Introduction to CMB: overview and observational status

Carlo Burigana
INAF-IASF Bologna
burigana@iasfbo.inaf.it

On behalf of the
Planck Collaboration
for related topics

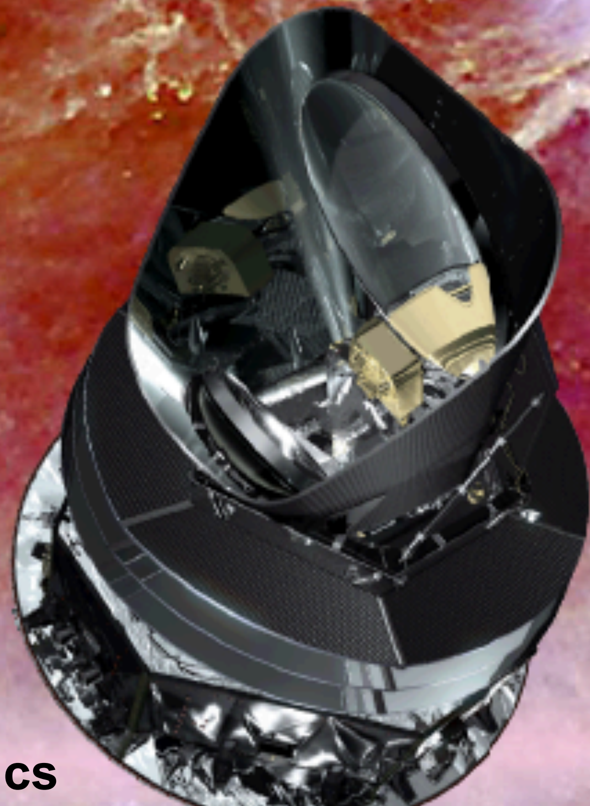

Ferrara, 7 September 2015
Astrophysical Probes of Fundamental Physics
A PhD School at University of Ferrara, 7-11/09/2015
(Dept. of Physics and Earth Science)

CMB: history of non-discoveries: 1

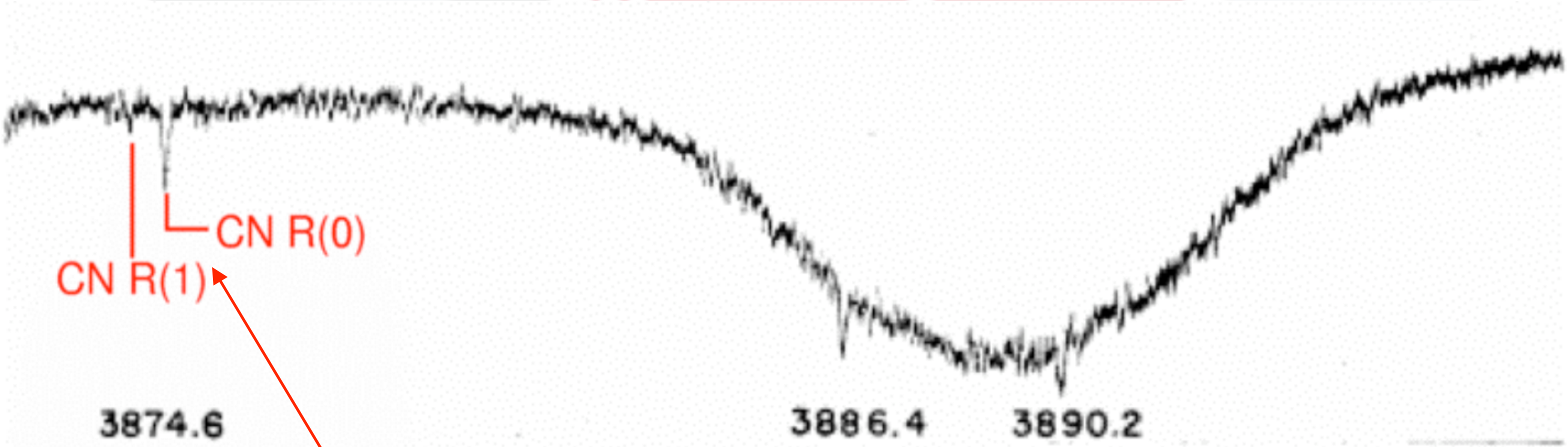

Gerard Herzberg (1904-1999), Nobel Prize for Chemistry 1971
“Spectra of Diatomic Molecules”, 1950:

noticed that from intensity of lines of CN at K=0 e K=1 it was possible to derive a temperature of 2.3 K, but obviously it does not have a particular meaning …

So Herzberg missed his second Nobel…

CMB: history of non-discoveries: 2, 3, 4

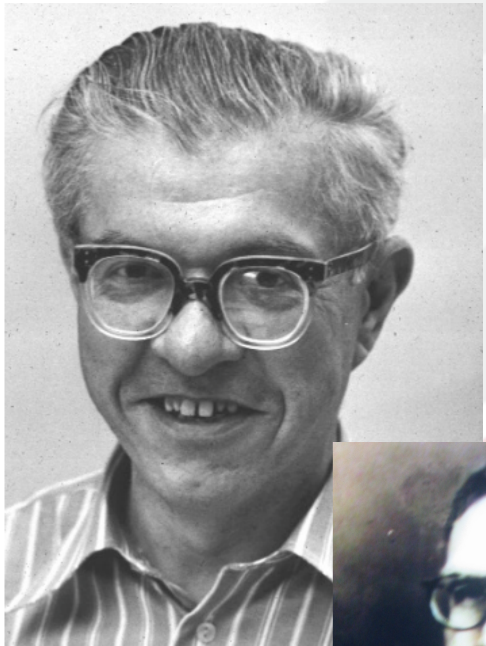

Fred Hoyle

George Gamow

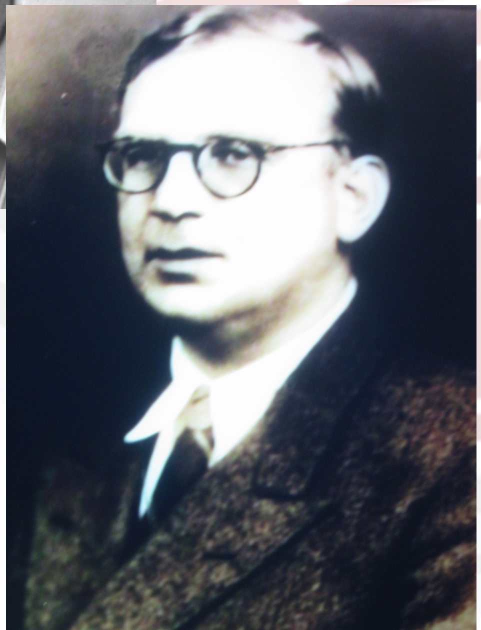

- Gamow (1948) predicted T=50 K, then (1956) T=6 K
- Alpher & Herman (1948) predicted T=5 K (!)
- Hoyle (1950) evaluated all of this not realistic suggesting that Big Bang theory is fully wrong
- Shmaonov (1957) “reobserved” CMB at 4±3 K. Nobody (even the author) recognized its meaning!

And finally … the discovery (1964)

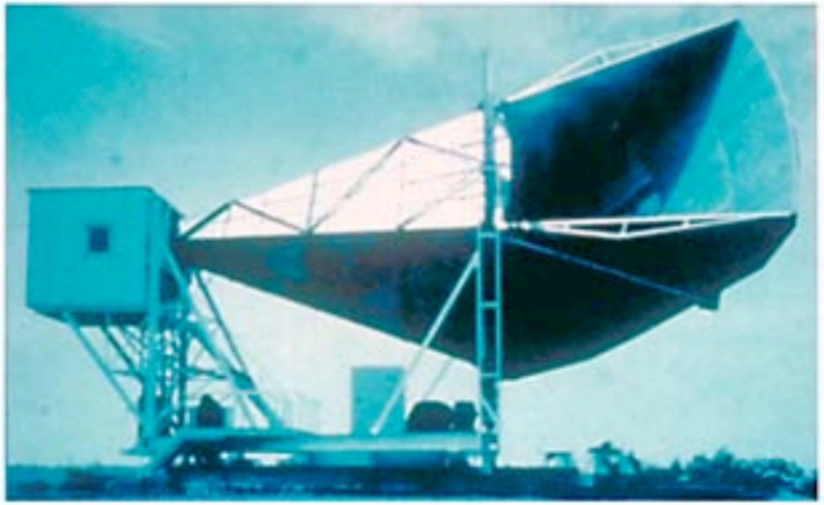

Microwave Receiver

Arno Penzias

Robert Wilson

First Nobel Prize for the CMB!

Another "non discovery": Relikt

RELIKT-1 a russian mission (launched in 1983)
aimed at measuring the CMB at 37 GHz with 6.6 deg angular resolution.
Galactic emisison and cosmic dipole were measured.
In 1986 they planned RELIKT-2, never launched because of the URSS disgregation after 1993.

1987 – Relikt-1: upper limits!
"Standard" Big Bang model was close to be rejected …
"The multipole analysis gave the estimates of $(\Delta T/T)_2 \leq 3\times10^{-5}$ and $(\Delta T/T)_3 \leq 7\times10^{-5}$ for the quadrupole and octupole respectively. "

Finally …

1993 – COBE: anisotropy discovery!
$6\times10^{-6} < \Delta T_2/T < 3.3\times10^{-5}$ with 90% confidence including systematic errors …"

COBE (1992)

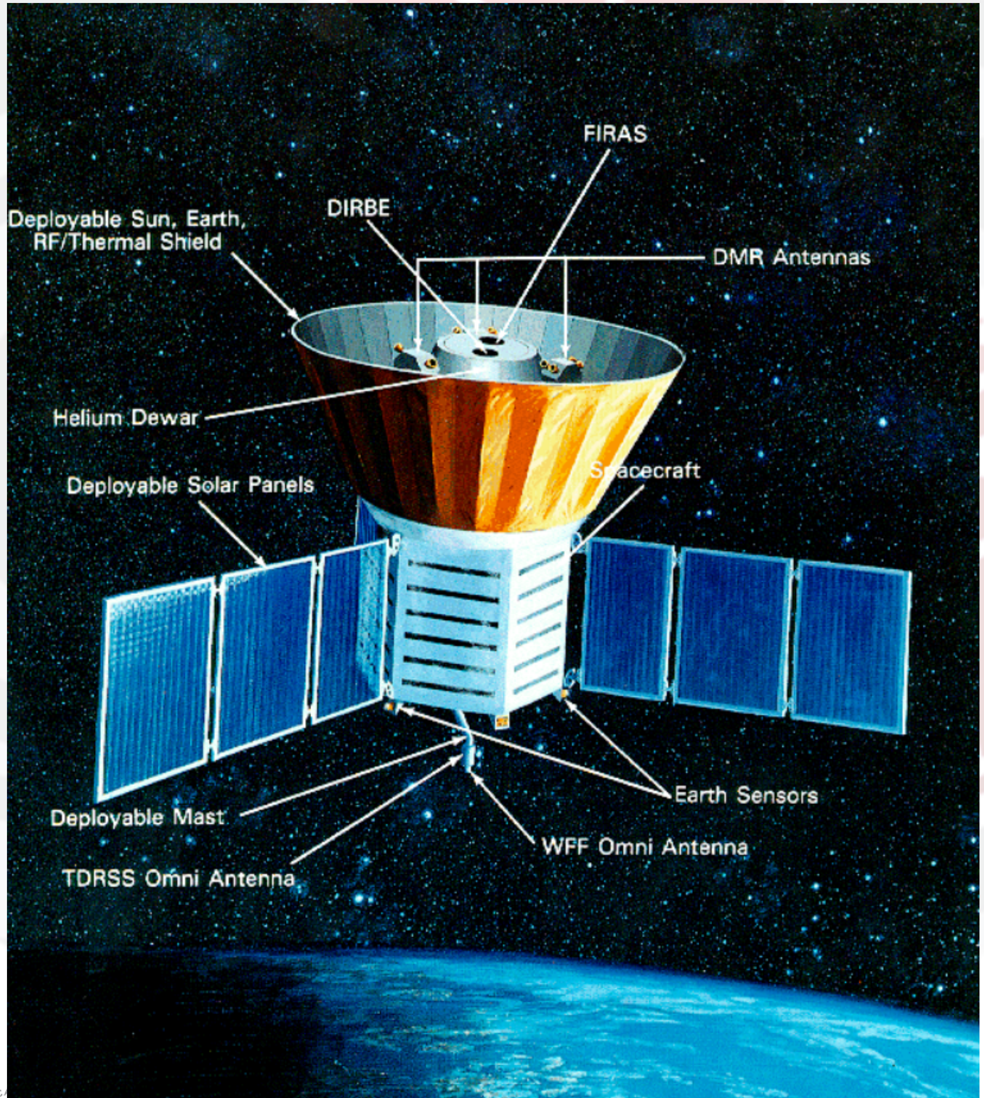
FIRAS
DIRBE
Deployable Sun, Earth, RF/Thermal Shield
DMR Antennas
Helium Dewar
Deployable Solar Panels
Spacecraft
Earth Sensors
Deployable Mast
WFF Omni Antenna
TDRSS Omni Antenna

THE TIMES

25 April 1992

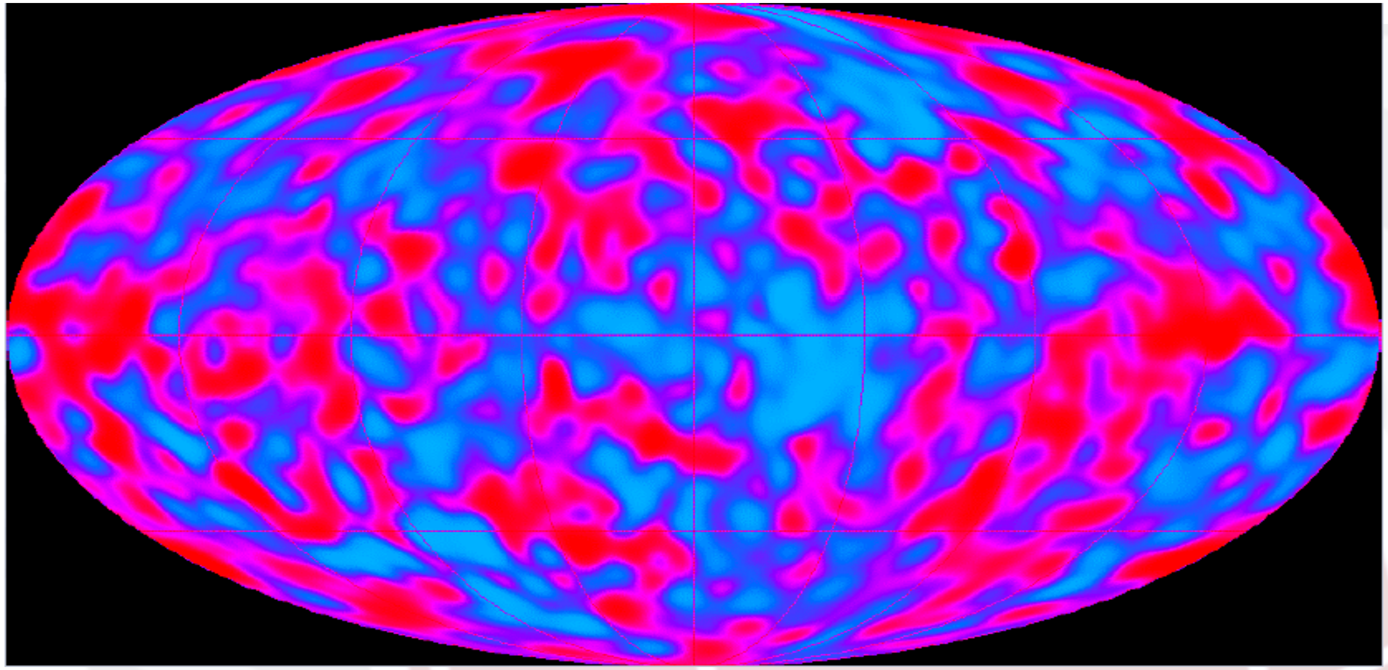

COBE - DMR

Stephen Hawking defined it as
the most important discovery of the century if not of all times

Mather & Smoot
2006, second
Nobel Prize
for the CMB

A Scientist's Mail.

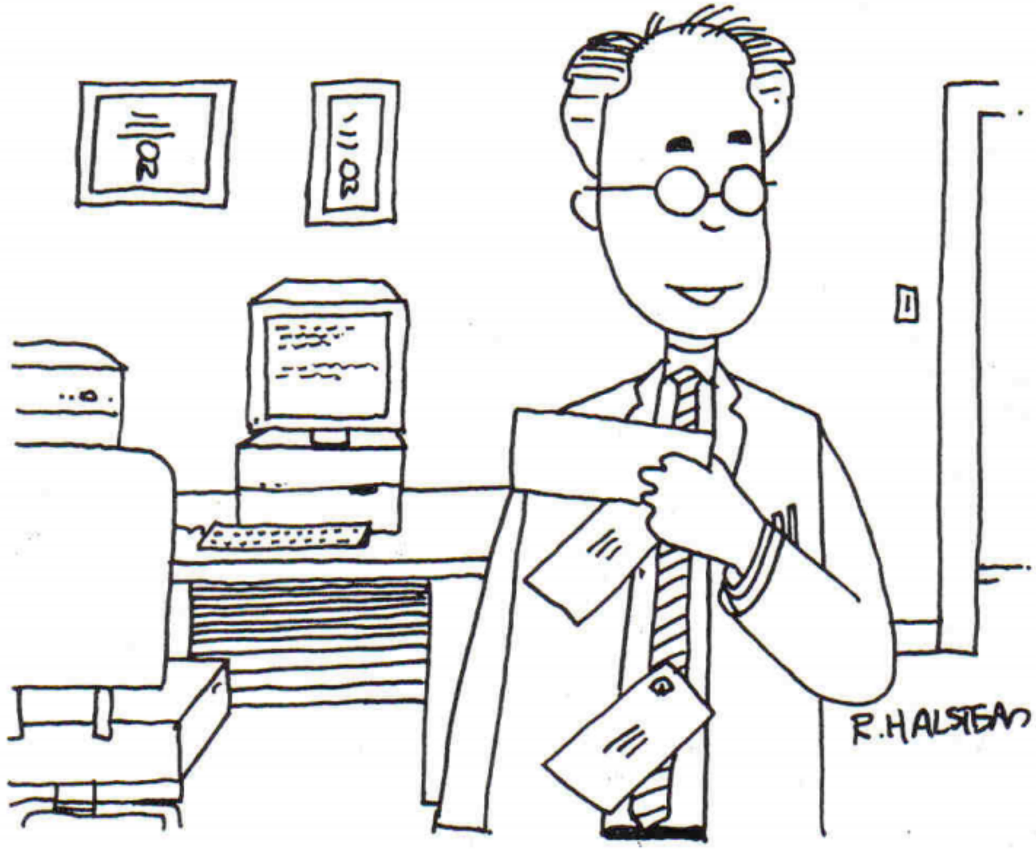

"You may have already won the Nobel Prize...."

John Mather

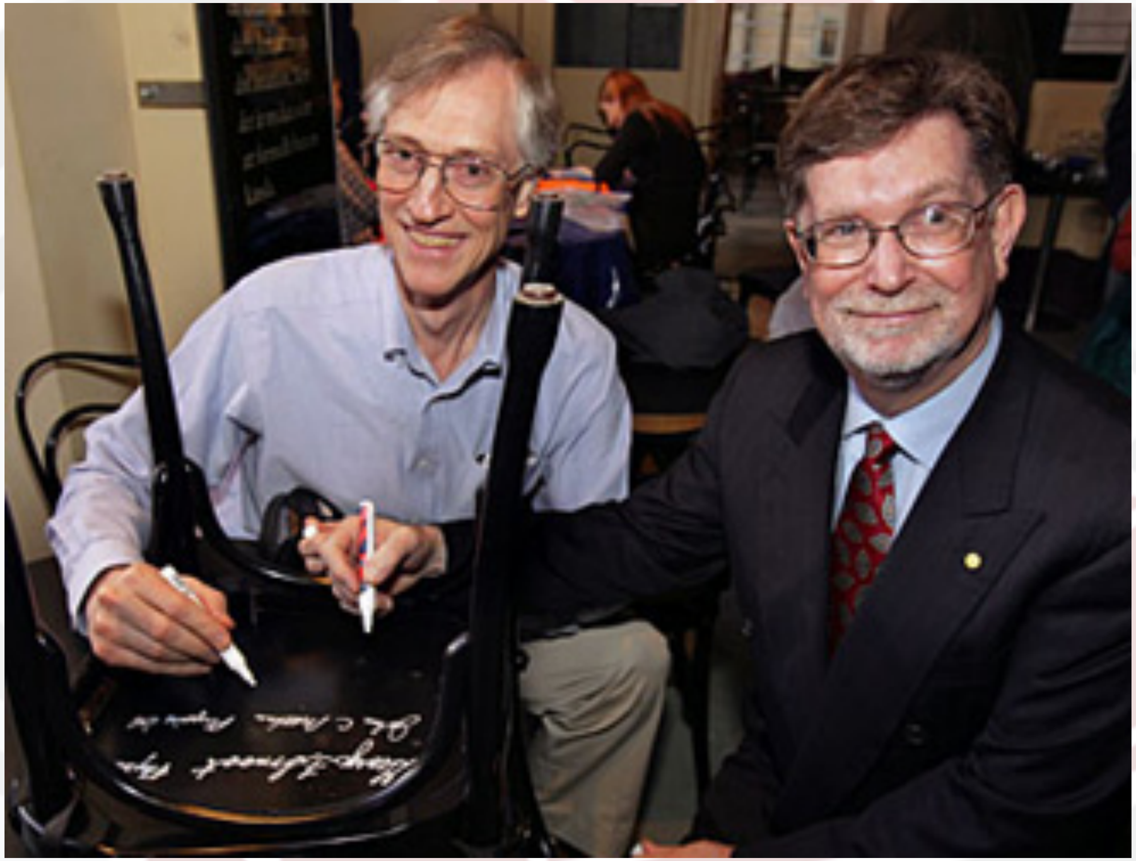

George Smooth

Nobel Prize for Physics 2006

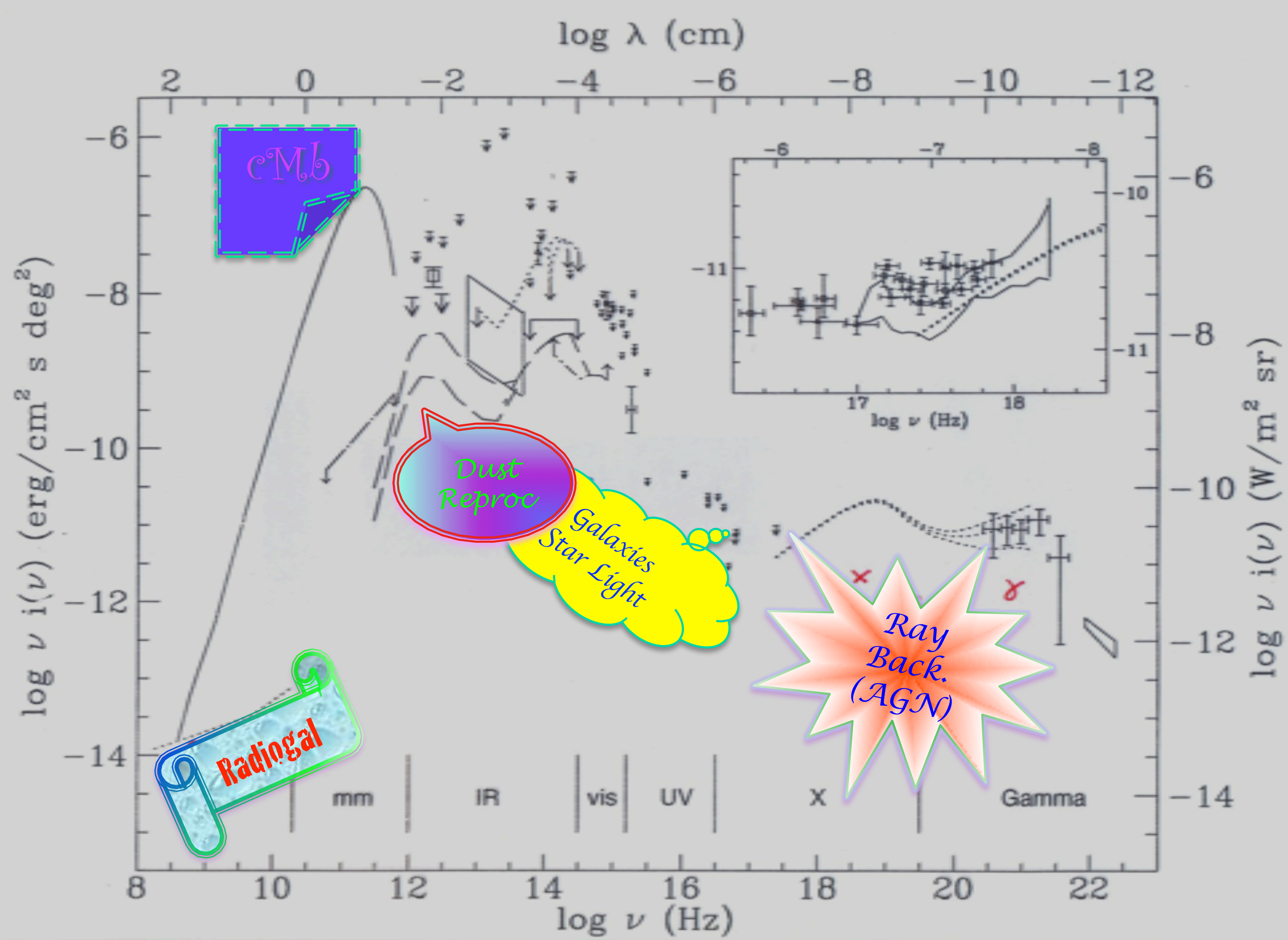

Adapted from de Zotti & Burigana 1992, Highlights of Astronomy, 9, 265

Multifrequency view of cosmic backgrounds

Cosmic Microwave Background Radiation

Anisotropies

- $$\frac{\Delta T}{T}(\hat{\mathbf{n}})$$

Map of CMB anisotropies

Angular power spectrum

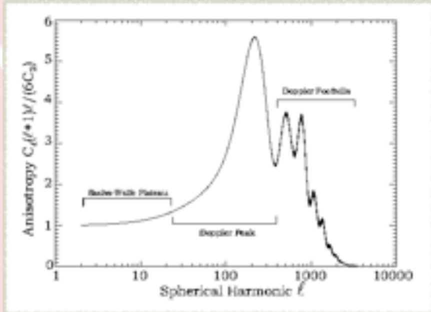

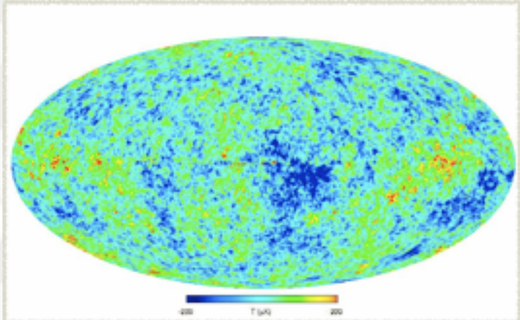

Polarization

- $$P^2 = Q^2 + U^2$$

Main contribution:

Thomson Scattering of radiation with quadrupole anisotropy generates linear polarization

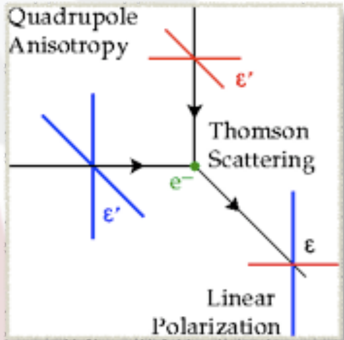

Spectrum

- Photon distribution function

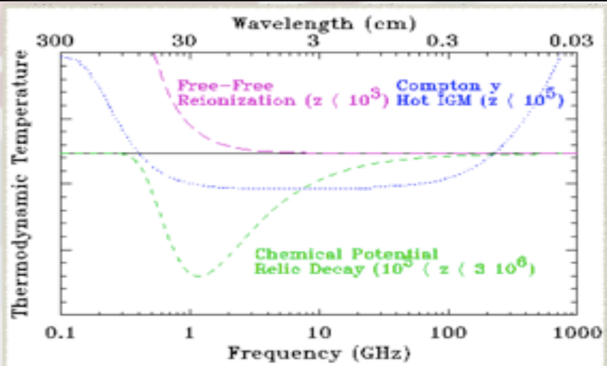

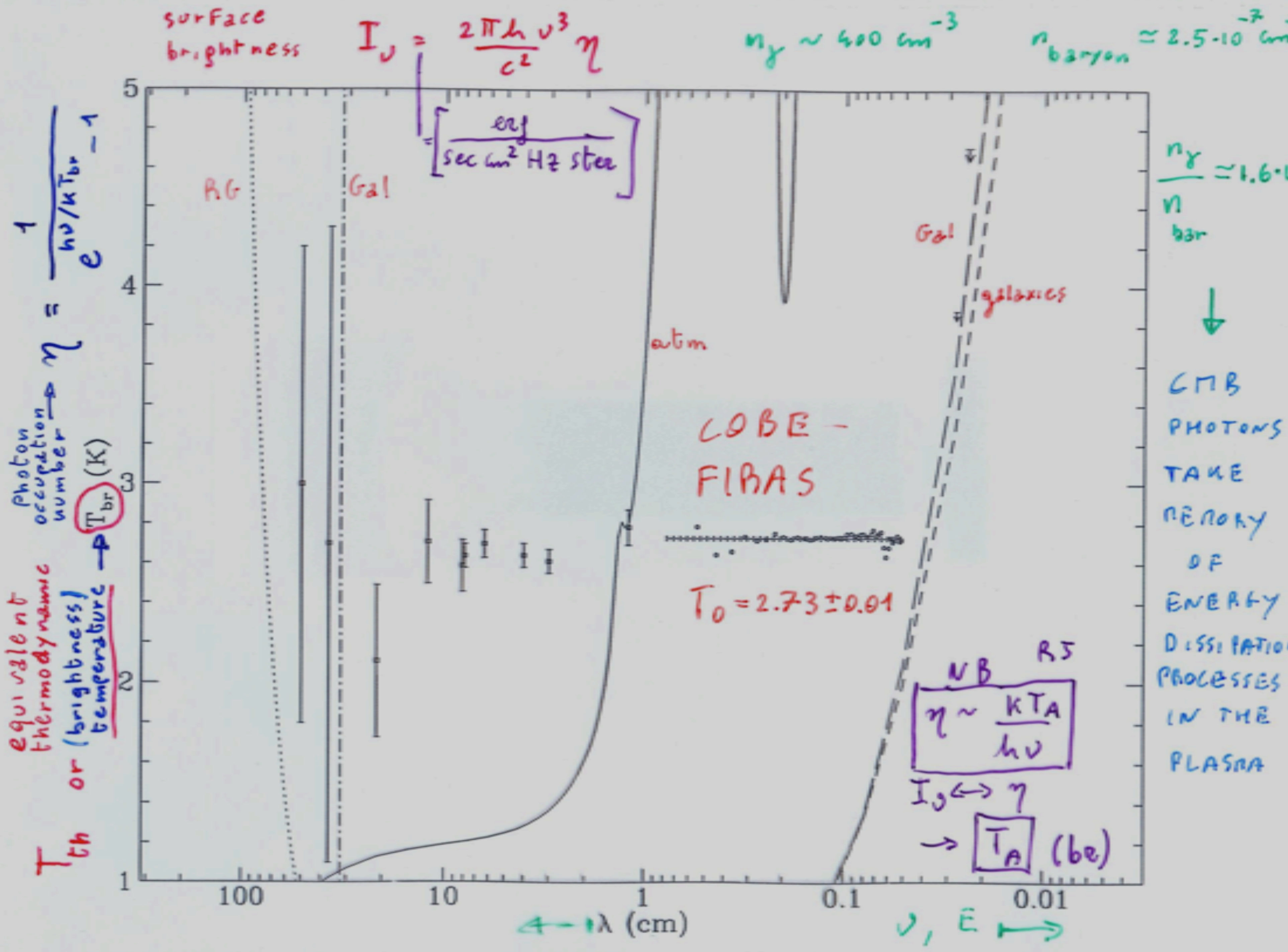
surface brightness
$I_\nu = \frac{2\pi h \nu^3}{c^2}\eta$
$= \left[\frac{erg}{sec\ cm^2\ Hz\ ster}\right]$
$n_\gamma \sim 400\ cm^{-3}$
$n_{baryon} \simeq 2.5\cdot 10^{-7}\ cm^{-3}$
$\frac{n_\gamma}{n_{bar}} \simeq 1.6\cdot 10^9$
CMB PHOTONS TAKE MEMORY OF ENERGY DISSIPATION PROCESSES IN THE PLASMA
T_{th} equivalent thermodynamic or (brightness) temperature → T_{br} (K)
photon occupation number → $\eta = \frac{1}{e^{h\nu/kT_{br}} - 1}$
RG
Gal
atm
Gal
galaxies
COBE - FIRAS
$T_0 = 2.73 \pm 0.01$
RJ
NB
$\eta \sim \frac{kT_A}{h\nu}$
$I_\nu \leftrightarrow \eta$
→ T_A (be)
5
4
3
2
1
100
10
1
0.1
0.01
λ (cm)
ν, E

CMB temperature as function of redshift

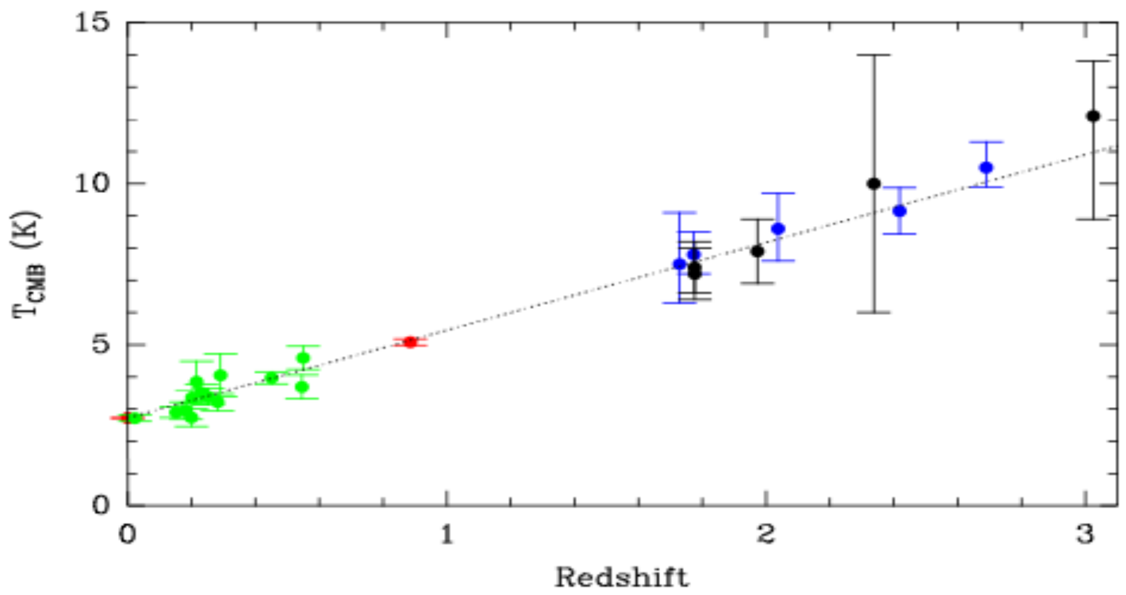

Fig. 5. Measurements of the CMB temperature as a function of redshift. Data points in green correspond to S-Z measurements toward galaxy clusters, in black to C I and C II absorption studies, in blue to CO absorption (see Noterdaeme et al. 2011 and references therein), and the value derived toward the PKS 1830−211 SW absorption is marked in red. The dotted line corresponds to the law $T_{CMB}=T_0\times(1+z)$.

Important verification of fundamental principles in cosmology

Recent progress:
Muller et al. 2013, A&A, 551, id. A109
Observation:
T_{CMB}=5.08±0.10 K
at 68% CL @ z=0.89
Prediction: T_{CMB}=5.14 K

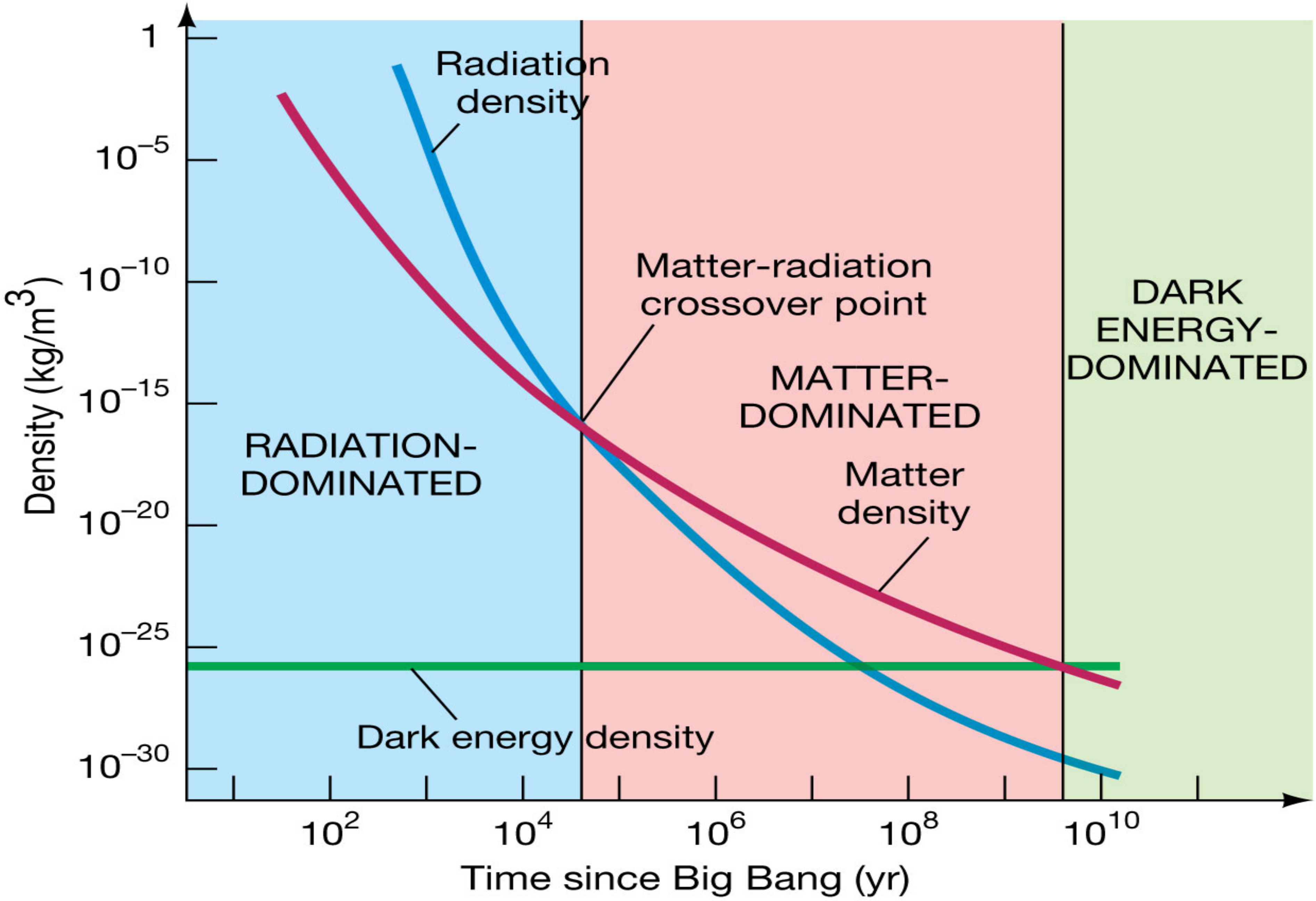

Radiation density
Matter-radiation crossover point
DARK ENERGY-DOMINATED
MATTER-DOMINATED
RADIATION-DOMINATED
Matter density
Dark energy density
Density (kg/m³)
1
10⁻⁵
10⁻¹⁰
10⁻¹⁵
10⁻²⁰
10⁻²⁵
10⁻³⁰
10²
10⁴
10⁶
10⁸
10¹⁰
Time since Big Bang (yr)

Cosmic history: "early" vs "late" epochs

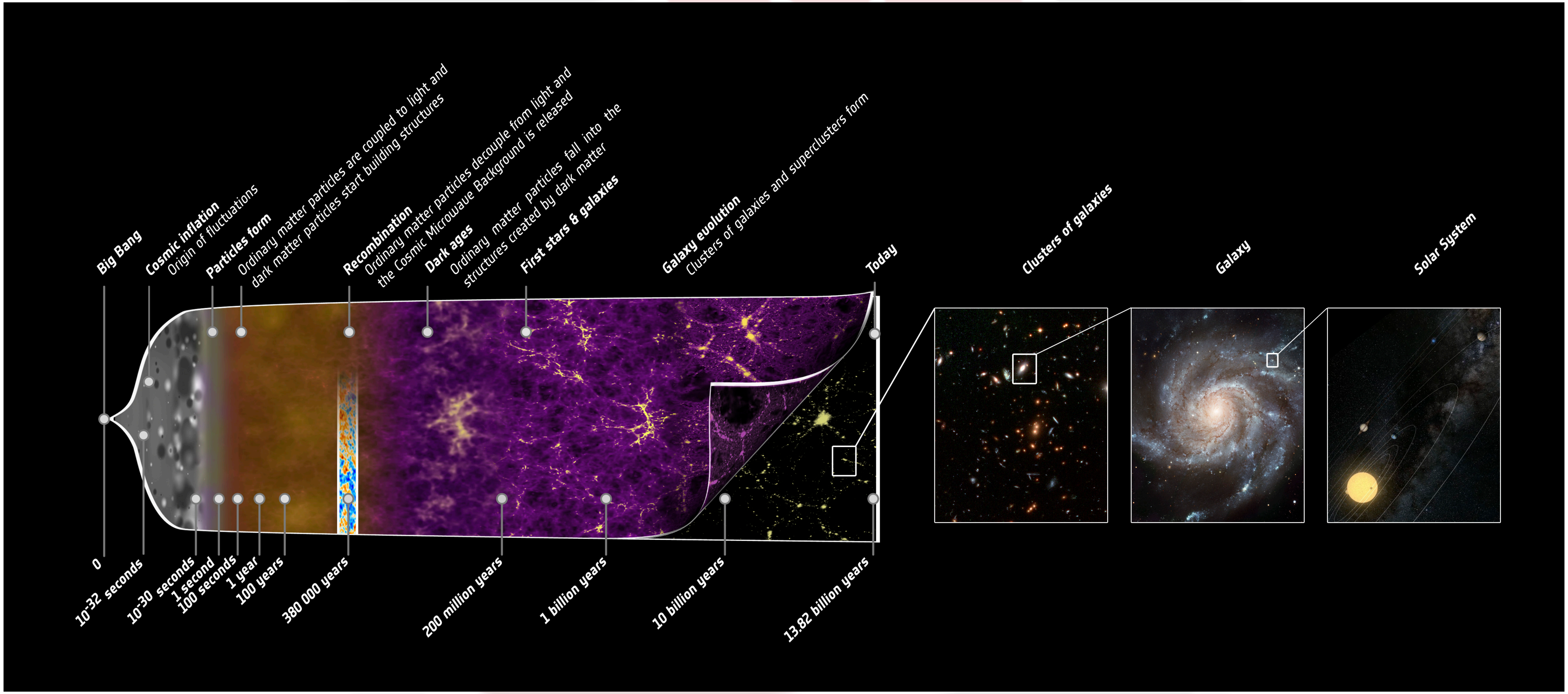

[http://www.esa.int/Our_Activities/Space_Science/Planck/History_of_cosmic_structure_formation]

Total Intensity (Temperature) Anisotropies of the Cosmic Microwave Background

C. Burigana – Ferrara 7/9/2015

CMB space mission experiments overview – Planck: 3rd Generation

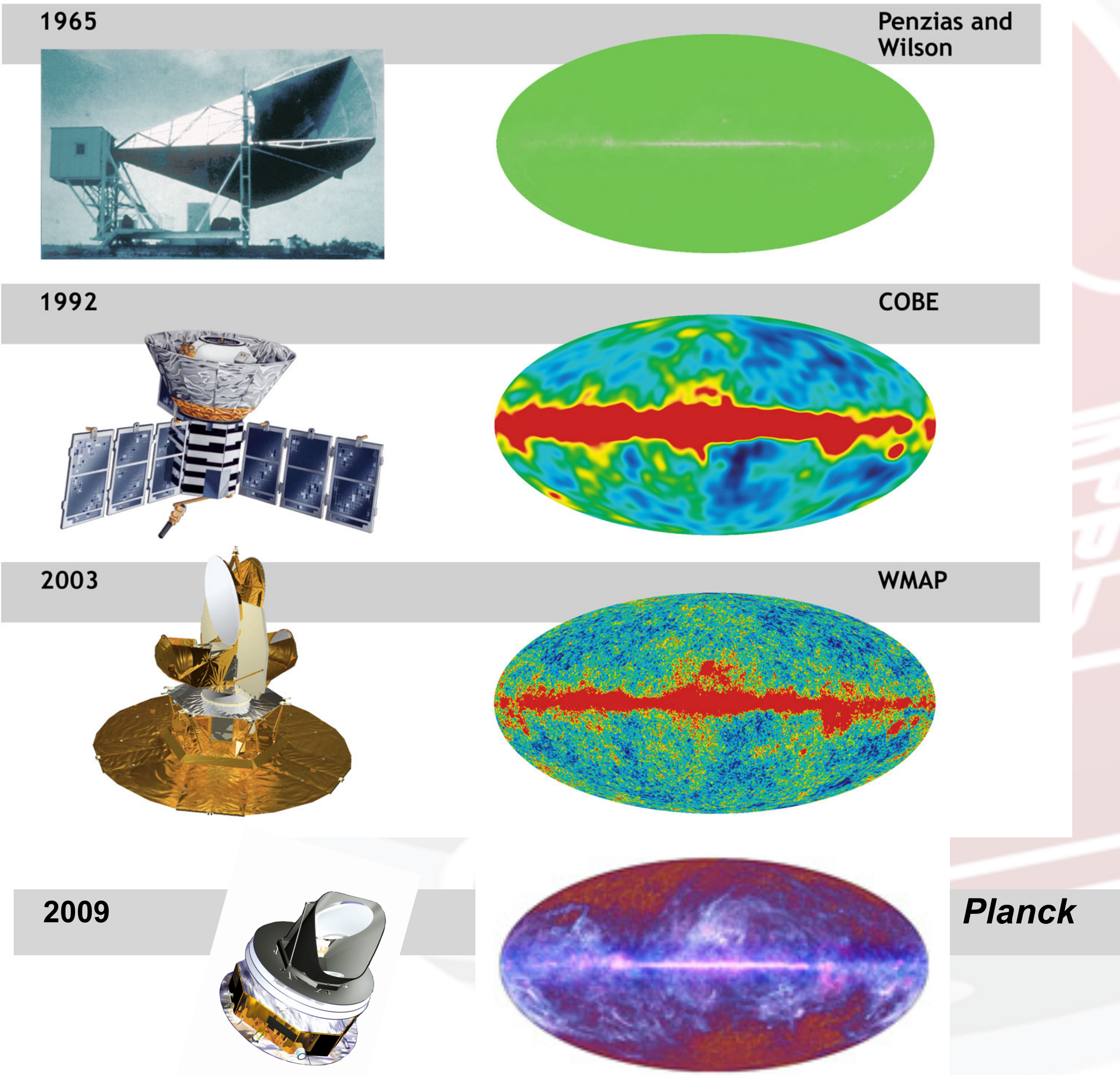

The oldest light or the first light of the Universe

Discovered the remnant afterglow from the **Big Bang**. → **2.7 K**
Blackbody radiation, Discovered the patterns (**anisotropy**) in the afterglow. → **angular scale ~ 7°** at a level $\Delta T/T$ of 10^{-5}
(Wilkinson Microwave Anisotropy Probe): → **angular scale ~ 15’**
→ **angular scale ~ 5’**, $\Delta T/T \sim 2\times10^{-6}$, 30~857 GHz

Planck Scientific Objectives

The unrivalled accuracy of *Planck* on the whole sky will allow us to:

– Pin down the basic characteristics of the Universe: age, contents, dynamics, geometry, …

– Examine the origins of the Universe and test inflation

– Probe physics at extremely high energies, e.g. superstrings, neutrinos

– Probe the birth of the first stars and galaxies

& also

– Understand the evolution of structures, galaxies and clusters of galaxies; Observe our own Galaxy as never seen before …

→ Key non-CMB science with *Planck* includes:

- ❖ The Cosmic Infrared Background
- ❖ Sunyaev-Zeldovich selected sources
- ❖ Extragalactic sources and backgrounds
- ❖ Maps of Milky Way at frequencies 30-1000 GHz

… and all related science ☺

Dipole and Galactic plane visible

30 GHz

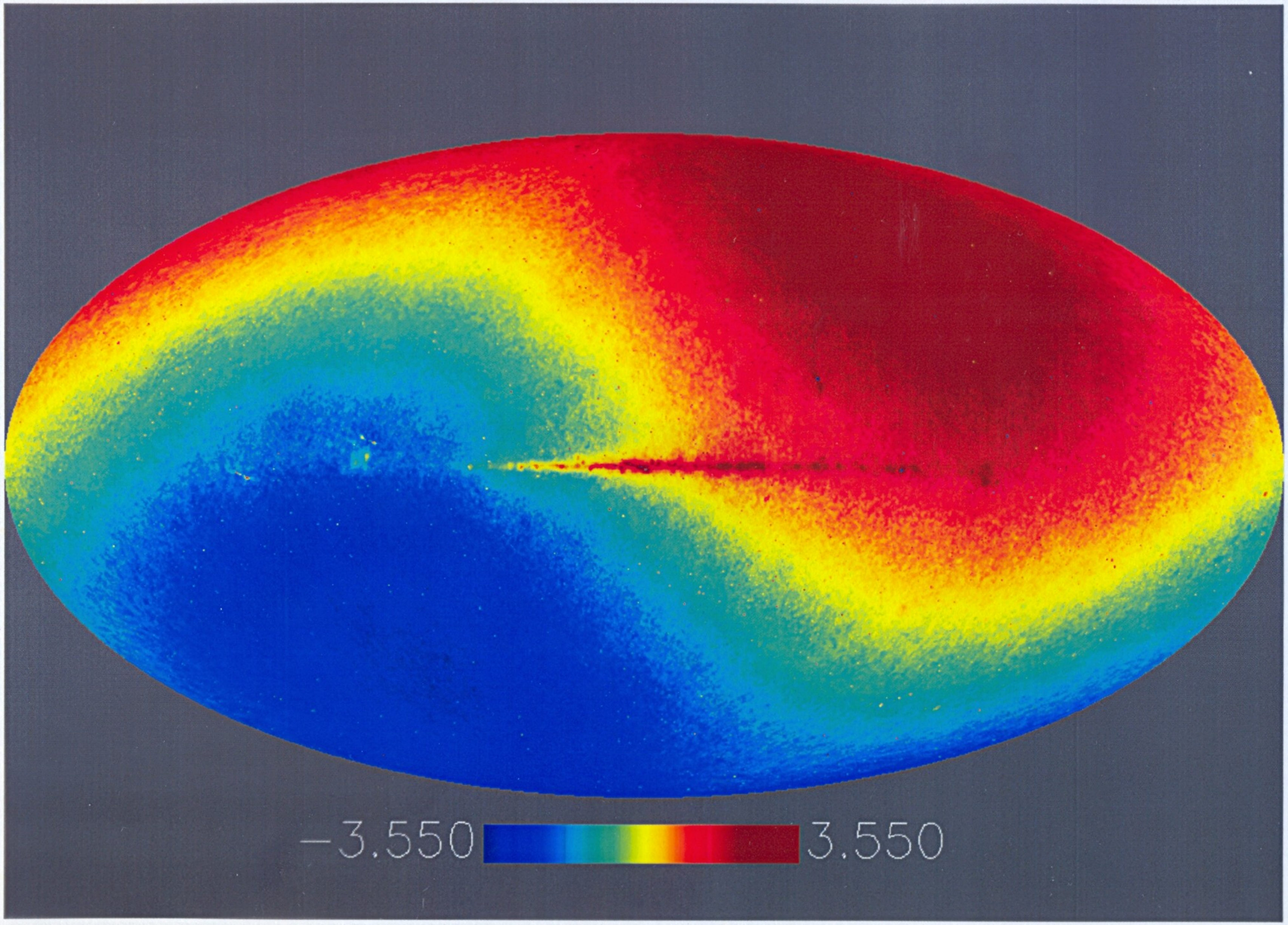

mK

The CMB seen by *Planck* & its cosmological implications

2015

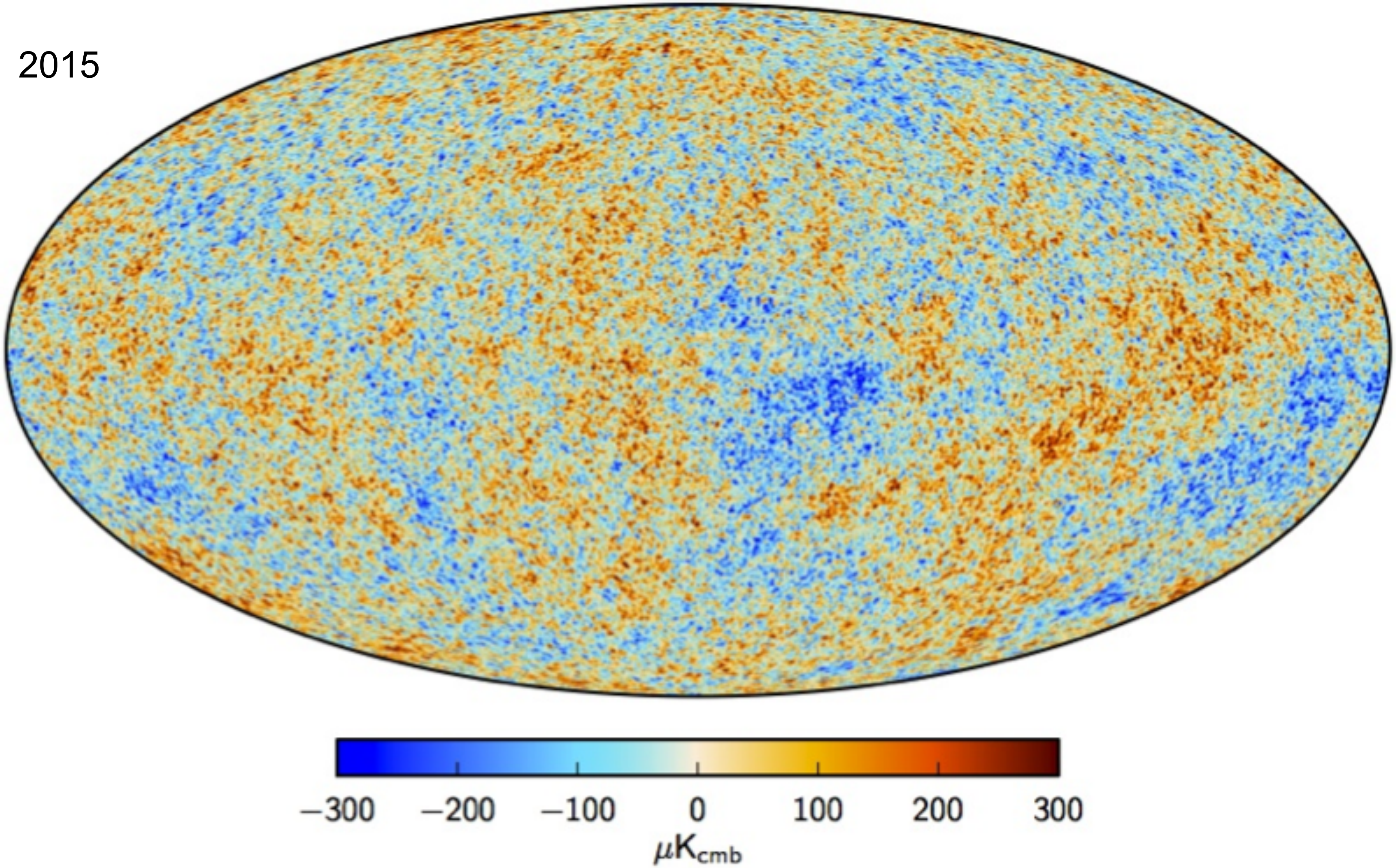

❖ Temperature anisotropy pattern

$\Downarrow$ Statistical moments

$\Downarrow$ $\langle T \rangle = T_0 \simeq (2.725 \pm 0.002)\,K$

Monopole, Mather et al. '99

RMS FLUCTS.

they depend on scale
(and, observationally, experiment resolution, pixel size)

◆ → All-sky observations → spherical harmonics expansion

$$\frac{\delta T}{T}(\vec{\gamma}) = \sum_{\ell=1}^{\infty} \sum_{m=-\ell}^{\ell} a_{\ell m} Y_{\ell m}(\vec{\gamma})$$

$$C(\theta) = \left\langle \frac{\delta T}{T}(\vec{\gamma}_1) \frac{\delta T}{T}(\vec{\gamma}_2) \right\rangle = \frac{1}{4\pi} \sum_{\ell} (2\ell+1) C_\ell P_\ell(\cos\theta)$$

$$C_\ell = 2\pi \int d\cos\theta \, P_\ell(\cos\theta) \cdot C(\theta)$$

Isotropy → $\langle a_{\ell m} \rangle = 0$

$$C_\ell = \langle |a_{\ell m}^2| \rangle = \frac{1}{2\ell+1} \sum_m a_{\ell m}^2$$

✧ Multipoles regimes

$\ell \sim \frac{180}{\theta(\mathrm{DEG})}$

$\ell \lesssim 50$ Low multipoles, large scales

$100 \lesssim \ell \lesssim 10^3$ Acoustic peaks region, intermediate multipoles/scales

$\ell \gtrsim 10^3$ Silk damping region
high multipoles, small scales

Particle horizon
Given a phenomena at a given (**x**, t)
Is it observable by an observer at (**x**', t') ?

It divides space into 2 regions:
observed objects < -- > not observed objects
causally connected regions < -- > not causally connected regions

Observer in	$r = 0$	time	t
Signal	r_1		t_1

Observer receives signals from $r < r_1$

$$\int_0^{r_1} \frac{dr}{\sqrt{1-kr^2}} = \int_{t_1}^{t} \frac{dt'}{R(t')}$$

If it converges when $t_1 \rightarrow 0$ then horizon exists

$$\int_0^{r_H(t)} \frac{dr}{\sqrt{1-kr^2}} = \int_0^{t} \frac{dt'}{R(t')}$$

→ Proper distance of horizon

$$d_H(t) = R(t) \int_0^{r_H(t)} \frac{dr}{\sqrt{1-kr^2}} = R(t) \int_0^{t} \frac{dt'}{R(t')}$$

N.B.: at $z \lesssim z_{eq}$ $R(t)$ dominated by Ω_m

$d_H(t) \longrightarrow \theta(t) \sim \theta(z)$

distance / separation of angular distance

$\theta \approx \frac{1}{z^{1/2}} \Omega^{1/2} \approx 2\,\deg\, \Omega^{1/2}$ at $z \sim 10^3$

Angular scale ≅ particle horizon

at $z \sim 10^3$

$\simeq 1^\circ \longleftrightarrow \ell \sim 200$

$\Rightarrow$ Large scales $\ell \lesssim 50 \gtrsim$ horizon at $z = 10^3$

$\hookrightarrow$ keep memory of primordial perturbations

n_s $\qquad P(k) = A\, k^{n_s} \qquad n_s = \dfrac{d \ln P}{d \ln k}$

\+ reionization history (τ)

\+ tensor perturbations / scalar perturbations

- $ds^2 = a^2(\eta)\left[-d\eta^2(1+2\psi) + dx^i dx^j \delta_{ij}(1-2\phi)\right]$

$a = 1/(1+z)$ $\qquad \phi, \psi$ PERT. SCAL.

- $H^2 = (\dot{a}/a)^2 = \left(\dfrac{da}{a^2 d\eta}\right)^2 = \dfrac{8\pi G}{3}\left[\dfrac{\rho_M}{a^3} + \dfrac{\rho_R}{a^4} + \rho_\nu(a) + \rho_\Lambda + \dfrac{\rho_K}{a^2}\right]$

$dt = a\, d\eta$ $\qquad w = p/\rho$ $\qquad \Lambda$/DE ?

- $\left[\dfrac{\delta T}{T}\right]_{OBS} = \left[\dfrac{\delta T}{T}\right]_{LS} + \left[\dfrac{\delta T}{T}\right]_{ISW} = \left[\psi + \dfrac{\delta T}{T}\Big|_{nod}\right]_{LS} + \int_{\eta_{LS}}^{\eta_0} (\phi+\psi)'\, d\eta$

ad. $\qquad \delta_\gamma = \dfrac{\delta\rho}{\rho}\Big)_\gamma \simeq -4aH\dfrac{\theta}{k^2}, \qquad \theta = 2k^2\psi / aH(3+3w)$

velocity potential

$\left[\dfrac{\delta T}{T}\right]_{LS} = \left[\psi + \dfrac{\delta_\gamma}{4}\right]_{LS} \simeq \left[\dfrac{\psi}{3}\right]_{LS}$

Sachs-Wolfe '67

Ma & Bertschinger '95

Dodelson '03

IS. $\qquad \left[\dfrac{\delta T}{T}\right]_{LS} \simeq \left[2\psi\right]_{LS}$

❖ Multipole region of acoustic (or Doppler) peaks

$z < z_{rec} \sim 10^3$

photon-baryon fluid

p^+, e^- γ

\+ gravity → acoustic oscillations in the plasma / harmonic oscillator

gravity ≅ force , baryon ≅ inertia , photon ≅ pressure

recombination
≅ instantaneous →

$\Delta z_{rec} \ll z_{rec}$

radiation keeps memory of the
oscillatory state of different modes

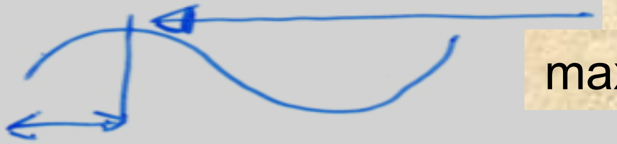

max overdensity <--> I° peak

1 / 4 oscillation

+ (1/2) + (1/2) + ... + (1/2) oscill.

→ 3°, 5°, 7° peak etc.

under-density modes → 2°, 4°, 6° peak etc.

valleys ≅ max of velocity
opposite in phase
with max of density

→ Structure of acoustic peaks
(depending on cosmological parameters, type and amplitude
of primordial perturbations, …)

$$C_\ell = \langle |a_{\ell m}|^2 \rangle \simeq 16\pi \int_0^\infty \frac{dk}{k} P_{rad}(k)\, T^2(k)\, J_\ell^2(k\tau_0)$$

$\tau_0 = \frac{2}{H_0}$ $(\Omega_0 = 1)$ conf. time @ $z=0$

low ℓ large scale $T^2(k) \simeq 1$

$P_{rad}(k) \propto k^n$, $n = 1$

$\propto \frac{1}{\ell(\ell+1)}$ $\Rightarrow \ell(\ell+1) C_\ell \simeq \text{const}$

J_ℓ Bessel sph. function

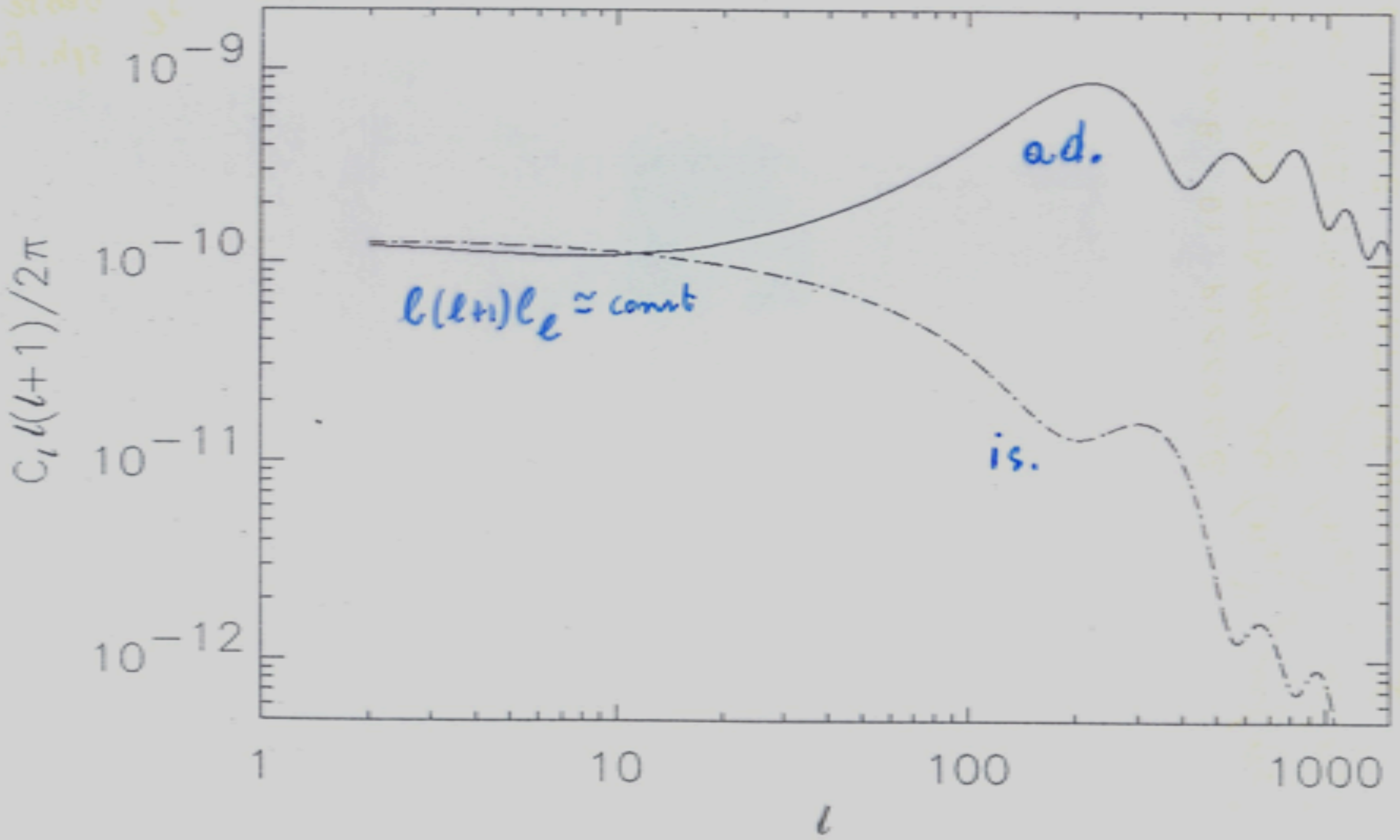

- Small scales $(\ell \gtrsim 10^3)$

where mechanisms of damping of perturbations operate

non-linear dissipation

$z \gtrsim 10^6$

$$\lambda_{ne} \simeq \frac{2}{\sqrt{3}} \cdot 4.1 \cdot 10^5 \left(\frac{T_0}{2.7K}\right)^{-2} \frac{\delta_\gamma^i}{1+z} \ \mathrm{Mpc}$$

$i = 1, 2, 3$ Zeldovich & Novikov '83

diffusion

$z \lesssim 10^6$ (Silk '67)

$$\lambda_{diff} \simeq \left(\frac{8}{15}\right)^{1/2} \pi \left(ct \cdot ct_{diff}\right)^{1/2} (1+z)$$

$$ct_{diff} = \frac{1}{n_e \sigma_T}$$

$$ct \simeq \begin{cases} (1+z)^{-2} & z > z_{eq} \\ (1+z)^{-3/2} & z < z_{eq} \end{cases}$$

distortions of CMB spectrum

ANIS.

A) → generation of small spectral distortions

early, (intermediate), late type distortions $\mu(n_s)$, $u(n_s)$

B) → damping of perturbations & CMB anisotropies, in particular in the case of reionization

$$C_\ell \longrightarrow \simeq C_\ell \cdot \exp(-\tau), \quad \ell \gtrsim 50$$

CMB photons are almost unperturbed in their journey from the last scattering surface …
but not completely … **LENSING EFFECT**

MATTER DISTRIBUTION DEFLECTS THE LIGHT PATH LENSING THE CMB PHOTONS

The effect is similar to a de-focusing of the maps

PLANCK 2013 **HAS A 25 SIGMA DETECTION OF CMB LENSING!**

PLANCK 2015 **HAS A 40 SIGMA DETECTION OF CMB LENSING!**

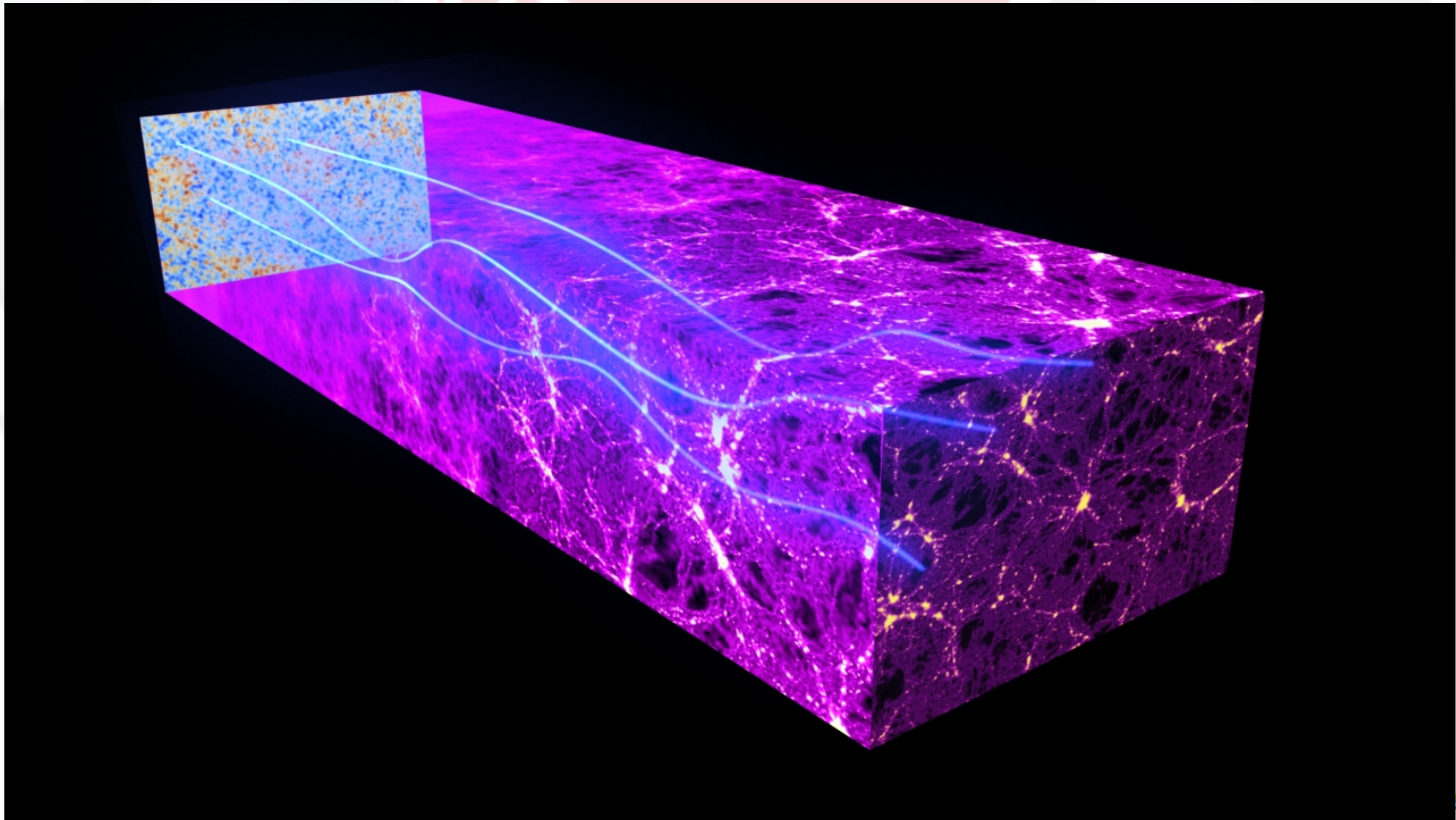

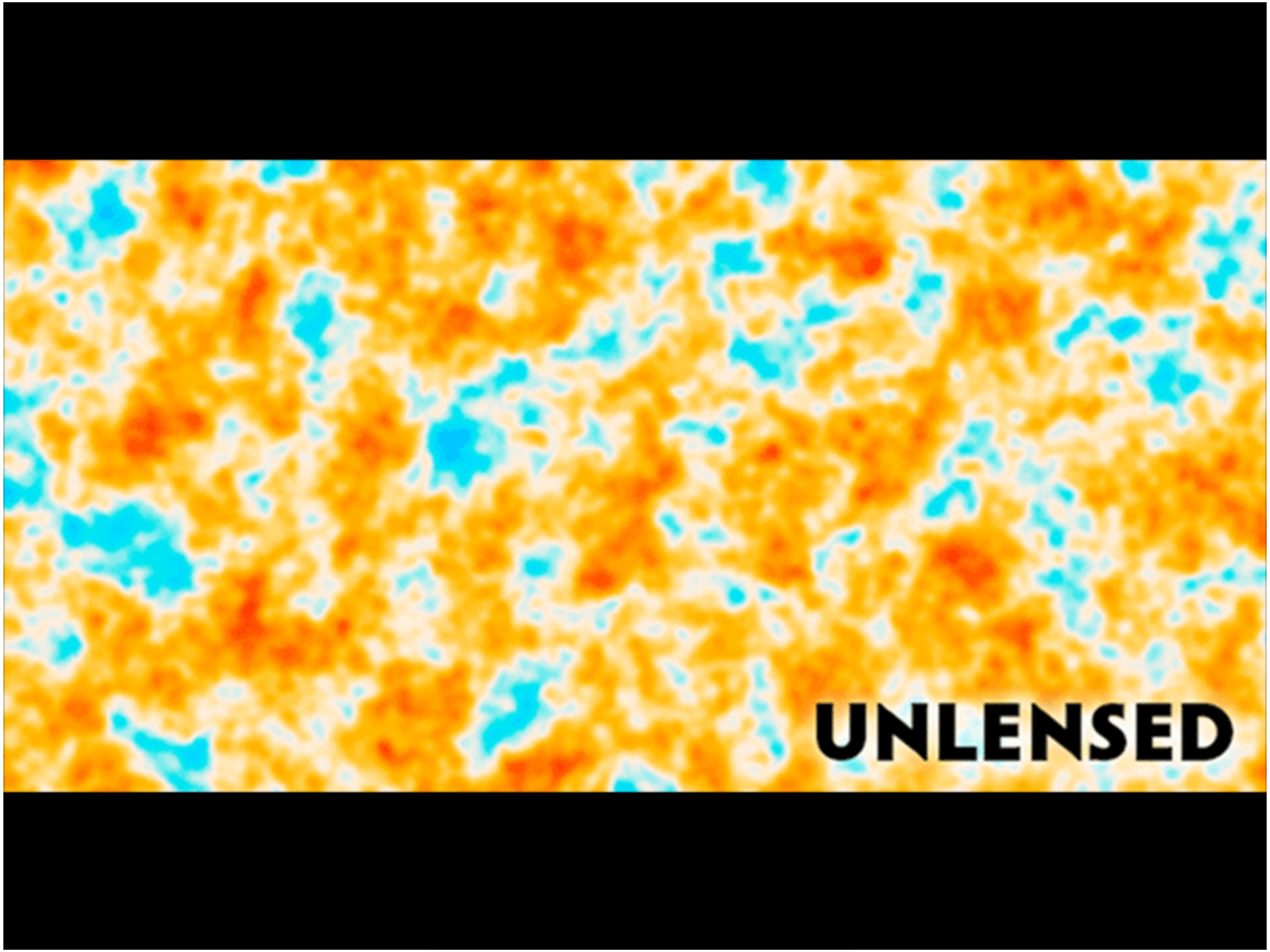
UNLENSED

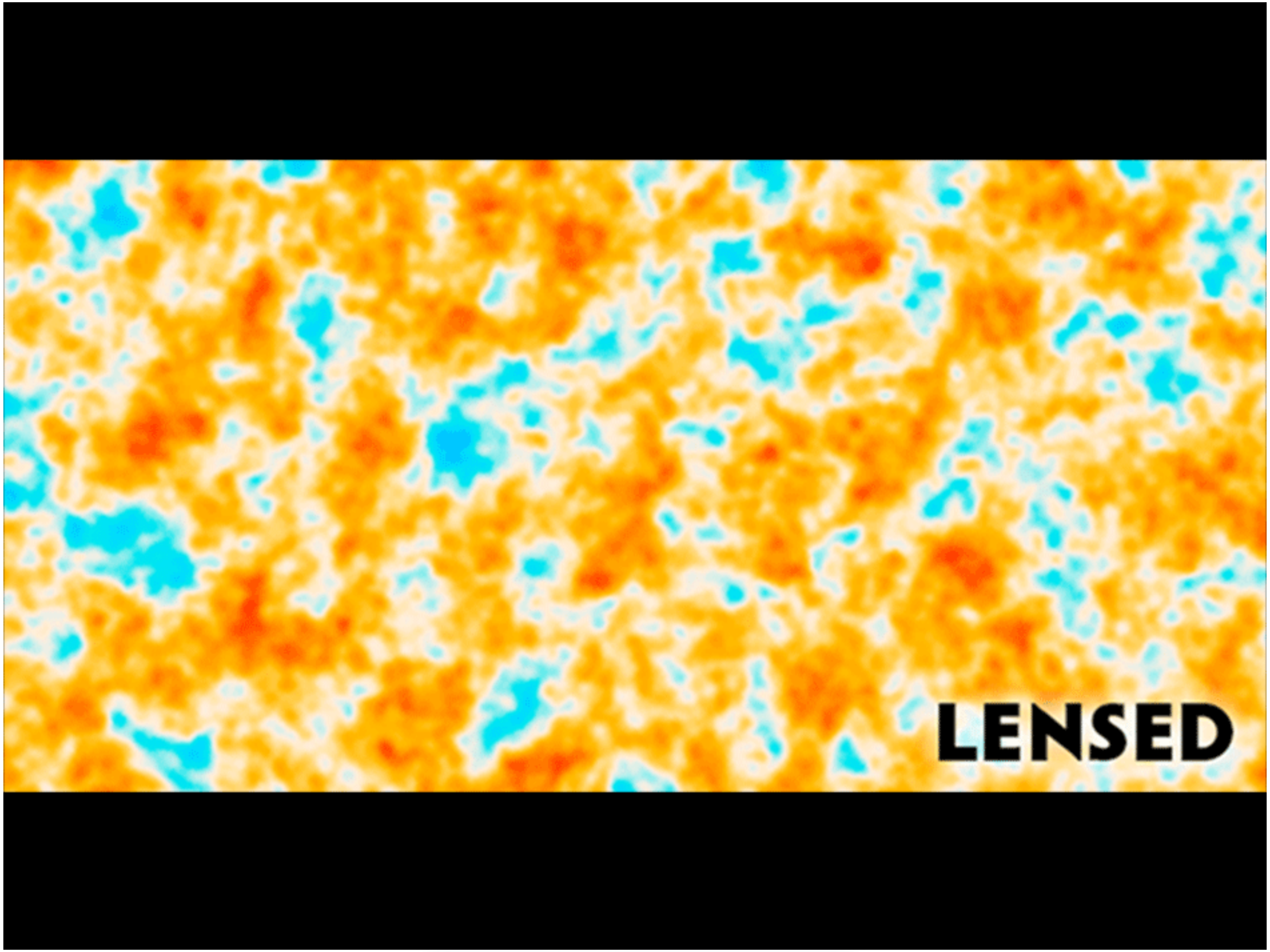
LENSED

Gravitational lensing potential power spectrum

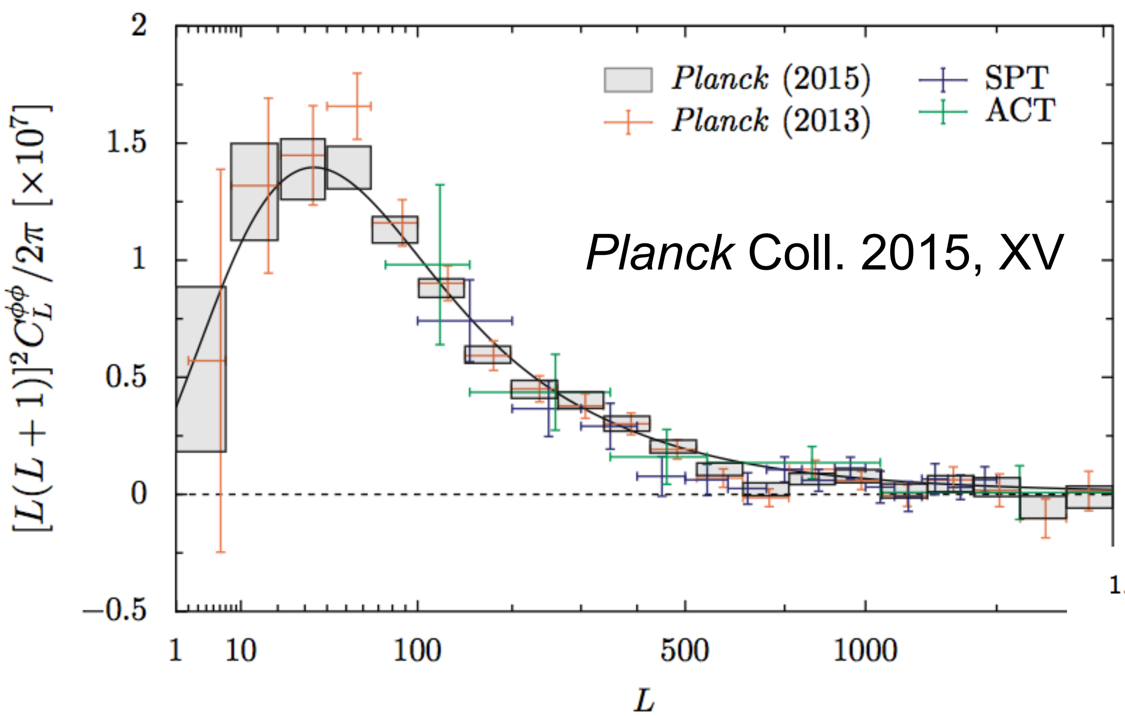

... & cosmological parameters from CMB lensing alone in the ΛCDM model. Solid coloured contours show 68% & 95% constraints when including: BAO (SDSS & 6DF - Anderson et al. 2014; Ross et al. 2014; Beutler et al. 2011; blue), and fixing the CMB acoustic-scale parameter. Solid black contours: constraint from the *Planck* CMB APS.

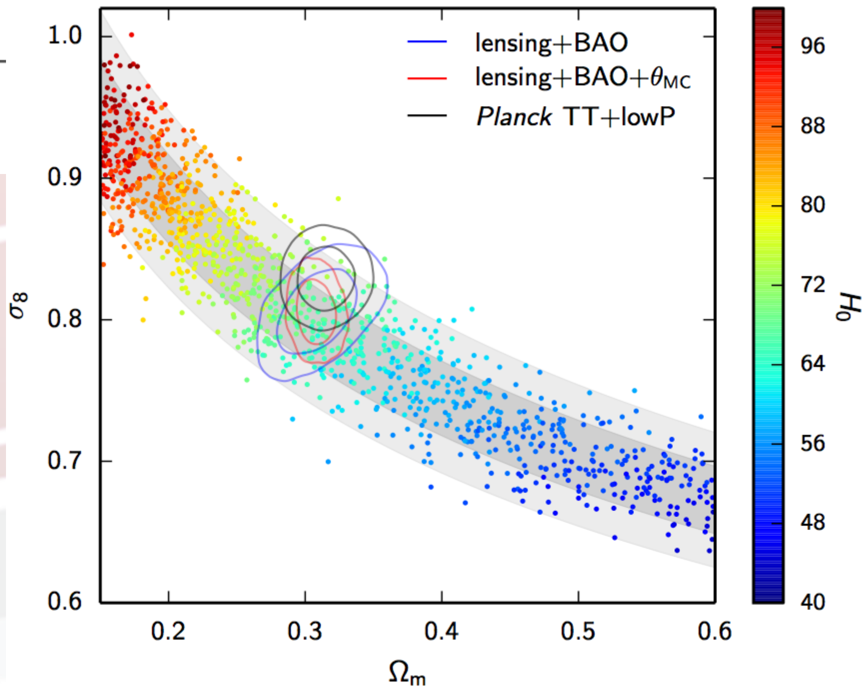

Planck 2015 full-mission, earlier measurements from *Planck* 2013 nominal-mission temperature data (*Planck* Collaboration XVII 2014), the South Pole Telescope (SPT, van Engelen et al. 2012), and the Atacama Cosmology Telescope (ACT, Das et al. 2014).
Black solid line: fiducial ΛCDM theory power spectrum.

Planck CMB map & multipole components = 2, 3, 4

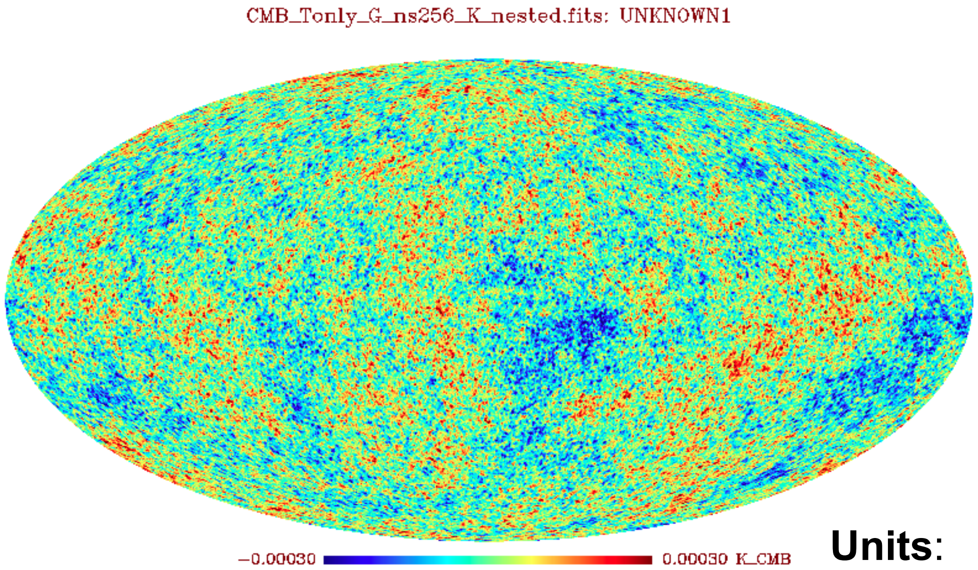

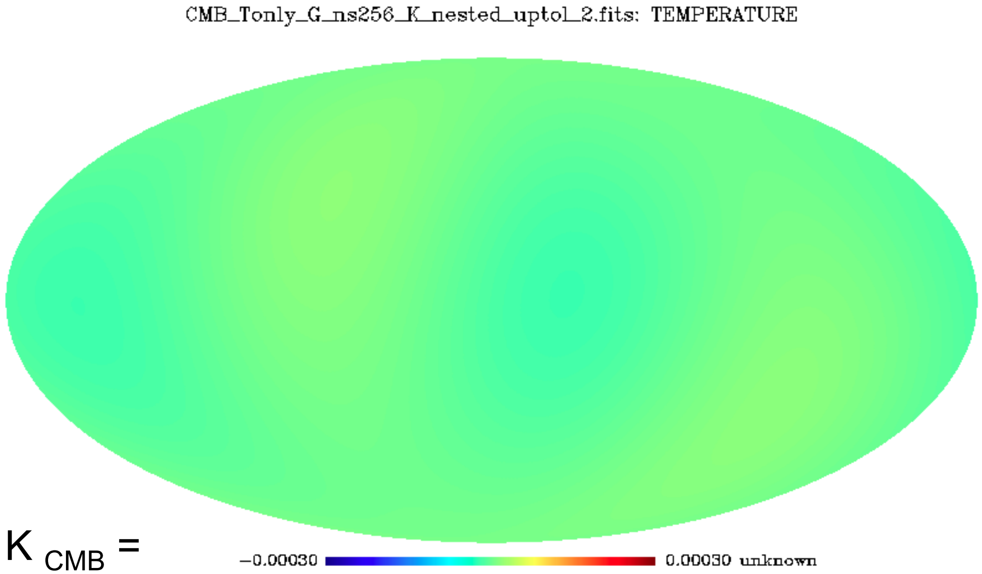

Units: K $_{CMB}$ =
Eq. Therm.Temp.

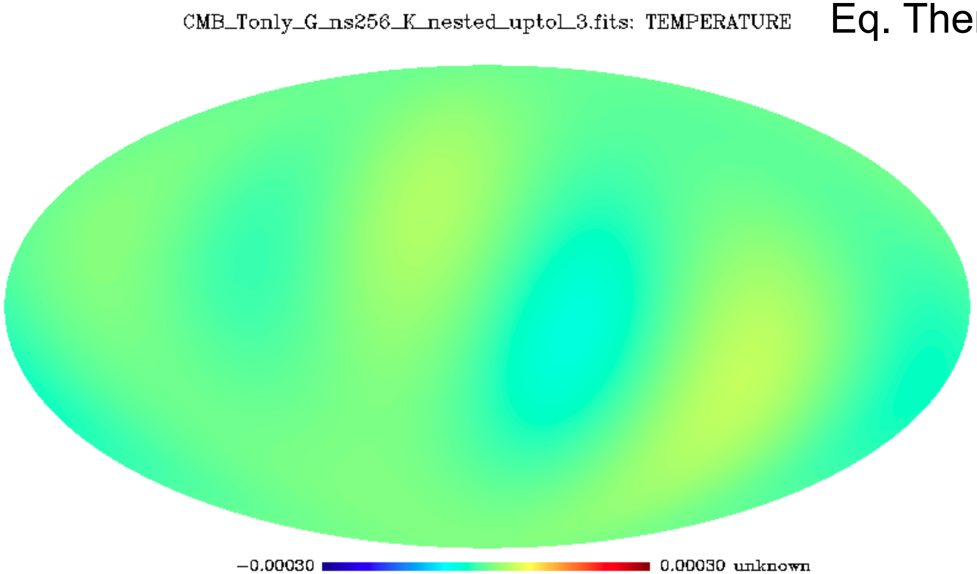

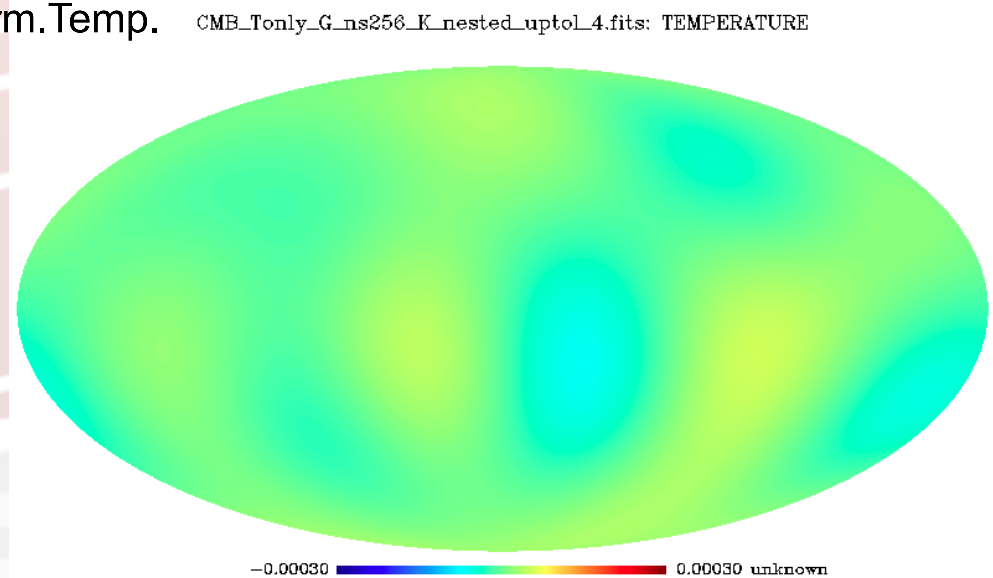

multipole components = 5, 6, 7, 8

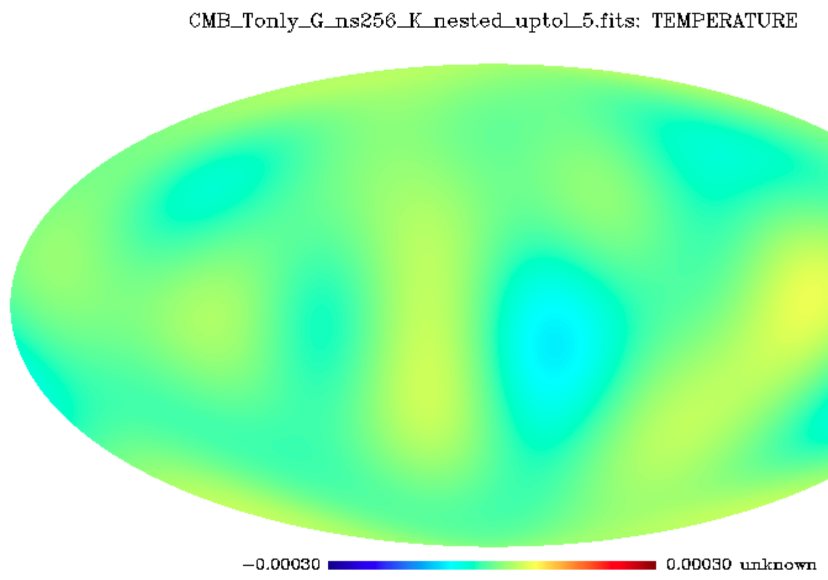

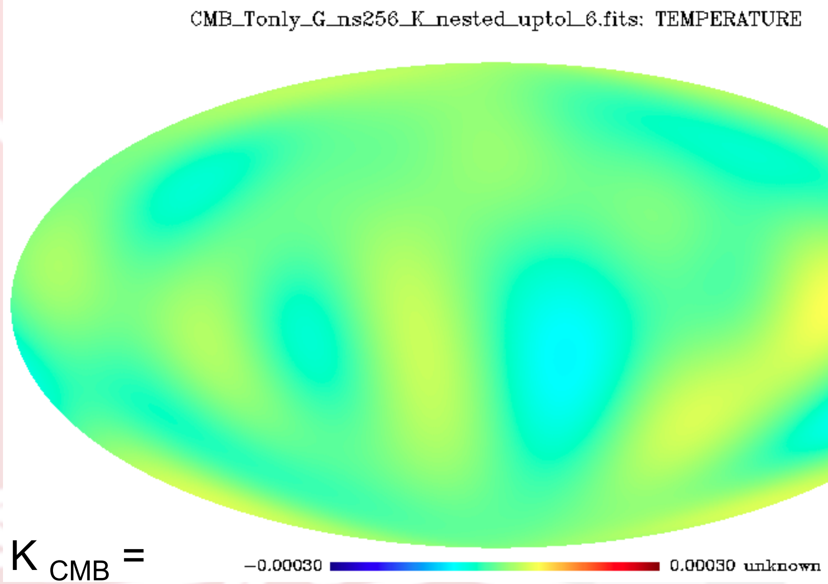

Units: K_{CMB} = Eq. Therm.Temp.

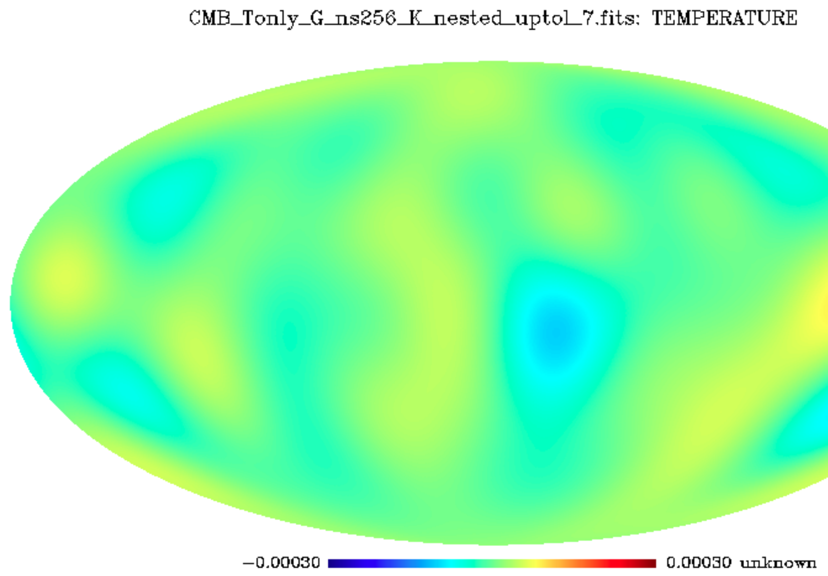

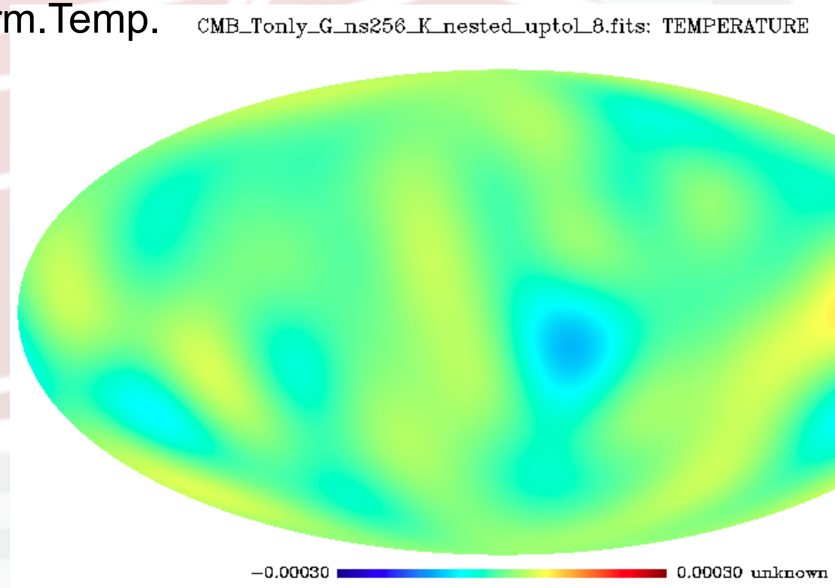

multipole components = 9, 10, 11 & *Planck* CMB map

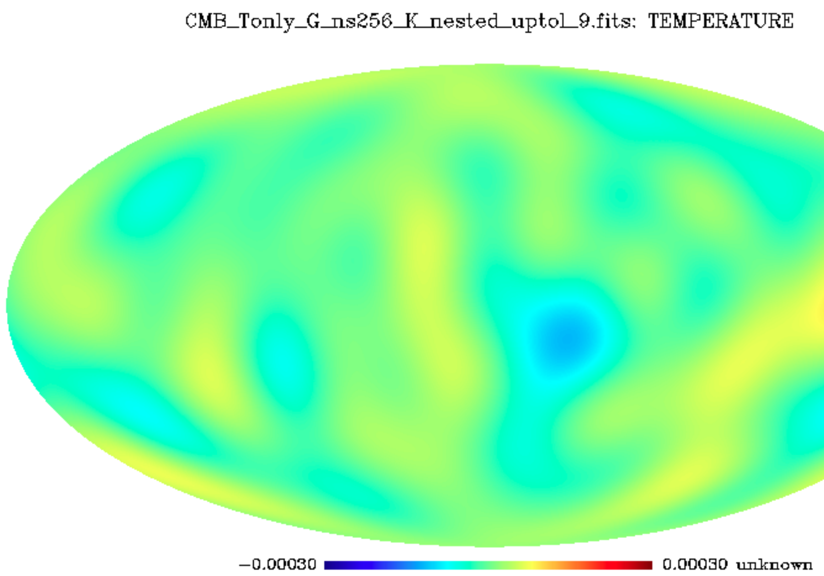

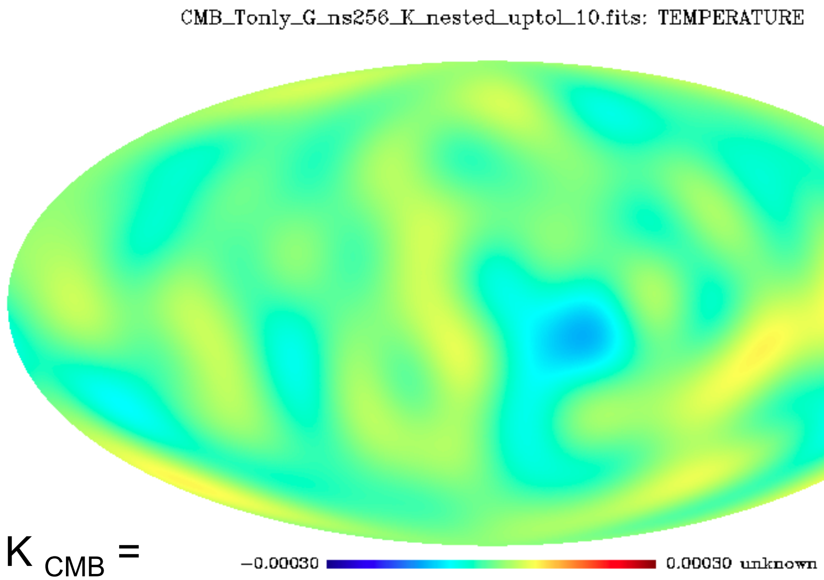

Units: K_{CMB} = Eq. Therm.Temp.

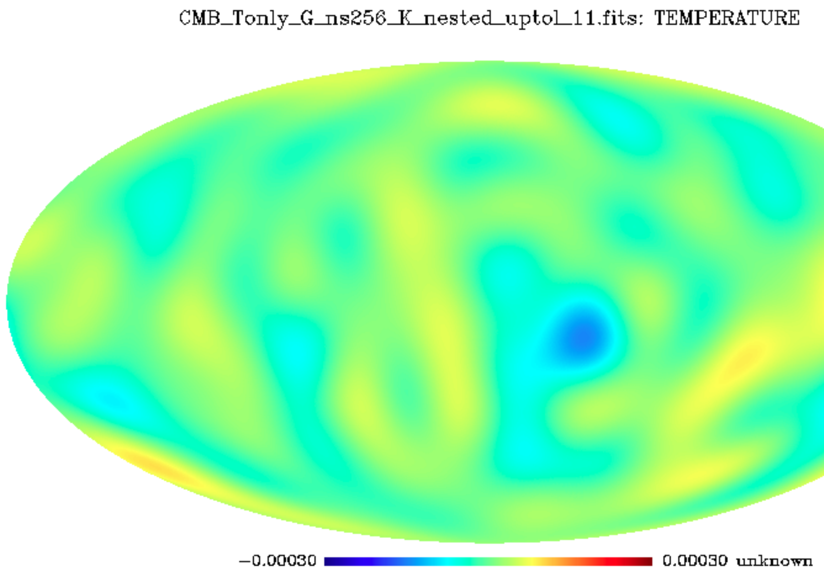

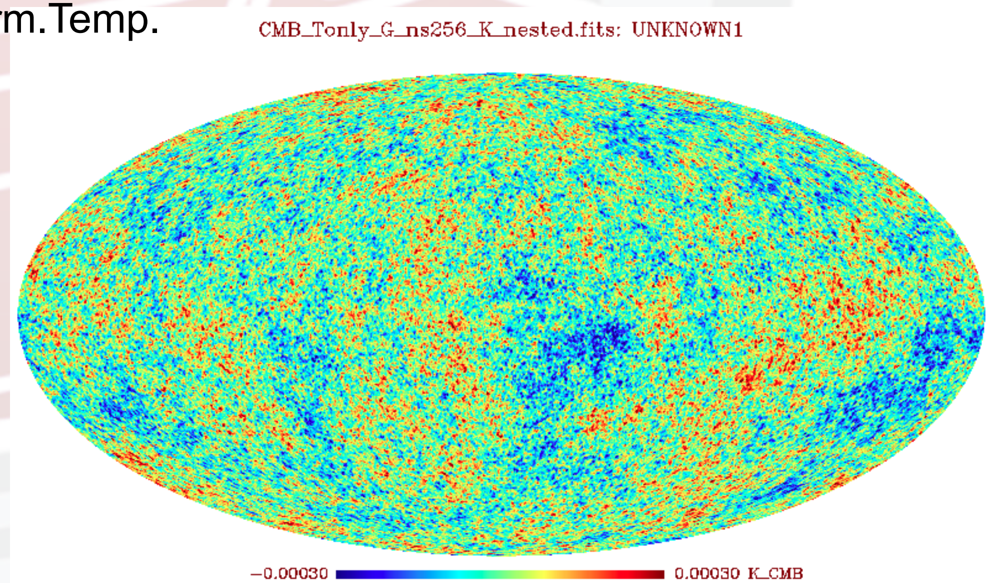

Large scales
Planck results: flat-decoupled-Bianchi model?

There is an elephant
in the room? ☺

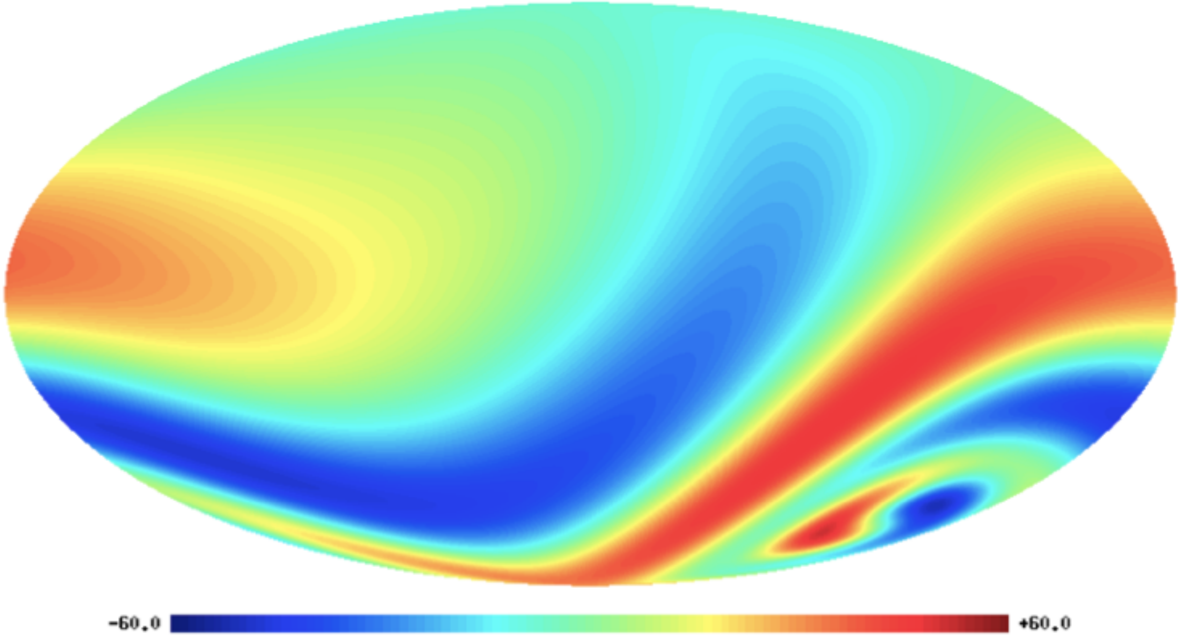

Omogeneous but anisotropic
Generalization of the standard model generated by 3-parameter Lie groups: Bianchi IX (closed) vs Bianchi VIIh (open)

Biaxial symmetric Bianchi IX
→ "squashed 3-sphere" Universe

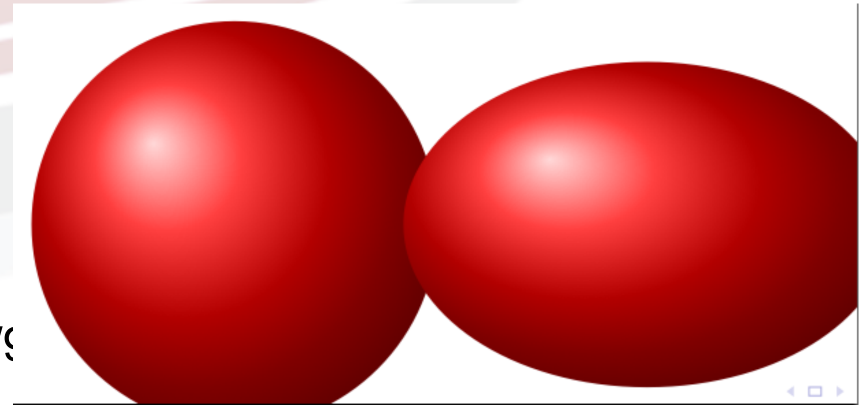

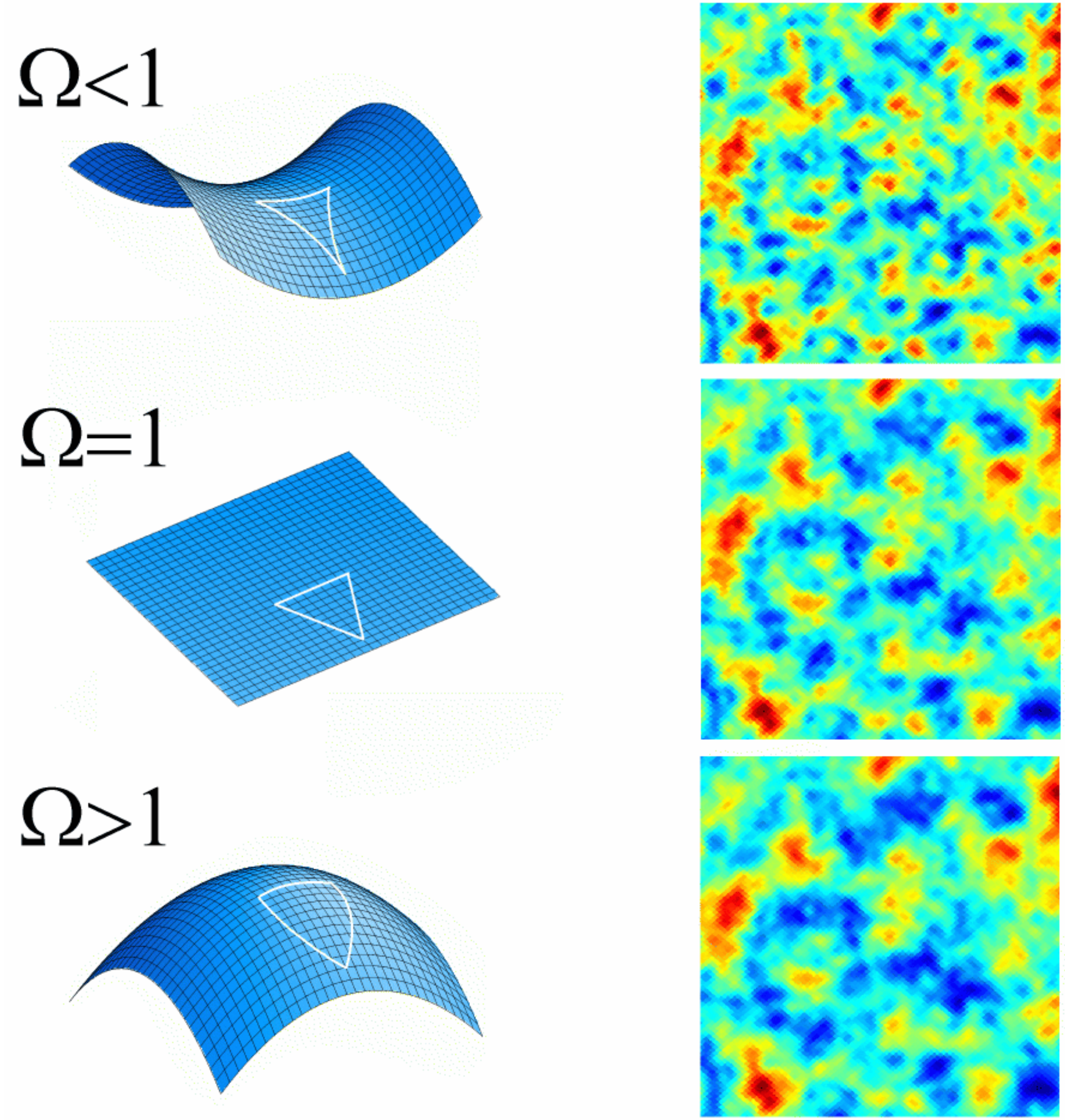

Geometry of the Universe with CMB anisotropy at about 1 deg resolution

CMB ANISOTROPIES ARE ANALYZED IN A STATISTICAL WAY

$$\Delta T(\vec{x}, \hat{n}, \tau) = \Sigma_{l=1}^{\infty} \Sigma_{m=-l}^{l} a_{lm}(\vec{x}, \tau) Y_{lm}(\hat{n})$$

THE ANGULAR POWER SPECTRUM $C_l = \frac{1}{2l+1} \Sigma_m \langle a_{lm}^* a_{lm} \rangle$

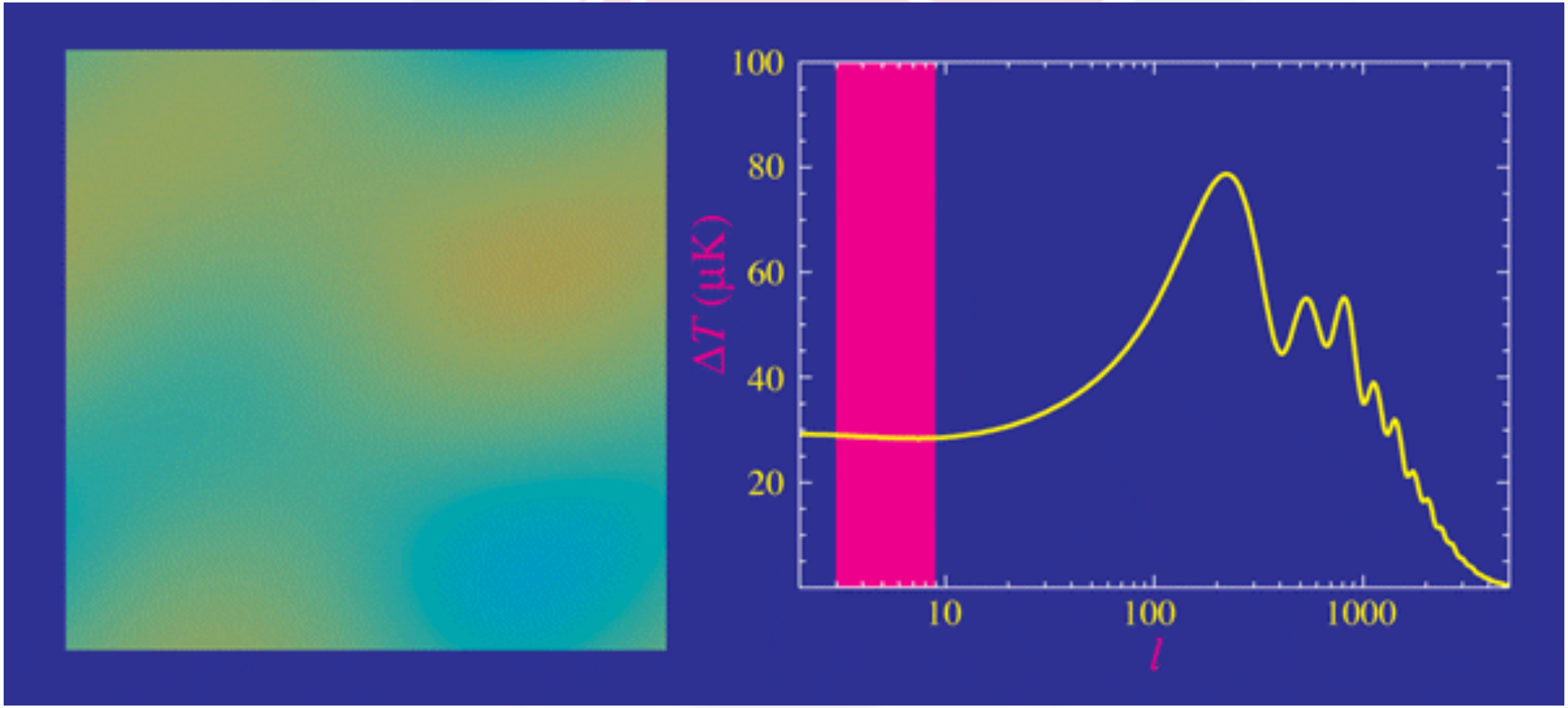

Waine Hu http://background.uchicago.edu/~whu/metaanim.html

SENSITIVITY IN TERMS OF ANGULAR POWER SPECTRUM

The statistics of temperature anisotropy is typically analyzed in spherical harmonics $Y_{\ell m}$: ($\hat{\gamma}$ is the observation unit direction vector)

$$\frac{\delta T}{T}(\hat{\gamma}) = \sum_{\ell=1}^{\infty} \sum_{m=-\ell}^{\ell} a_{\ell m} Y_{\ell m}(\hat{\gamma}) \,, \qquad (1)$$

Isotropy around the observer → $a_{\ell m}$ should have zero mean, $\langle a_{\ell m} \rangle = 0$, and variance C_ℓ $-- \vartheta/\mathrm{deg} = 180/\ell$

Dimensionless temperature fluctuation $\delta T/T$ – (Physical) temperature fluctuation δT

Given the CMB monopole temperature = 2.725 K (Mathe J.C., Fixsen D.J., Shafer R.A., Mosier C., Wilkinson D.T., 1999, ApJ, 512, 511)

the dimensionless C_ℓ will be $\simeq 7.4 \times 10^{12}$ smaller than the C_ℓ expressed in terms of μK^2 (in thermodynamic temperature).

$$C_\ell \equiv \langle | \, a_{\ell m}^2 \, | \rangle = \frac{1}{2\ell+1} \sum_m a_{\ell m}^2 = 2\pi \int d\cos\theta C(\theta) P_\ell(\cos\theta) \qquad (2)$$

$$C(\theta) \equiv \langle \frac{\delta T}{T}(\hat{\gamma}_1) \frac{\delta T}{T}(\hat{\gamma}_2) \rangle = \frac{1}{4\pi} \sum_l (2l+1) \, C_\ell \, P_\ell(\cos\theta) \,; \qquad (3)$$

here $\cos\theta = \hat{\gamma}_1 \cdot \hat{\gamma}_2$ and P_ℓ is the Legendre polynomial.

Since each given anisotropy field is a single realization of a stochastic process, it may be different from the average over the ensemble of all possible realizations of the given (true) model with given parameters. This translates into the fact that the $a_{\ell m}$ coefficients are random variables (possibly following a Gaussian distribution), at a given ℓ, and therefore their variance, C_ℓ, is χ^2 distributed with $2\ell+1$ degrees of freedom. The relative variance δC_ℓ on C_ℓ is equal to $\sqrt{2/(2\ell+1)}$ which is quite relevant at low ℓ because of the relatively small number of available modes.

→ OVERALL UNCERTAINTY: (Knox L., 1995, Phys. Rev. D., 48, 3502)

$$\frac{\delta C_\ell}{C_\ell} = \sqrt{\frac{2}{f_{\rm sky}(2\ell+1)}}\left[1+\frac{A\sigma^2}{NC_\ell W_\ell}\right], \qquad (4)$$

A=size of the surveyed area, σ=rms noise per pixel, N=total number of observed pixel, W_ℓ=beam window function.

For a symmetric Gaussian beam → $W_\ell = \exp(-\ell(\ell+1)\sigma_{\rm B}^2)$ where $\sigma_{\rm B} = {\rm FWHM}/\sqrt{8\ln 2}$.

→ "COSMIC VARIANCE": it defines the ultimate limit on the accuracy at which a given model defined by an appropriate set of parameters can be constrained by the angular power spectrum.

Another similar variance in anisotropy experiments is related to the SKY COVERAGE. This variance depends on the observed sky fraction, $f_{\rm sky}$.

At the largest multipoles achievable with a given experiment the most relevant uncertainties are related to the EXPERIMENT RESOLUTION and SENSITIVITY.

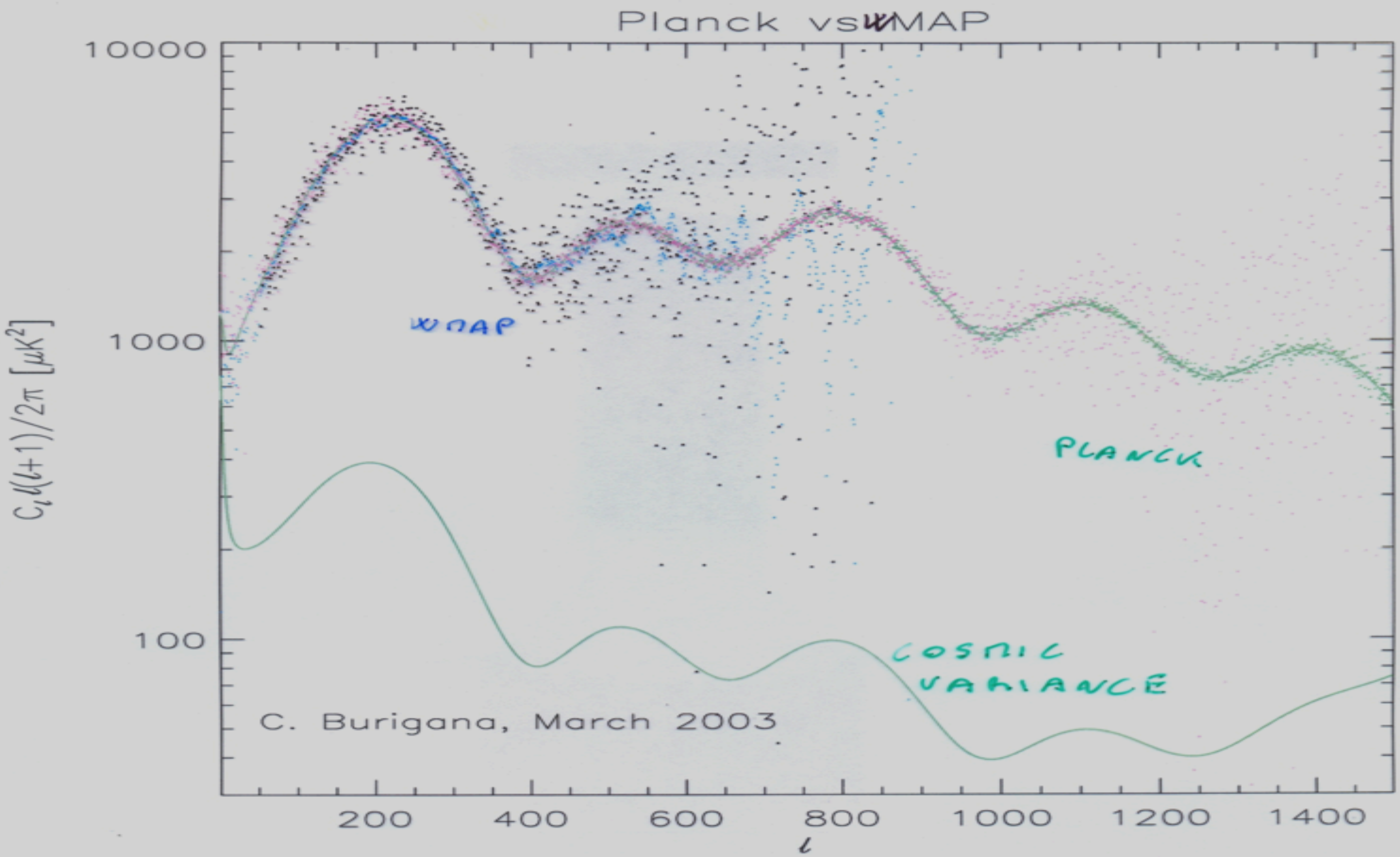
Planck vs WMAP
10000
1000
100
$C_\ell \ell(\ell+1)/2\pi\ [\mu K^2]$
WMAP
PLANCK
COSMIC
VARIANCE
C. Burigana, March 2003
200
400
600
800
1000
1200
1400
ℓ

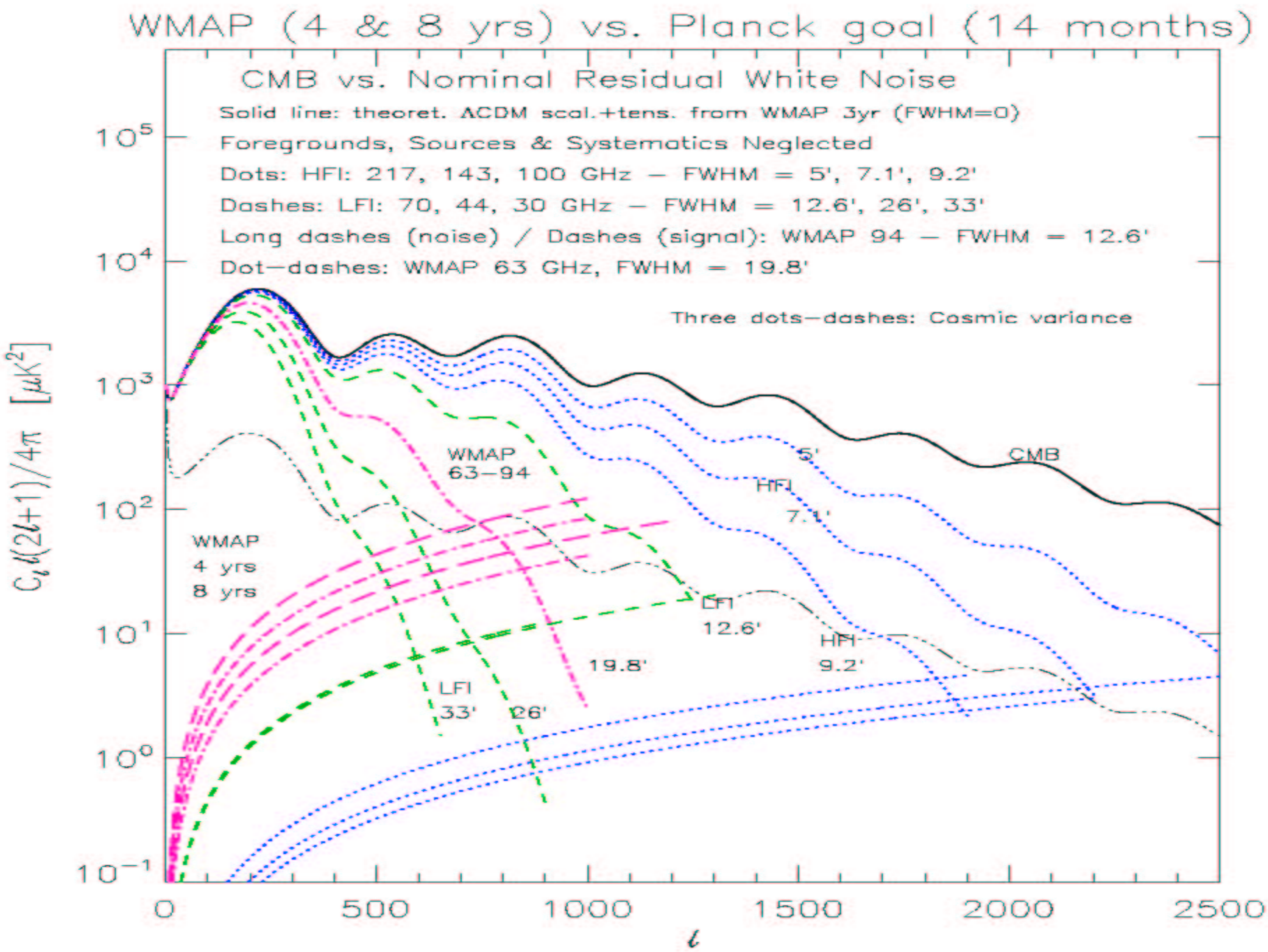
WMAP (4 & 8 yrs) vs. Planck goal (14 months)
CMB vs. Nominal Residual White Noise
Solid line: theoret. ΛCDM scal.+tens. from WMAP 3yr (FWHM=0)
Foregrounds, Sources & Systematics Neglected
Dots: HFI: 217, 143, 100 GHz – FWHM = 5', 7.1', 9.2'
Dashes: LFI: 70, 44, 30 GHz – FWHM = 12.6', 26', 33'
Long dashes (noise) / Dashes (signal): WMAP 94 – FWHM = 12.6'
Dot-dashes: WMAP 63 GHz, FWHM = 19.8'
Three dots-dashes: Cosmic variance
WMAP 63-94
WMAP 4 yrs 8 yrs
CMB
5'
HFI
7.1'
LFI
12.6'
HFI
9.2'
19.8'
LFI
33'
26'
$C_\ell \ell(2\ell+1)/4\pi$ [μK^2]
ℓ
10^5
10^4
10^3
10^2
10^1
10^0
10^{-1}
0
500
1000
1500
2000
2500

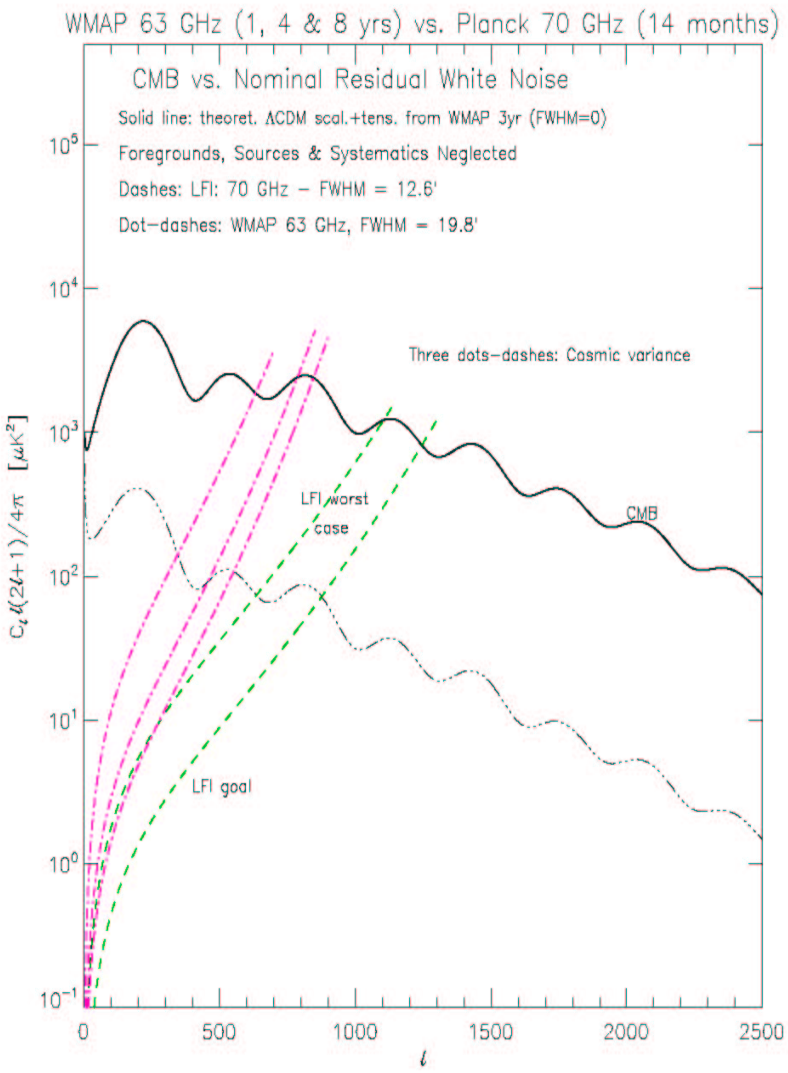

WMAP 63 GHz (1, 4 & 8 yrs) vs. Planck 70 GHz (14 months)
CMB vs. Nominal Residual White Noise
Solid line: theoret. ΛCDM scal.+tens. from WMAP 3yr (FWHM=0)
Foregrounds, Sources & Systematics Neglected
Dashes: LFI: 70 GHz – FWHM = 12.6'
Dot-dashes: WMAP 63 GHz, FWHM = 19.8'
Three dots-dashes: Cosmic variance
LFI worst case
LFI goal
CMB
$C_\ell \ell(2\ell+1)/4\pi$ [μK^2]
ℓ

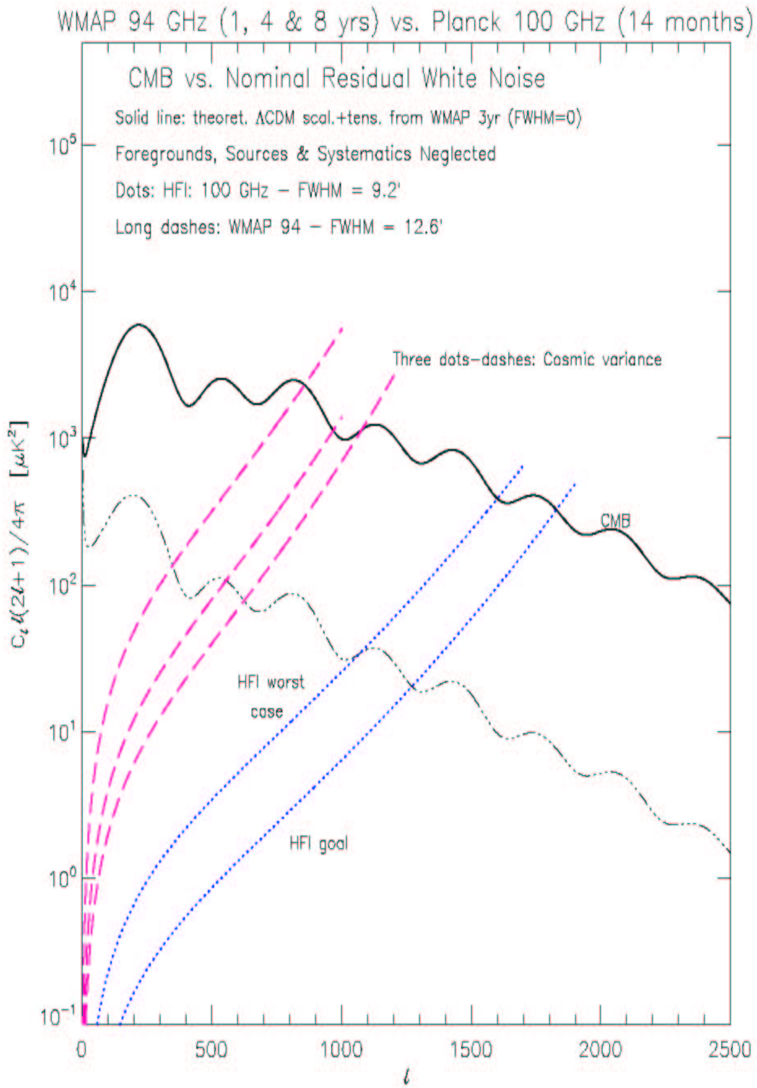

WMAP 94 GHz (1, 4 & 8 yrs) vs. Planck 100 GHz (14 months)
CMB vs. Nominal Residual White Noise
Solid line: theoret. ΛCDM scal.+tens. from WMAP 3yr (FWHM=0)
Foregrounds, Sources & Systematics Neglected
Dots: HFI: 100 GHz – FWHM = 9.2'
Long dashes: WMAP 94 – FWHM = 12.6'
Three dots-dashes: Cosmic variance
HFI worst case
HFI goal
CMB
$C_\ell \ell(2\ell+1)/4\pi$ [μK^2]
ℓ

APS DEPENDENCE ON COSMOLOGICAL PARAMETERS

Planck: a single experiment spanning a wide multipole range!

Theta → first peak position

Baryon Density → height difference between even and odd peaks

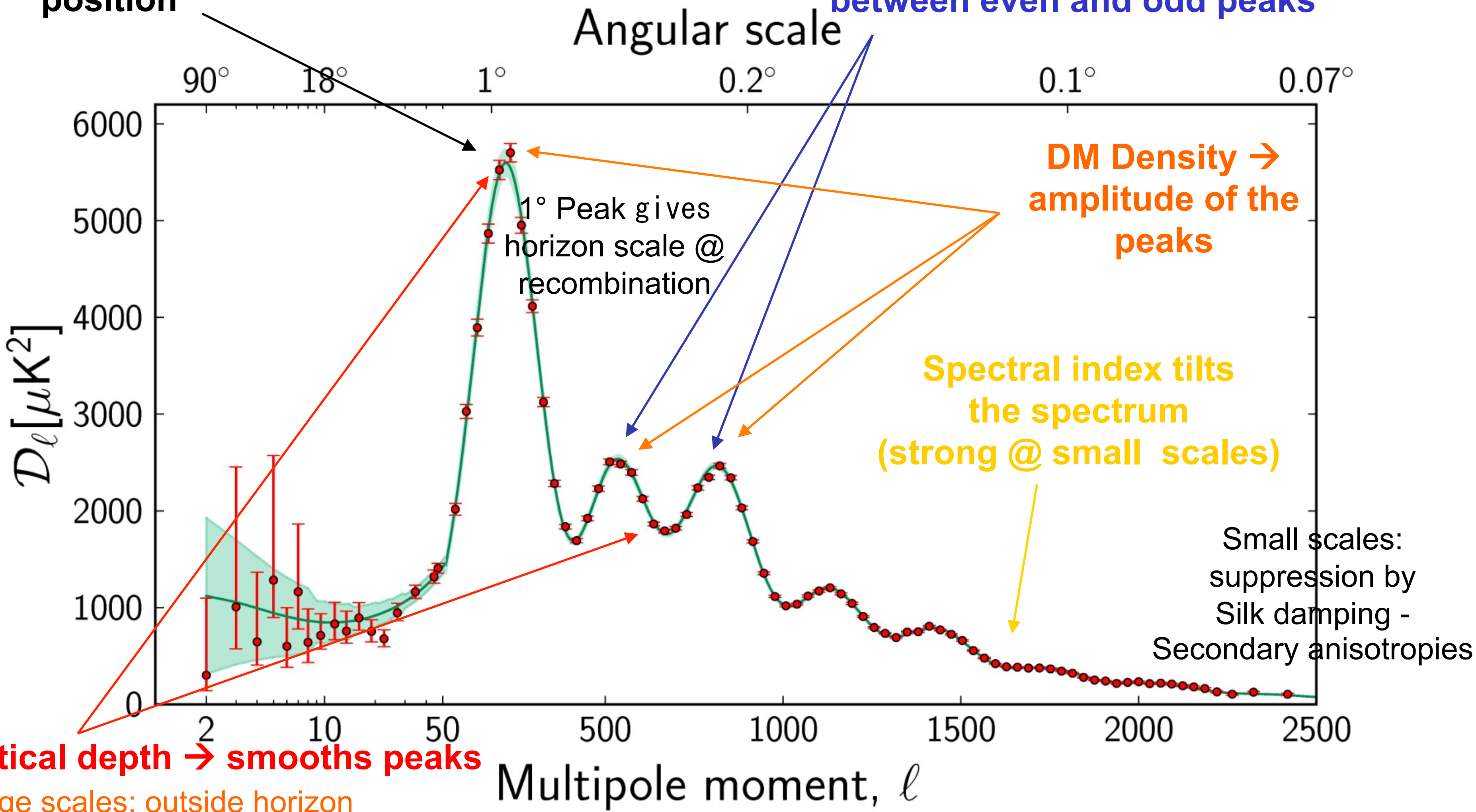

Optical depth → smooths peaks

Large scales: outside horizon @ recombination – only gravity

Intermediate scales: photon-baryon fluid acoustic oscillations - DM potential well vs radiation pressure

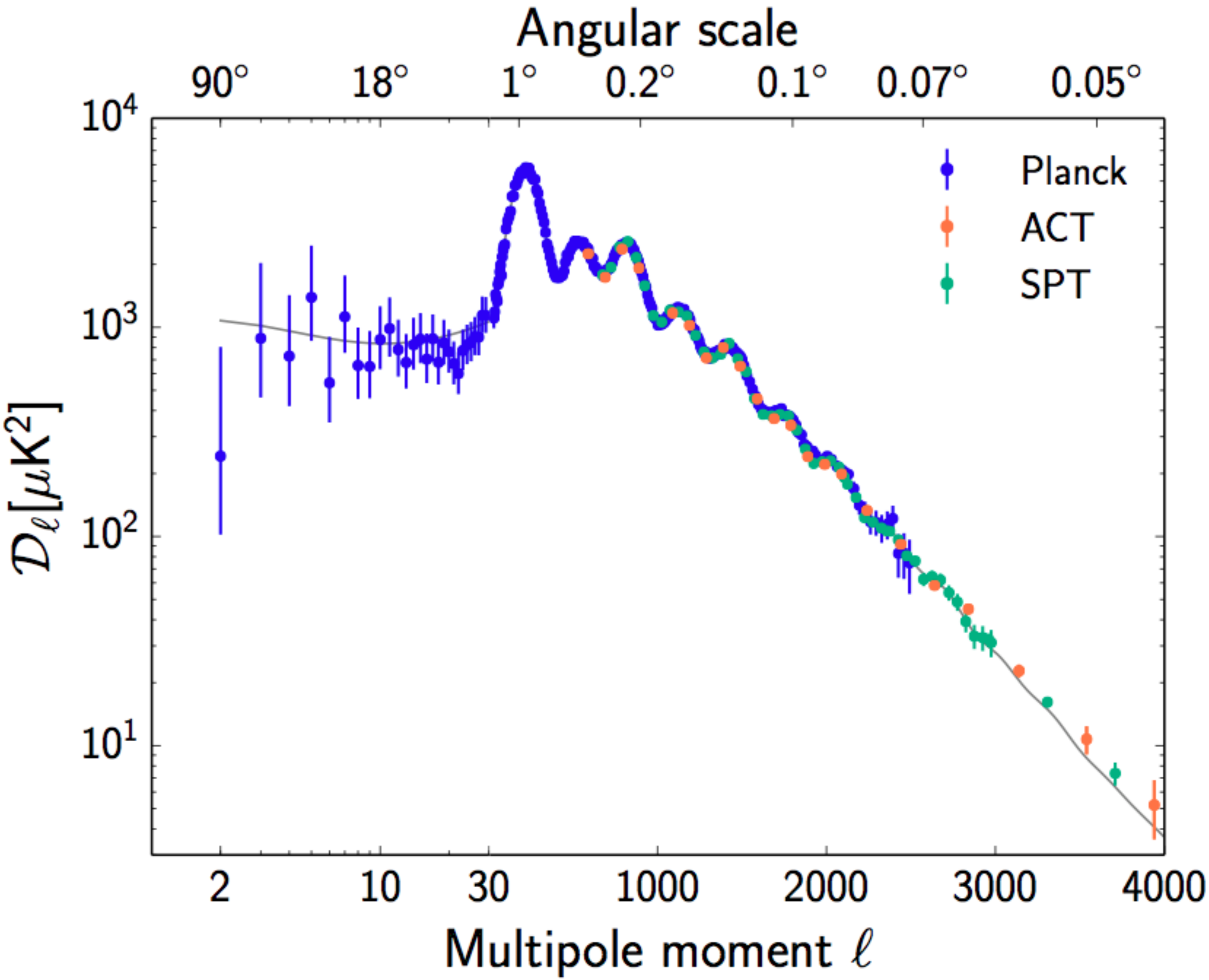

Angular scale
90°
18°
1°
0.2°
0.1°
0.07°
0.05°
10^4
10^3
10^2
10^1
$\mathcal{D}_\ell[\mu K^2]$
Planck
ACT
SPT
2
10
30
1000
2000
3000
4000
Multipole moment ℓ

$C_\ell \longleftrightarrow \delta T_\ell(\nu) = [\ell(\ell+1) C_\ell(\nu)/2\pi]^{1/2}$

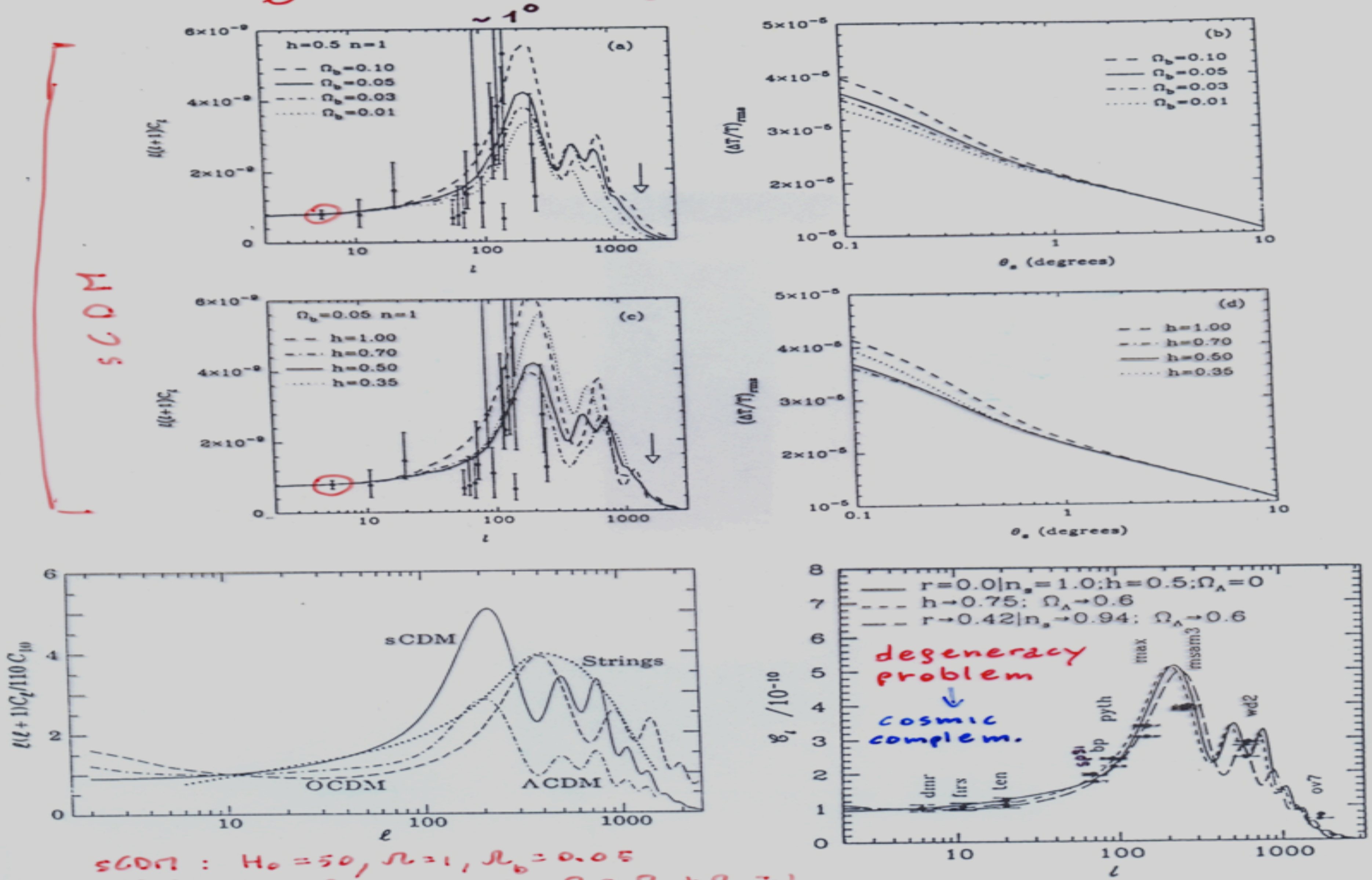

sCDM : $H_0 = 50$, $\Omega = 1$, $\Omega_b = 0.05$

ΛCDM : $H_0 = 80$, $\Omega_\Lambda = 0.3$, $\Omega = \Omega_\Lambda + \Omega_b = 1$

OCDM : $H_0 = 75$, $\Omega = 0.3$

Smoot e Scott '96

Bond '95

In spite of such richness of information in TT APS ...

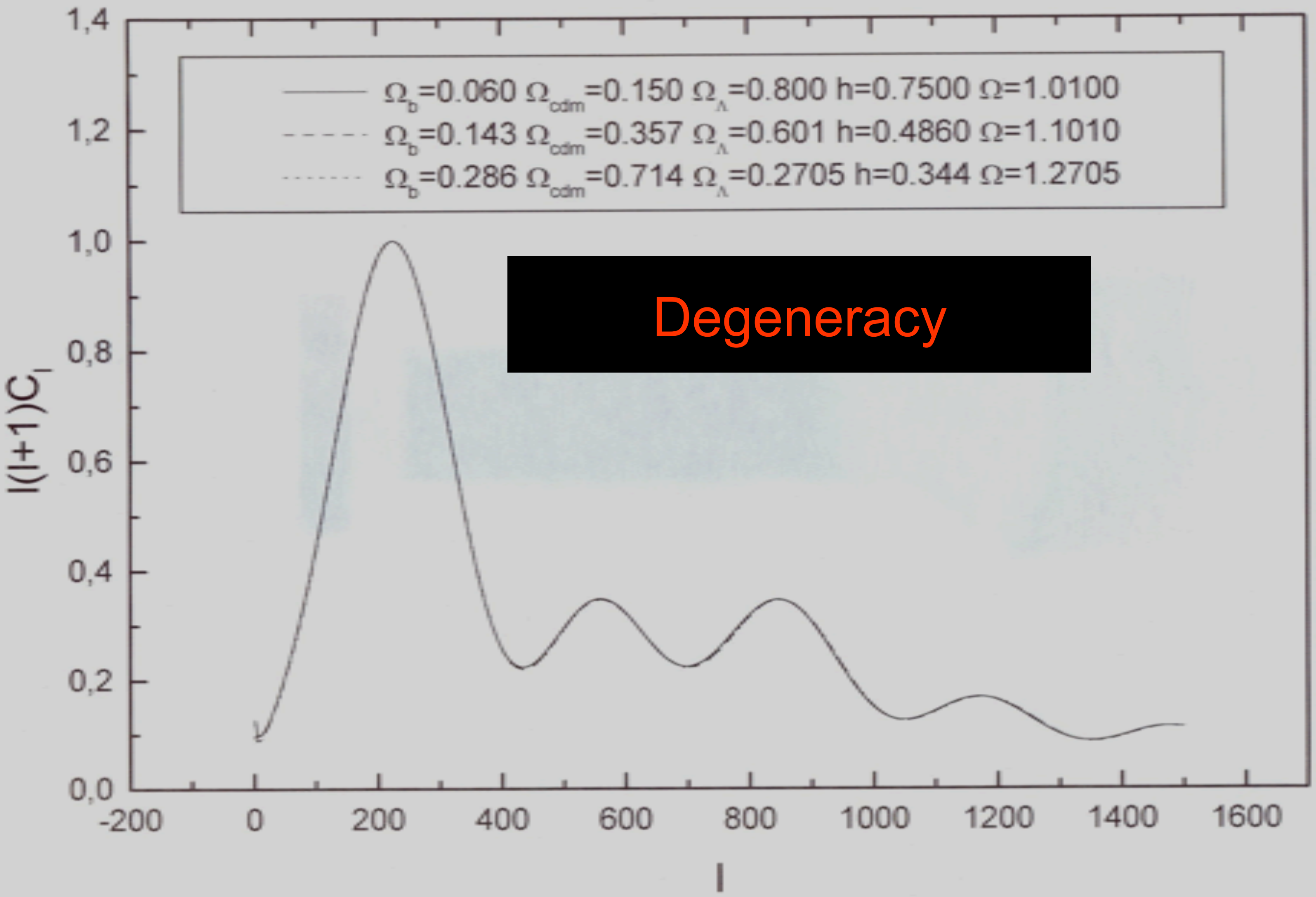

Polarization Anisotropies of the Cosmic Microwave Background

C. Burigana – Ferrara 7/9/2015

POLARIZATION

STOKES PARAMETERS $\quad I,\ \underbrace{Q,\ U}_{\text{lin. pol.}},\ V$

V: circular pol. $\longrightarrow 0$

$$T(\vec{\gamma}) = I(\vec{\gamma}) + Q(\vec{\gamma})\cos 2\alpha + U(\vec{\gamma})\sin 2\alpha$$

Q, U analyzed in spin spher. harmonics ${}_2Y_{\ell m}$

$\approx$ nonsimple transformation under rotation

$\Downarrow$

E & B modes $\qquad$ FLAT FIELD APPROX.

$$E(\vec{\ell}) = \int d^2\vec{\theta}\,[Q(\vec{\theta})\cos(2\phi_\ell) + U(\vec{\theta})\sin(2\phi_\ell)]\,e^{-i\vec{\ell}\cdot\vec{\theta}}$$

$$B(\vec{\ell}) = \int \quad '' \quad [U(\vec{\theta}) \quad '' \quad - Q(\vec{\theta}) \quad '' \quad] \quad ''$$

components of two scalar fields in Fourier space

$$E(\vec{\theta}) = (2\pi)^{-2}\int d^2\vec{\ell}\, e^{i\vec{\ell}\cdot\vec{\theta}}\, E(\vec{\ell})$$

$$B(\vec{\theta}) = \quad '' \quad \int \quad '' \quad B(\vec{\ell})$$

$\leftarrow$ in real space

POLARIZATION , E, B MODES

4π DEF.

$\boxed{\ell, m}$

$$T(\hat{n}) = \sum_{\ell m} a_{\ell m} \, Y_{\ell m}(\hat{n})$$

$$Q(\hat{n}) \pm i U(\hat{n}) = \sum_{\ell m} a_{\mp 2, \ell m} \, {}_{\mp 2}Y_{\ell m}(\hat{n})$$

spin spherical harmonics

$$a_{\pm 2, \ell m} = E_{\ell m} \pm i B_{\ell m}$$

$$_N Y = (-1)^N \, {}_{-N}Y^*_{\ell, -m}$$

$$\int d\hat{n} \, {}_N Y_{\ell m}(\hat{n}) \, {}_N Y^*_{\ell' m'}(\hat{n}) = \delta_\ell^{\ell'} \delta_m^{m'}$$

$$\Longrightarrow \begin{matrix} E_{\ell m} \\ B_{\ell m} \end{matrix} \quad \left(\int \quad Q, \quad U \right)$$

$$E_{\ell m} = \frac{1}{2} \int d\hat{n} \left\{ Q(\hat{n}) \overbrace{\left[{}_2Y^*_{\ell m}(\hat{n}) + {}_{-2}Y^*_{\ell m}(\hat{n}) \right]}^{A} \right\}$$

$$- i \left\{ U(\hat{n}) \underbrace{\left[{}_2Y^*_{\ell m}(\hat{n}) - {}_{-2}Y^*_{\ell m}(\hat{n}) \right]}_{B} \right\}$$

$$B_{\ell m} = -\frac{1}{2} \int d\hat{n} \left\{ U(\hat{n}) \left[\quad A \quad \right] \right\}$$

$$+ i \left\{ Q(\hat{n}) \left[\quad B \quad \right] \right\}$$

$$C_\ell^{XY} = \langle a^X_{\ell m} \, a^{Y*}_{\ell m} \rangle$$

C_ℓ^{TT}, C_ℓ^{EE}, C_ℓ^{BB} ≥ 0

C_ℓ^{TE}, C_ℓ^{TB} $\gtreqless 0$

C_ℓ^{EB}.

B-mode / BPOL

1° slow-roll par.

$$\varepsilon_1 = -\frac{\dot{H}}{H^2}$$

$$R \sim \frac{C_\ell^T}{C_\ell^S} \sim \frac{T}{S} \sim 16\,\varepsilon_1 \quad , \quad @ \text{ inflation}$$

!!

epoch / energy scale of inflation

single field inflation

E and B Mode Polarization

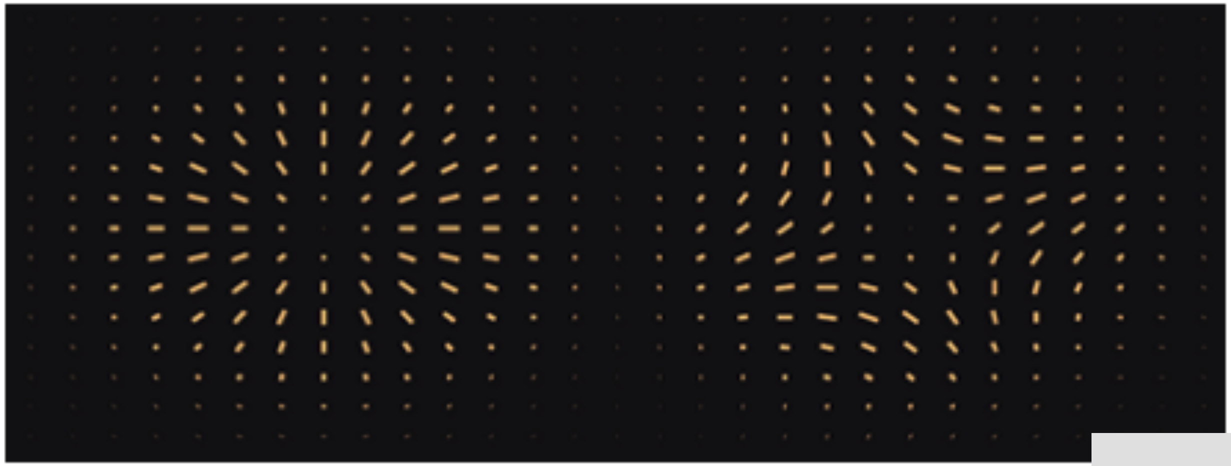

E mode

B mode

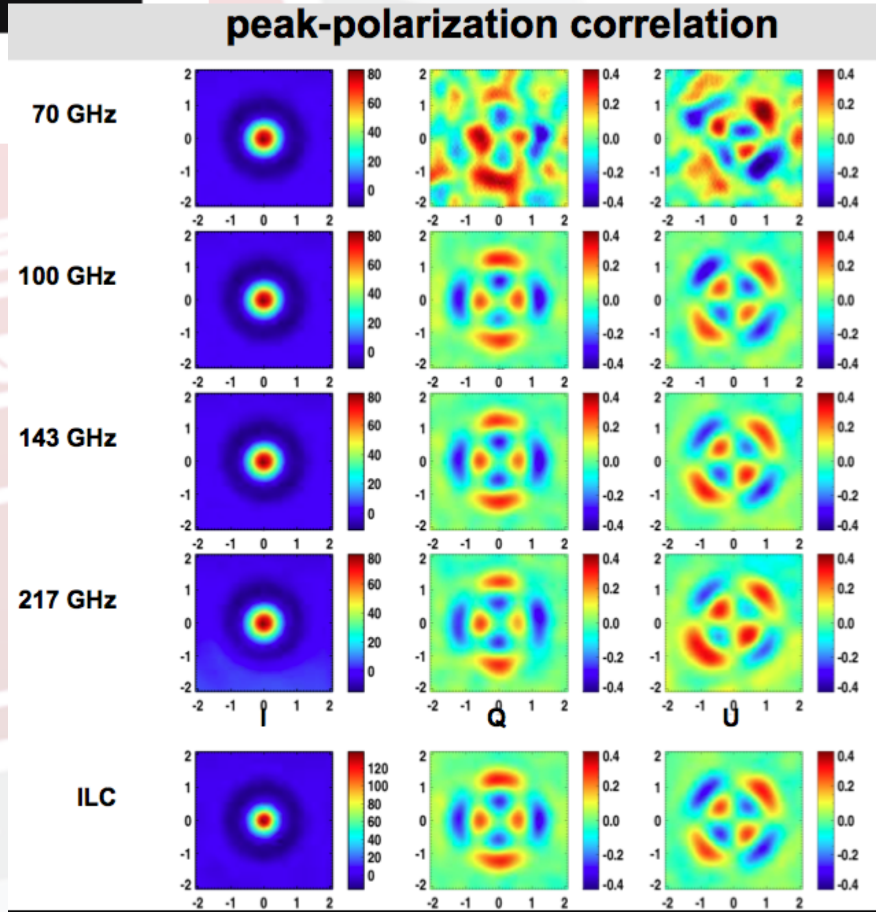

Polarization with *Planck*:

CMB map in Q,U (2015)

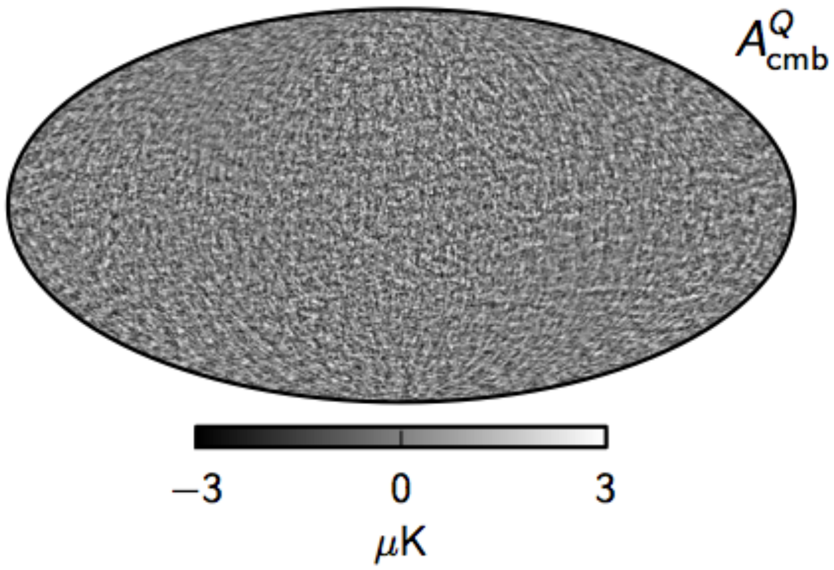

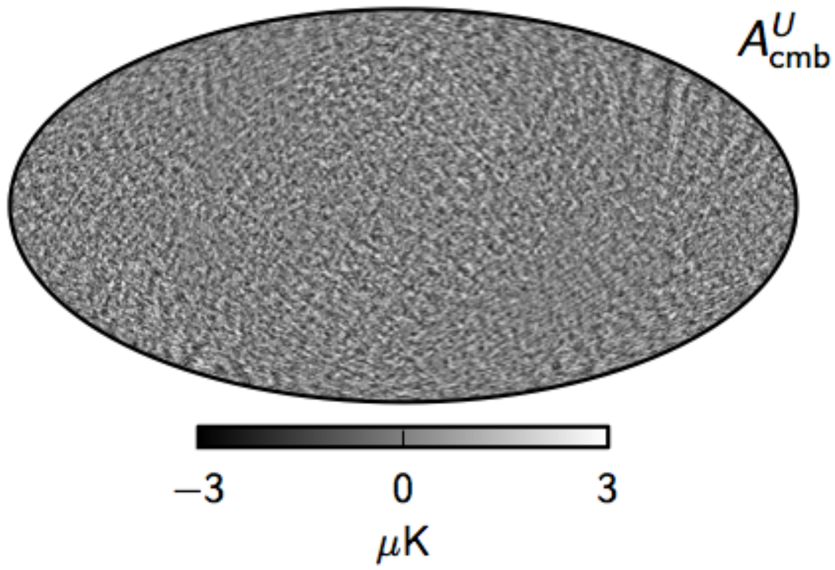

Maximum posterior amplitude Stokes Q (left) and U (right) maps derived from Planck observations between 30 and 353 GHz.
These maps have been high pass-filtered with a cosine-apodized filter between l= 20 and 40, and a 17% region of the Galactic plane has been replaced with a constrained Gaussian realization.

Planck 2015 Polarization map

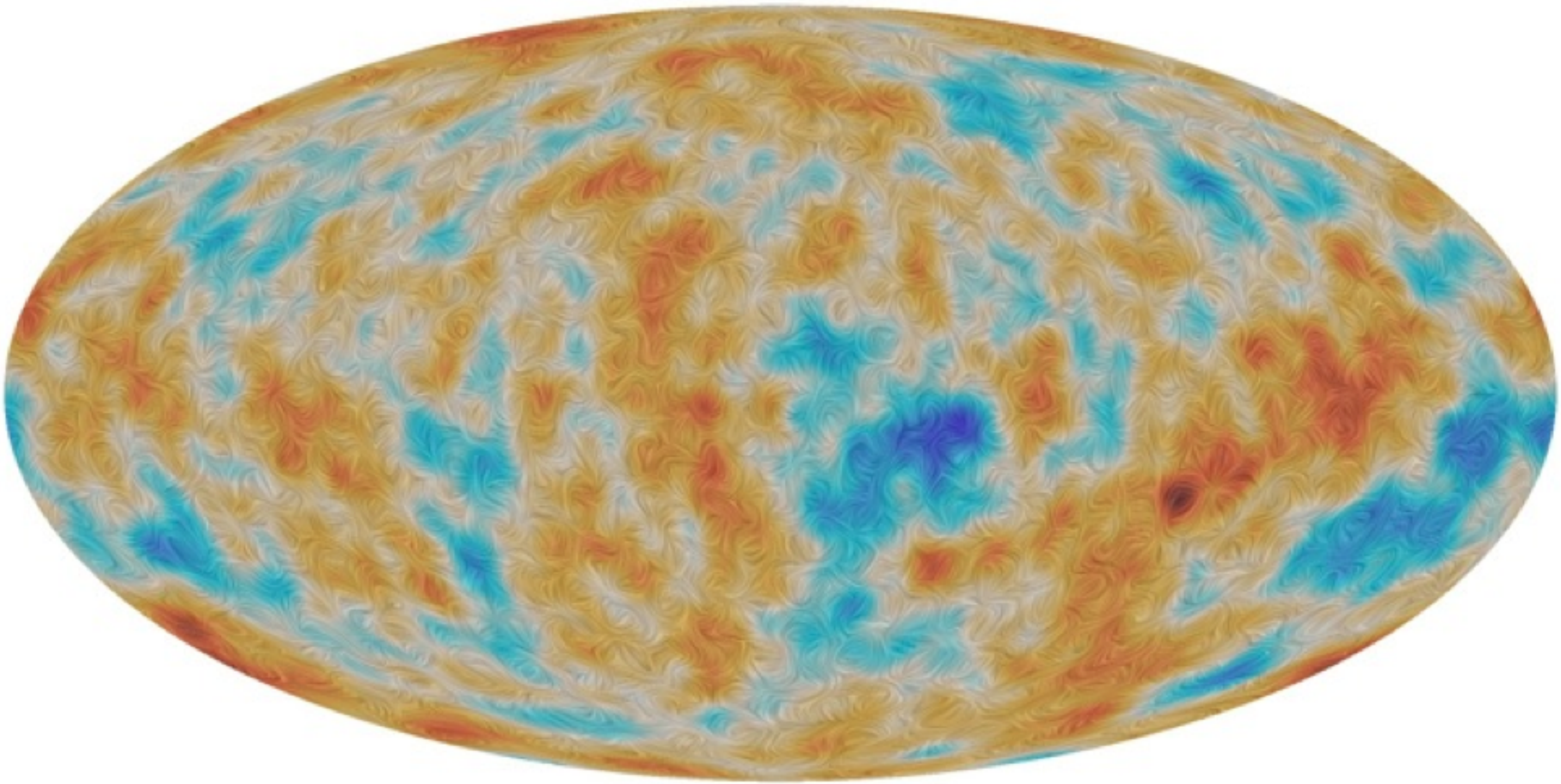

Planck 2015 APS

From Planck 2015 results. XX.

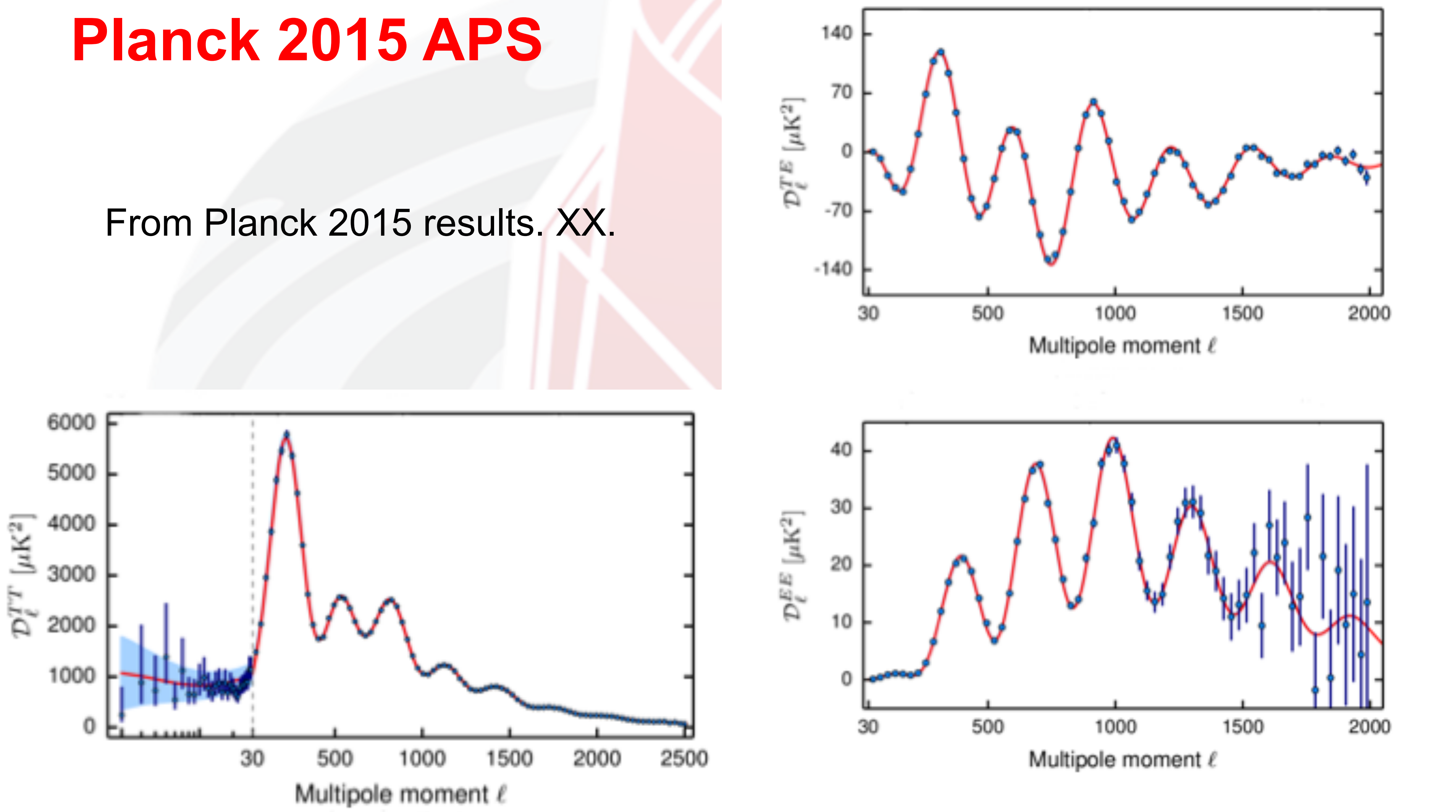

Fig. 2. *Planck TT* (top), high-ℓ TE (centre), and high-ℓ EE (bottom) angular power spectra. Here $\mathcal{D}_\ell \equiv \ell(\ell+1)C_\ell/(2\pi)$.

Systematic effects: LFI @ 70 GHz

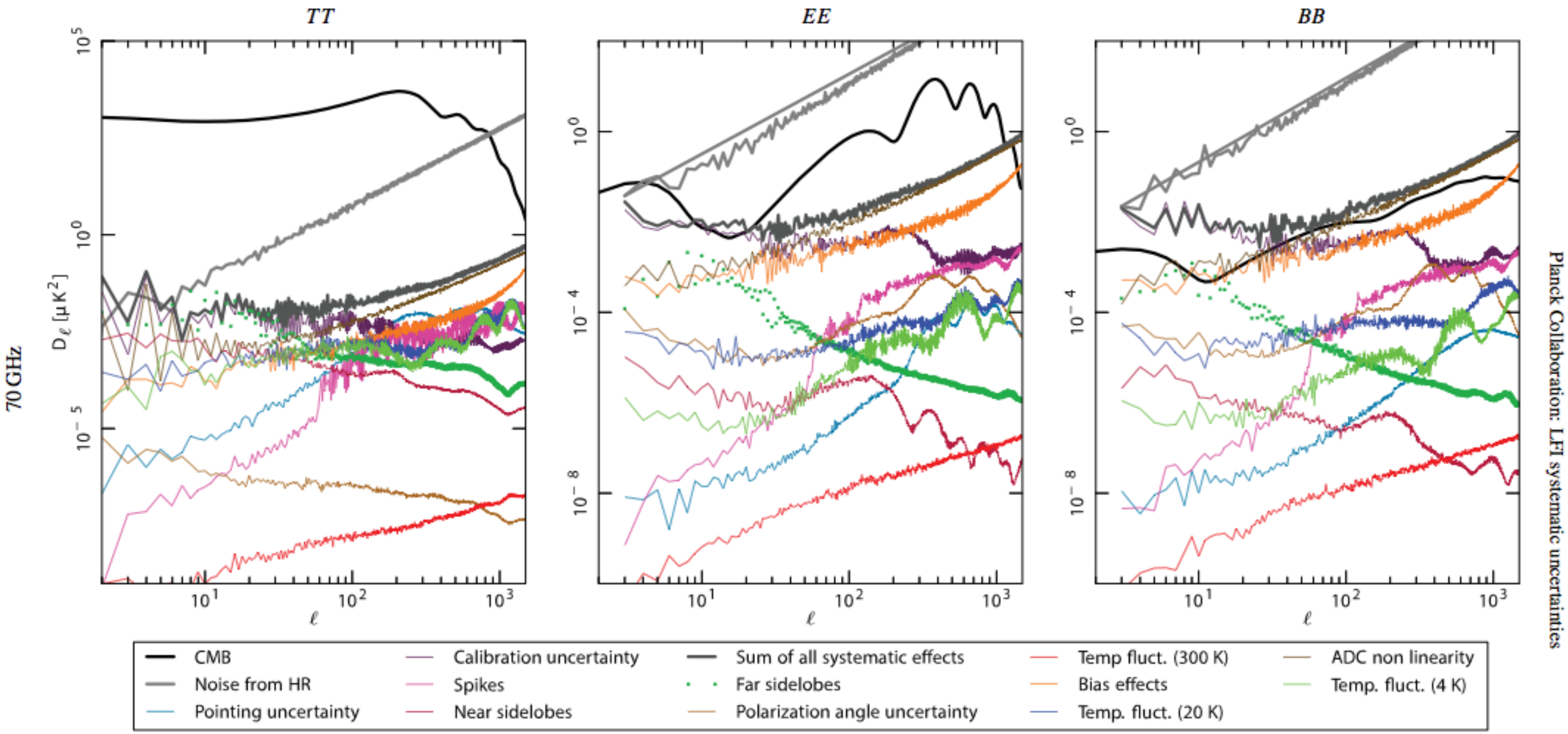

Fig. 3: Angular power spectra of the various systematic effects at 70 GHz, compared to the CMB temperature and polarization spectra and to the instrumental noise from half-ring (HR) difference maps. The CMB *TT* and *EE* spectra are best fits to the *Planck* cosmological parameters (see figures 9 and 10 in Planck Collaboration I 2015) filtered by the LFI window functions. The example CMB *B*-mode spectrum is based on *Planck*-derived cosmological parameters and assumes a tensor-to-scalar ratio $r = 0.1$, a tensor spectral index $n_T = 0$, and no beam-filtering. The thick dark-grey line represents the total contribution. The dotted dark-green line is the contribution from far the sidelobes that has been removed from the data and is therefore not considered in the total.

PLANCK COSMOLOGICAL PARAMETERS

The CMB anisotropy angular power spectrum shape and amplitude is strongly dependent on the underlying cosmological model.

Cosmological models are characterized by cosmological parameters

STANDARD VANILLA MODEL PARAMETERS

- Baryon Density today $\omega_b \equiv \Omega_b h^2$
- Dark Matter Density today $\omega_c \equiv \Omega_c h^2$
- Horizon @REC Angular Diameter Distance $100\theta_{MC}$
- Optical depth for reionization τ
- Cosmological perturbation tilt $P(k) = A_s k^n$ n_s
- Cosmological perturbation amplitude $\ln(10^{10} A_s)$

Some more information on parameter definition - I

- Evolution of cosmic scale factor $a=1/(1+z)$

  $H^2 = [(da/dt)/a]^2 = [da / (a^2 d\eta)]^2$

  $= (8\pi G/3) [\rho_M/a^3 + \rho_R/a^4 + \rho_v(a) + \rho_\Lambda + \rho_K/a^2]$

  where $d\eta=dt/a$, t =time, η=conformal time
- Ratio of energy densities relative to the total

  $\Omega_i=3\rho_i/(8\pi G H_0^2)$; $H_0 = H(@\ t=\text{today})$ = Hubble constant,
  $h=H_0/[100\text{Km/s/Mpc}]$ $1/H_0$ related to the age of the Universe

  for example: $t_0= (2/3)/H_0$ for a simple Einstein-de Sitter model

  $\rho_\Lambda= 3\Lambda/(8\pi G)$; $\rho_K= 3K/(8\pi G)$ (K=0,+1,-1) $\tau = \int \chi_e n_e \sigma_T c dt$
- Thomson optical depth due to reionization
  (integral from the raising of ionization fraction after “quiescent phase” following recombination up to current epoch)
- Redshift of last-scattering, $z_\star$, such that optical depth to Thomson scattering from $z = 0$ to $z = z_\star$ is unity, assuming no reionization

Some more information on parameter definition - II

- Angular scale of the sound horizon at last-scattering $\theta_* = r_s(z_*)/D_A(z_*)$
  where $r_s(z) = \int_0^{\eta(z)} \frac{d\eta'}{\sqrt{3(1+R)}}$, with $R \equiv 3\rho_b/(4\rho_\gamma)$
- Typically $100\times\theta_\star$ is given
- Baryon velocities decouple from the photon dipole when Compton drag balances the gravitational force, which happens at $\tau_d \sim 1$, where

$$\tau_d(\eta) \equiv \int_{\eta_0}^{\eta} \dot{\tau}\, d\eta'/R$$

- Drag redshift z_{drag} such that $\tau_d(\eta(z_{drag})) = 1$
- Sound horizon at the drag epoch $r_{drag} = r_s(z_{drag})$
- Characteristic wavenumber for damping, k_D

$$k_D^{-2}(\eta) = -\frac{1}{6}\int_0^{\eta} d\eta' \, \frac{1}{\dot{\tau}} \frac{R^2 + 16(1+R)/15}{(1+R)^2}$$

- Angular damping scale $\theta_D = \pi/(k_D D_A)$, D_A = comoving angular diameter distance to $z_\star$

PLANCK COSMOLOGICAL PARAMETERS: ΛCDM model

2015 Release

Table 3. Parameters of the base ΛCDM cosmology computed from the 2015 baseline *Planck* likelihoods illustrating the consistency of parameters determined from the temperature and polarization spectra at high multipoles. Column [1] uses the *TT* spectra at low and high multipoles and is the same as column [6] of Table 1. Columns [2] and [3] use only the *TE* and *EE* spectra at high multipoles, and only polarization at low multipoles. Column [4] uses the full likelihood. The last column lists the deviations of the cosmological parameters determined from the TT+lowP and TT,TE,EE+lowP likelihoods.

Parameter	[1] *Planck* TT+lowP	[2] *Planck* TE+lowP	[3] *Planck* EE+lowP	[4] *Planck* TT,TE,EE+lowP	$([1]-[4])/\sigma_{[1]}$
$\Omega_b h^2$	0.02222 ± 0.00023	0.02228 ± 0.00025	0.0240 ± 0.0013	0.02225 ± 0.00016	-0.1
$\Omega_c h^2$	0.1197 ± 0.0022	0.1187 ± 0.0021	$0.1150^{+0.0048}_{-0.0055}$	0.1198 ± 0.0015	0.0
$100\theta_{MC}$	1.04085 ± 0.00047	1.04094 ± 0.00051	1.03988 ± 0.00094	1.04077 ± 0.00032	0.2
τ	0.078 ± 0.019	0.053 ± 0.019	$0.059^{+0.022}_{-0.019}$	0.079 ± 0.017	-0.1
$\ln(10^{10}A_s)$	3.089 ± 0.036	3.031 ± 0.041	$3.066^{+0.046}_{-0.041}$	3.094 ± 0.034	-0.1
n_s	0.9655 ± 0.0062	0.965 ± 0.012	0.973 ± 0.016	0.9645 ± 0.0049	0.2
H_0	67.31 ± 0.96	67.73 ± 0.92	70.2 ± 3.0	67.27 ± 0.66	0.0
Ω_m	0.315 ± 0.013	0.300 ± 0.012	$0.286^{+0.027}_{-0.038}$	0.3156 ± 0.0091	0.0
σ_8	0.829 ± 0.014	0.802 ± 0.018	0.796 ± 0.024	0.831 ± 0.013	0.0
$10^9 A_s e^{-2\tau}$	1.880 ± 0.014	1.865 ± 0.019	1.907 ± 0.027	1.882 ± 0.012	-0.1

Main difference in τ since now polarization comes from *Planck*

Planck final performance in temperature & polarization

Average sensitivity, δT/T, per FWHM^2 resolution element (FWHM in arcmin) and white noise (per frequency channel for LFI and per detector for HFI) in 1 sec of integration (NET, in μK ·√s) in CMB temperature units. Acronyms: DT = detector technology, N of R (or B) = number of radiometers (or bolometers), EB = effective bandwidth (in GHz). At 100 GHz all bolometers are polarized, thus the temperature measure is derived combining data from polarized bolometers.

HFI	$\simeq$ 29.5 months	of integration	($\simeq$ 5 surveys)	
Frequency (GHz)	100	143	217	353
FWHM in T (P)	9.6 (9.6)	7.1 (6.9)	4.6 (4.6)	4.7 (4.6)
N of B in T (P)	(8)	4 (8)	4 (8)	4 (8)
EB in T (P)	33 (33)	43 (46)	72 (63)	99 (102)
NET in T (P)	100 (100)	62 (82)	91 (132)	277 (404)
δT/T [μK/K] in T (P)	2.04 (3.31)	1.56 (2.83)	3.31 (6.24)	13.7 (26.2)

HFI		
Frequency (GHz)	545	857
FWHM in T	4.7	4.3
N of B in T	4	4
EB in T	169	257
NET in T	2000	91000
δT/T [μK/K] in T	103	4134

LFI	$\simeq$ 29.5 + 21 months	of integration	($\simeq$ 8 surveys)
Frequency (GHz)	30	44	70
InP DT	MIC	MIC	MMIC
FWHM	33.34	26.81	13.03
N of R (or feeds)	4 (2)	6 (3)	12 (6)
EB	6	8.8	14
NET	159	197	158
δT/T [μK/K] (in T)	1.85	2.85	4.69
δT/T [μK/K] (in P)	2.61	4.02	6.64

CMB polarization with *Planck*
E & B – 30% binning, f_{sky}=74%

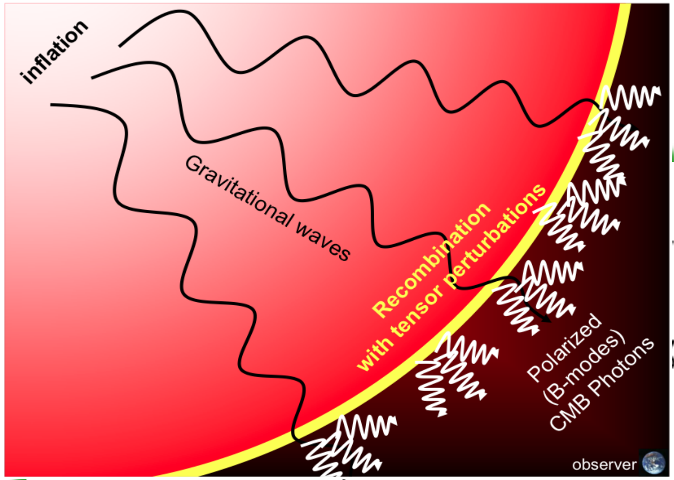

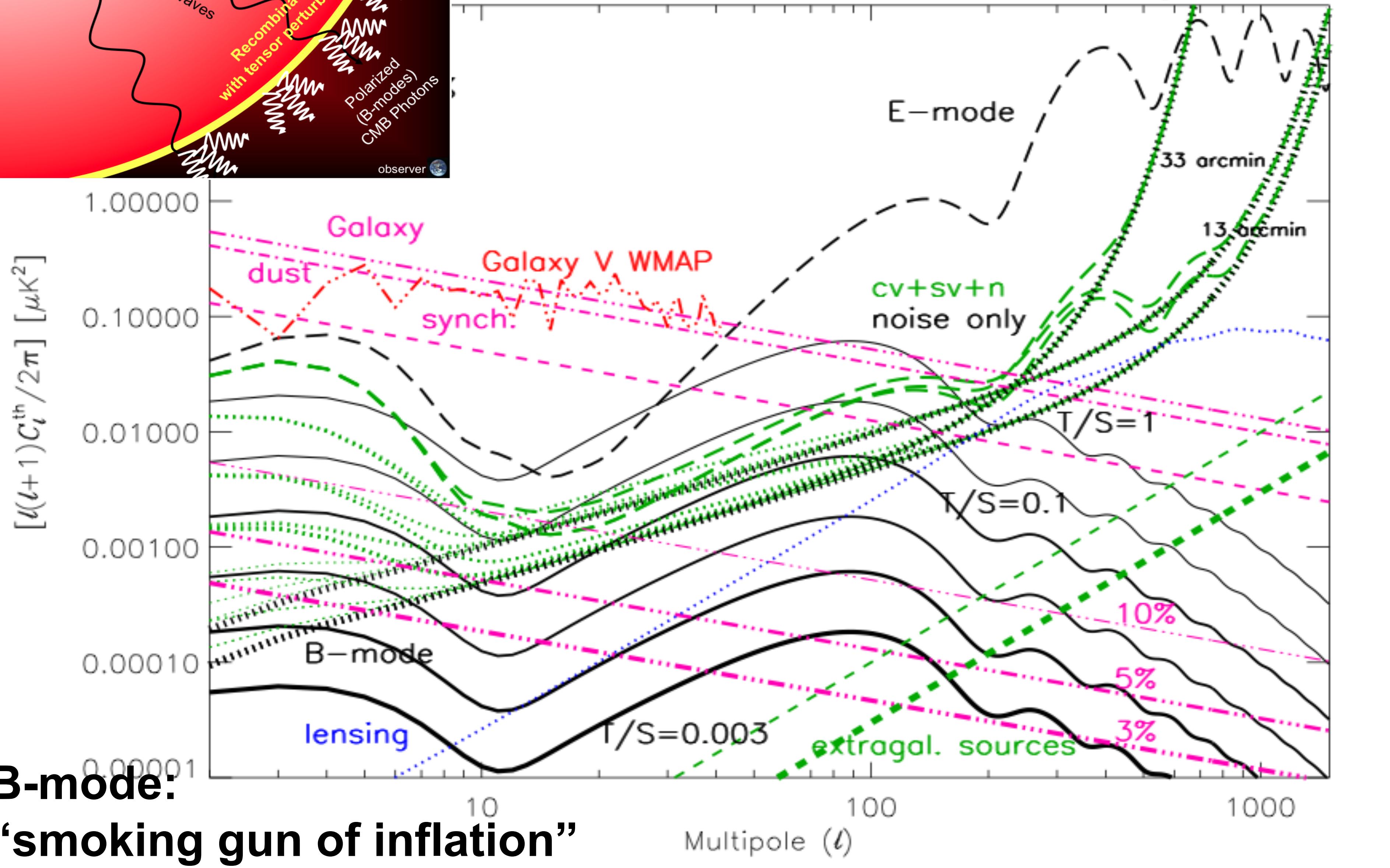

B-mode:
"smoking gun of inflation"
energy scale

B2+Keck 150 GHz T/Q/U maps of small sky patch

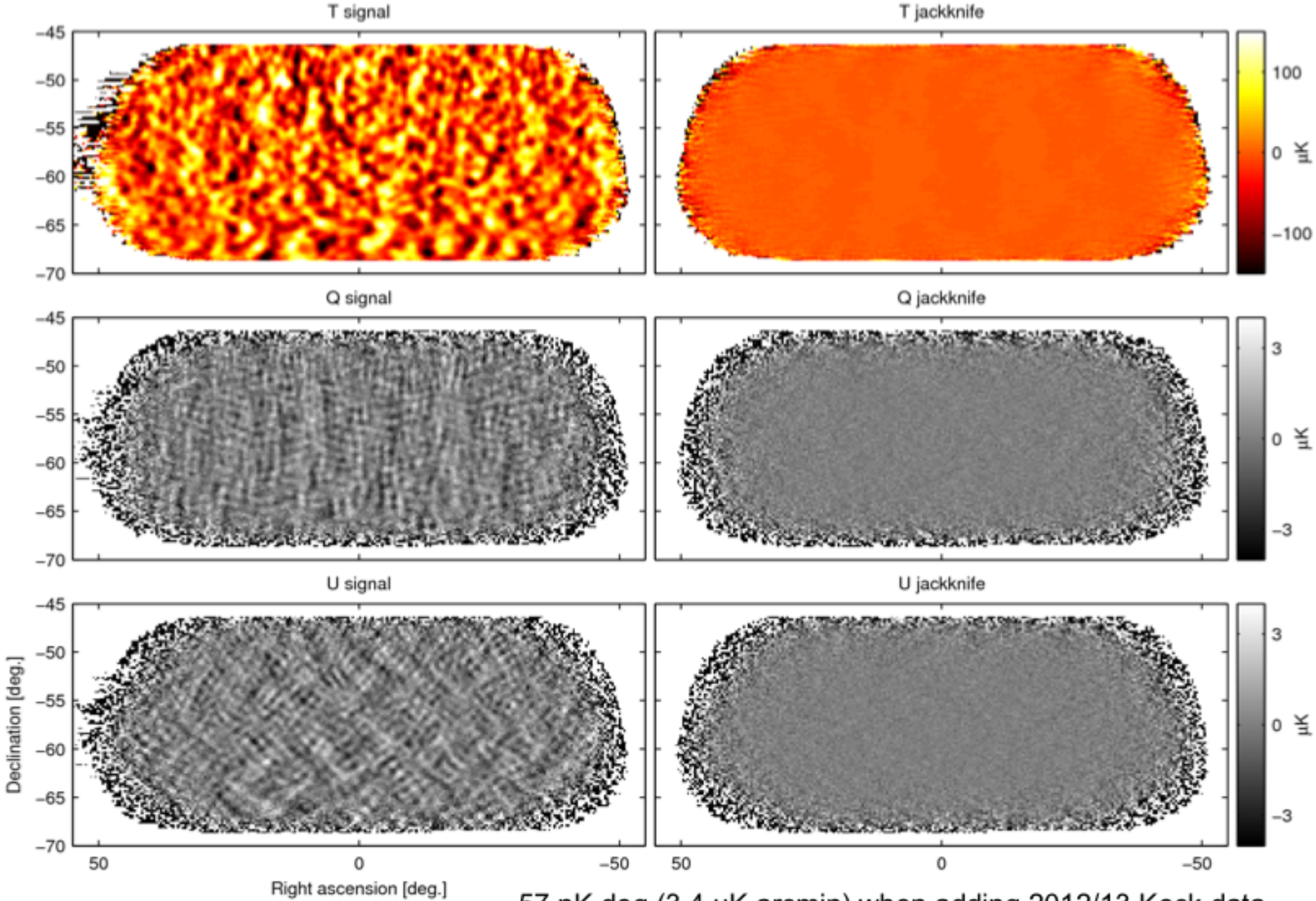

57 nK deg (3.4 μK arcmin) when adding 2012/13 Keck data - by far the deepest maps ever made - but apodized and filtered...

Bicep2, Keck Array and Planck Collaboration

Planck 353 GHz full sky maps in polarization

- 353 GHz polarized maps are dominated by Galactic dust emission

Q

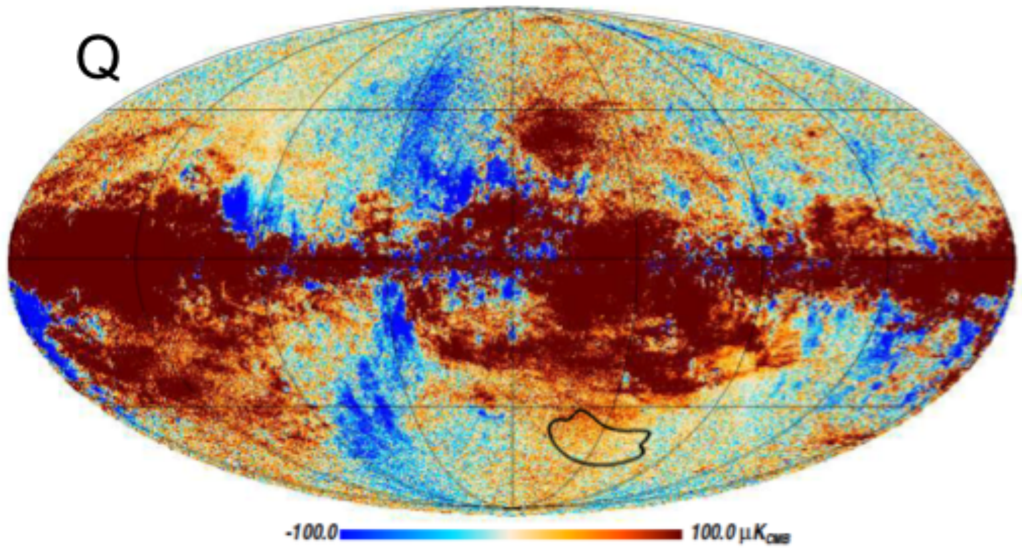

U

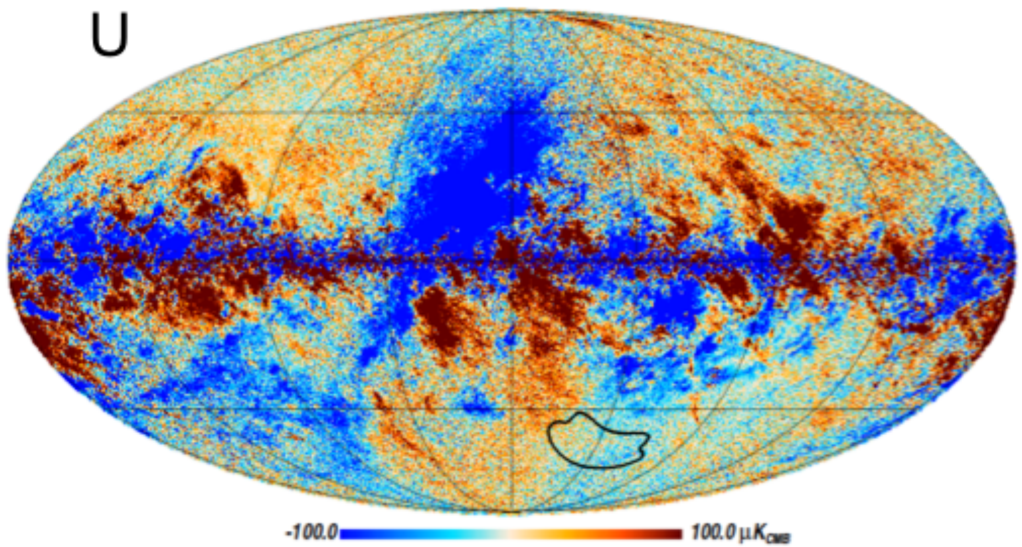

For comparison, Planck 70 GHz is close to the minimum of Galactic foreground emission

Q

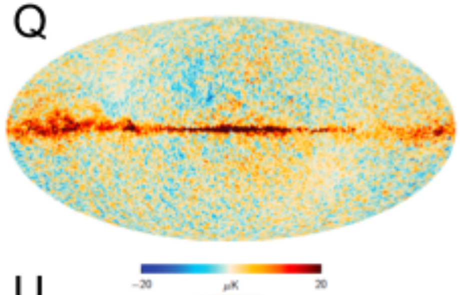

U

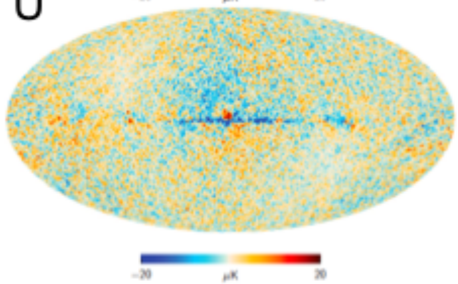

Bicep2, Keck Array and Planck Collaboration

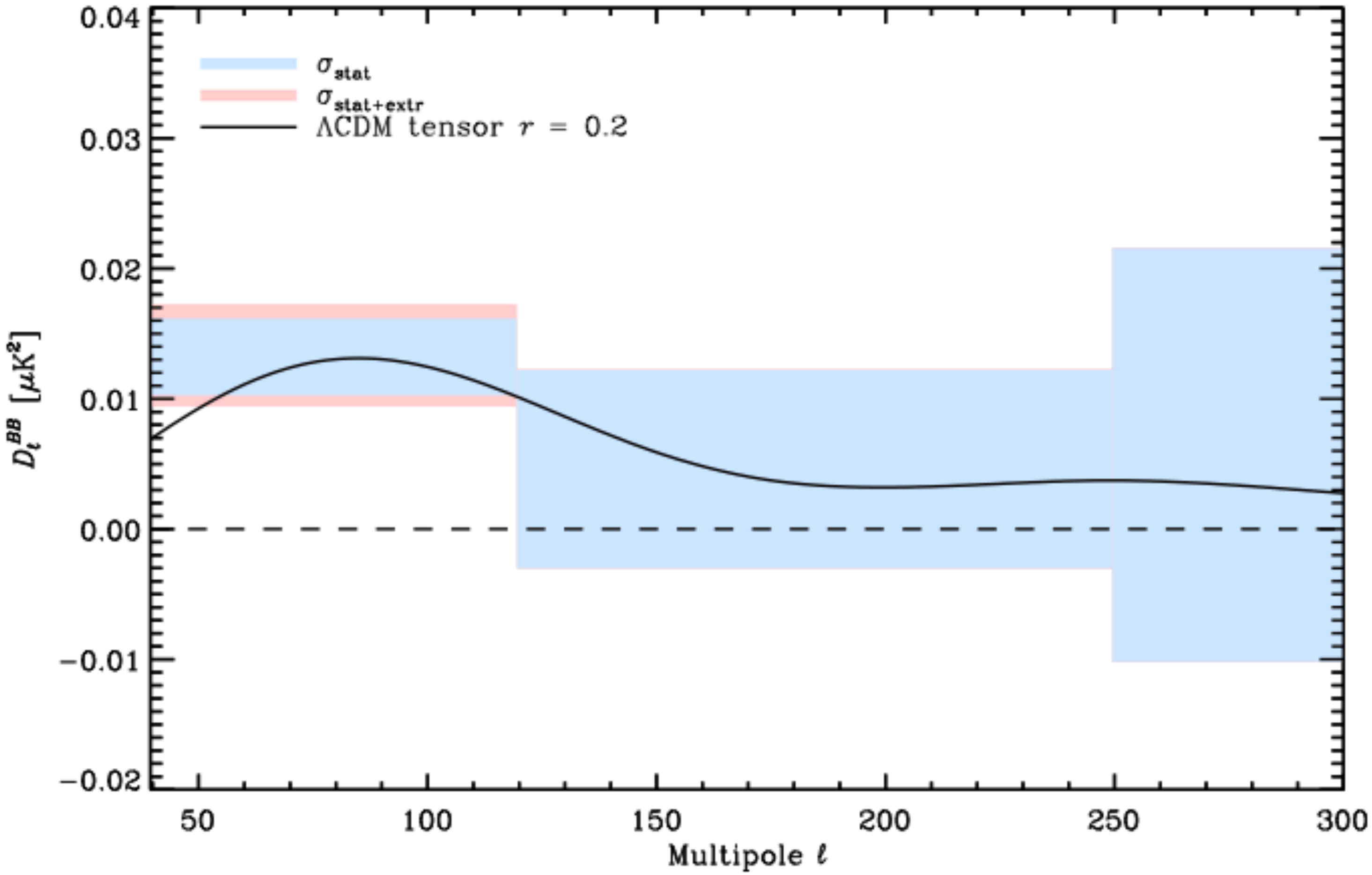

Fig. 9: *Planck* 353 GHz $\mathcal{D}_\ell^{BB}$ angular power spectrum computed on M_{B2} defined in Sect. 6.1 and extrapolated to 150 GHz (box centres). The shaded boxes represent the $\pm 1\,\sigma$ uncertainties: blue for the statistical uncertainties from noise; and red adding in quadrature the uncertainty from the extrapolation to 150 GHz. The *Planck* 2013 best-fit ΛCDM $\mathcal{D}_\ell^{BB}$ CMB model based on temperature anisotropies, with a tensor amplitude fixed at $r = 0.2$, is overplotted as a black line.

Compare BK 150 GHz (left) with Planck 353 GHz (right)

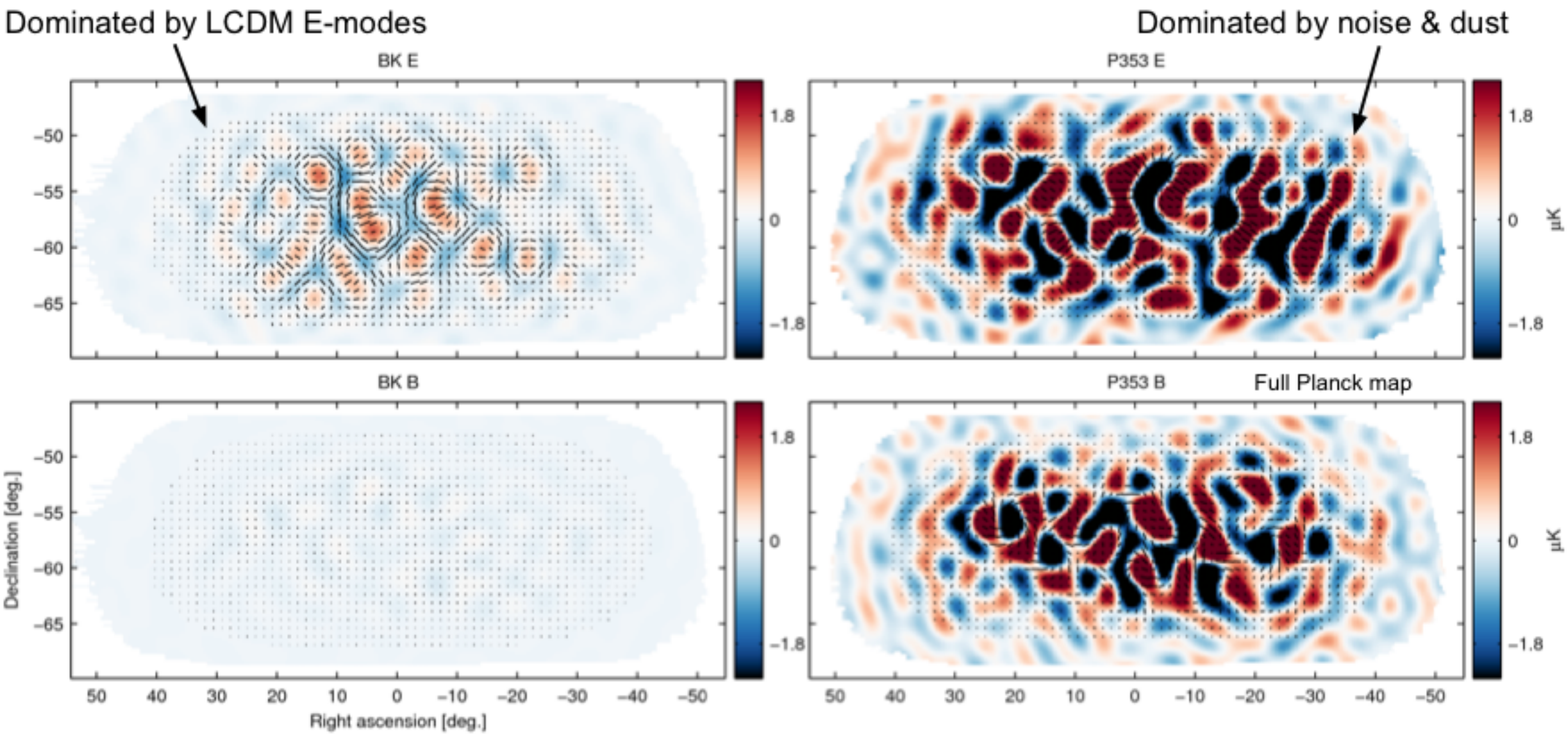

E-modes and B-modes filtered to range l=50-120

all maps shown with the same color stretch

The Real Data

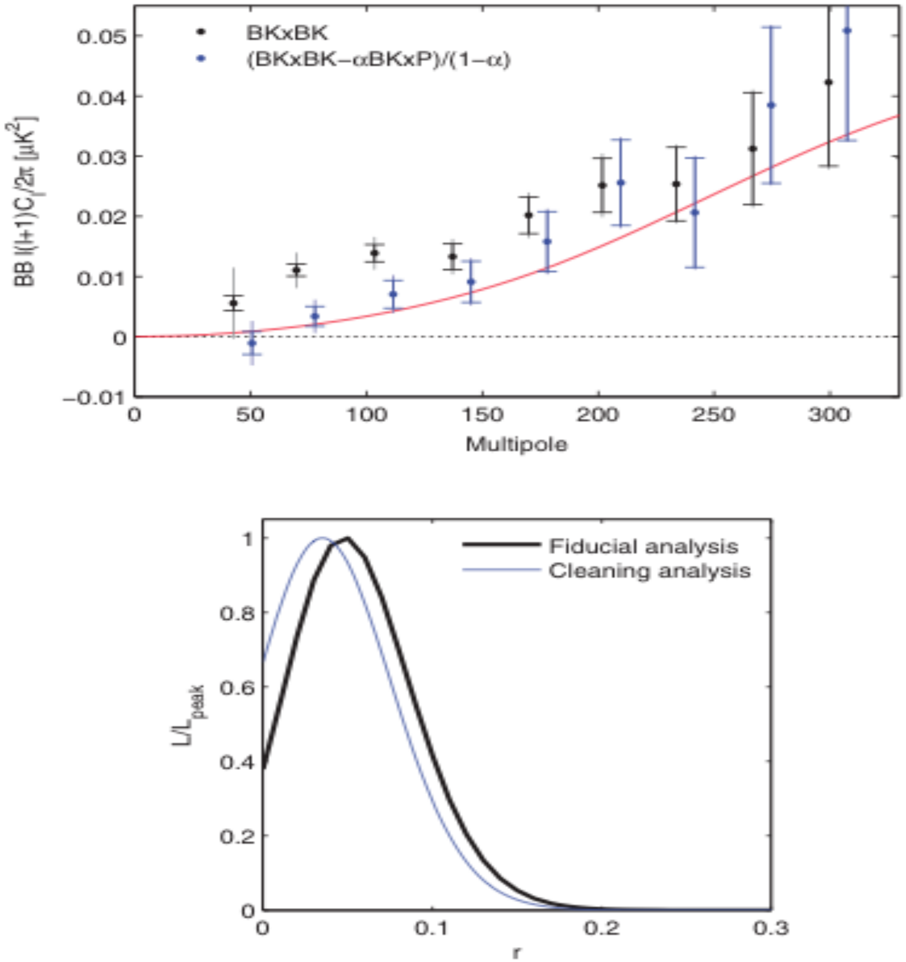

FIG. 12 (color). (Upper) *BB* spectrum of the BICEP2/*Keck* maps before and after subtraction of the dust contribution, estimated from the cross spectrum with *Planck* 353 GHz. The error bars are the standard deviations of simulations, which, in the latter case, have been scaled and combined in the same way. The inner error bars are from lensed-ΛCDM + noise simulations as in the previous plots, while the outer error bars are from the lensed-ΛCDM + noise + dust simulations. The red curve shows the lensed-ΛCDM expectation. (Lower) Constraint on r derived from the cleaned spectrum compared to the fiducial analysis shown in Fig. 6.

❖ The fundamental conclusion is that dust is detected at high significance, and r < 0.12 at 95% confidence.

○ Multi-component likelihood gives σ(r) ~ 0.035 -- This is a very direct constraint on tensors!

○ No significant evidence for r > 0. Currently r = 0 and r = 0.1 are at equal likelihood.

○ There may yet be a gravitational wave signal, but if there is it must be considerably smaller thanthe full signal.

❖ We have checked the stability of the analysis under variations of the data selection and other details.

○ Most variations make little difference. There is some difference in the results depending onwhether BICEP2 or Keck data is used but this is shown to be within noise fluctuation.

Non-Gaussianity … mainly through CMB bispectrum

"smoking gun of inflation" dynamics

$$B^{m_1 m_2 m_3}_{\ell_1 \ell_2 \ell_3} \equiv \langle a_{\ell_1 m_1} a_{\ell_2 m_2} a_{\ell_3 m_3} \rangle$$

$$= \mathcal{G}^{\ell_1 \ell_2 \ell_3}_{m_1 m_2 m_3}\, b_{\ell_1 \ell_2 \ell_3}$$

Gaunt integrals

$$\mathcal{G}^{\ell_1 \ell_2 \ell_3}_{m_1 m_2 m_3} \equiv \int Y_{\ell_1 m_1}(\hat{\boldsymbol{n}})\, Y_{\ell_2 m_2}(\hat{\boldsymbol{n}})\, Y_{\ell_3 m_3}(\hat{\boldsymbol{n}})\, d^2\hat{\boldsymbol{n}}$$
$$= h_{\ell_1 \ell_2 \ell_3} \begin{pmatrix} \ell_1 & \ell_2 & \ell_3 \\ m_1 & m_2 & m_3 \end{pmatrix},$$

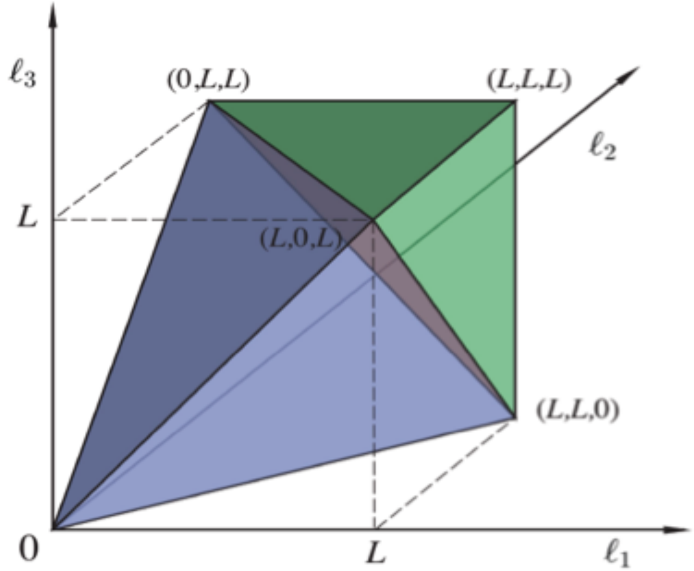

Triangle condition: $\ell_1 \le \ell_2 + \ell_3$ for $\ell_1 \ge \ell_2, \ell_3$, +perms.

Parity condition: $\ell_1 + \ell_2 + \ell_3 = 2n\,, \quad n \in \mathbb{N}\,,$

Resolution: $\ell_1, \ell_2, \ell_3 \le \ell_{\max}\,, \quad \ell_1, \ell_2, \ell_3 \in \mathbb{N}\,.$

(1) Multiple fields (local models, non-linearities develop outside horizon)
(2) Non-canonical kinetic term of quantum fields (higher derivative interactions; Dirac-Born-Infeld, K-inflation)
(3) Non-vacuum initial conditions

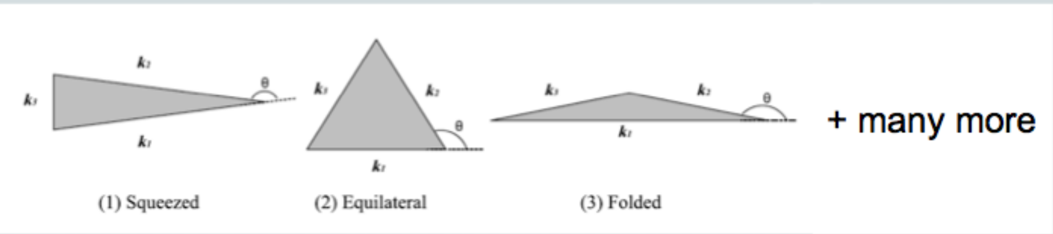

Spectrum (Absolute temperature) of the Cosmic Microwave Background

CMB spectrum: current status

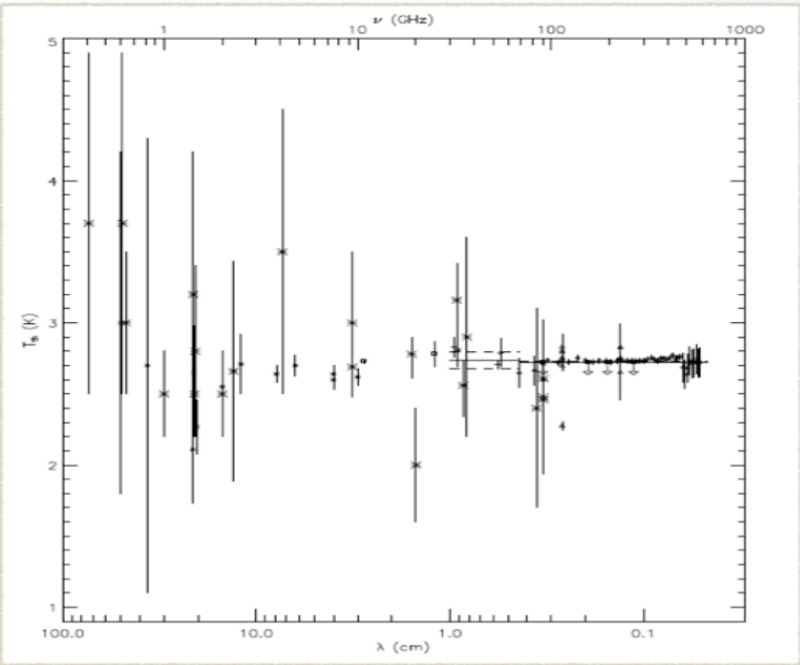

$T_0 = 2.725$
± 0.002 °K

Mather, J.C., et al., 1999, ApJ, 512, 511

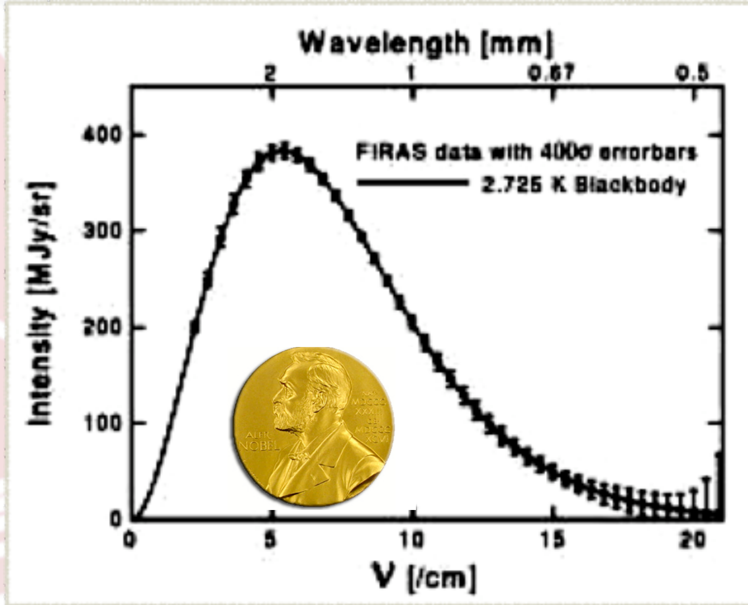

FIRAS measures: typical error ±0.0001 K

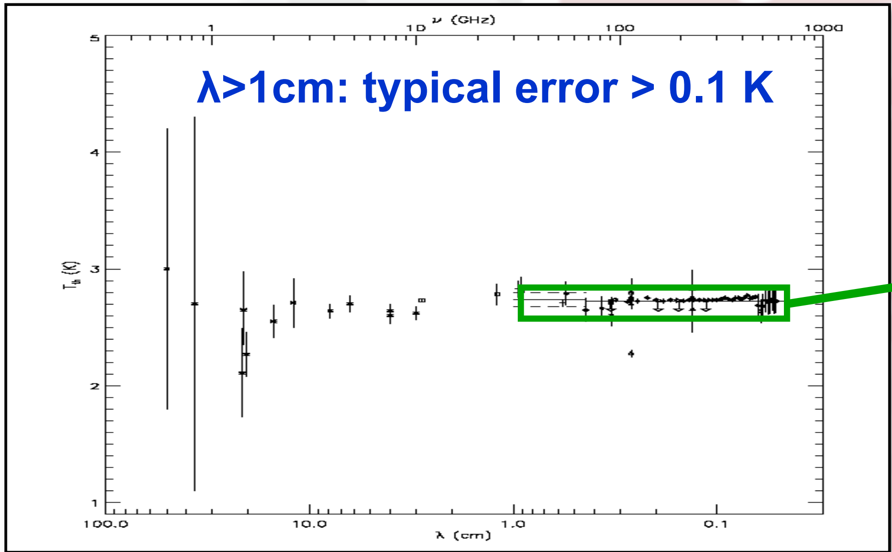

Measures of CMB spectrum (collected by C. Burigana & R.Salvaterra, 1999, arXiv: 0206350)

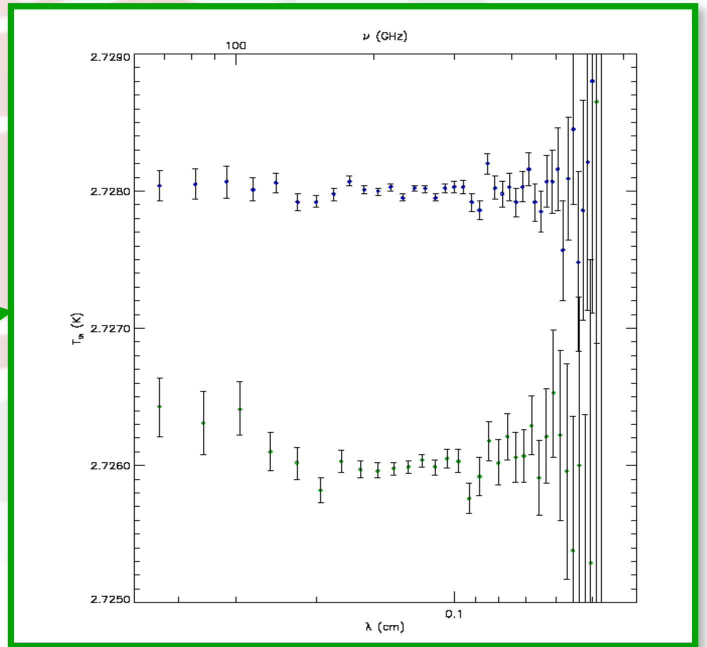

The assessement of Planckian spectrum disproved previous claim!

Matsumoto excess (1988, ApJ 329, 567)

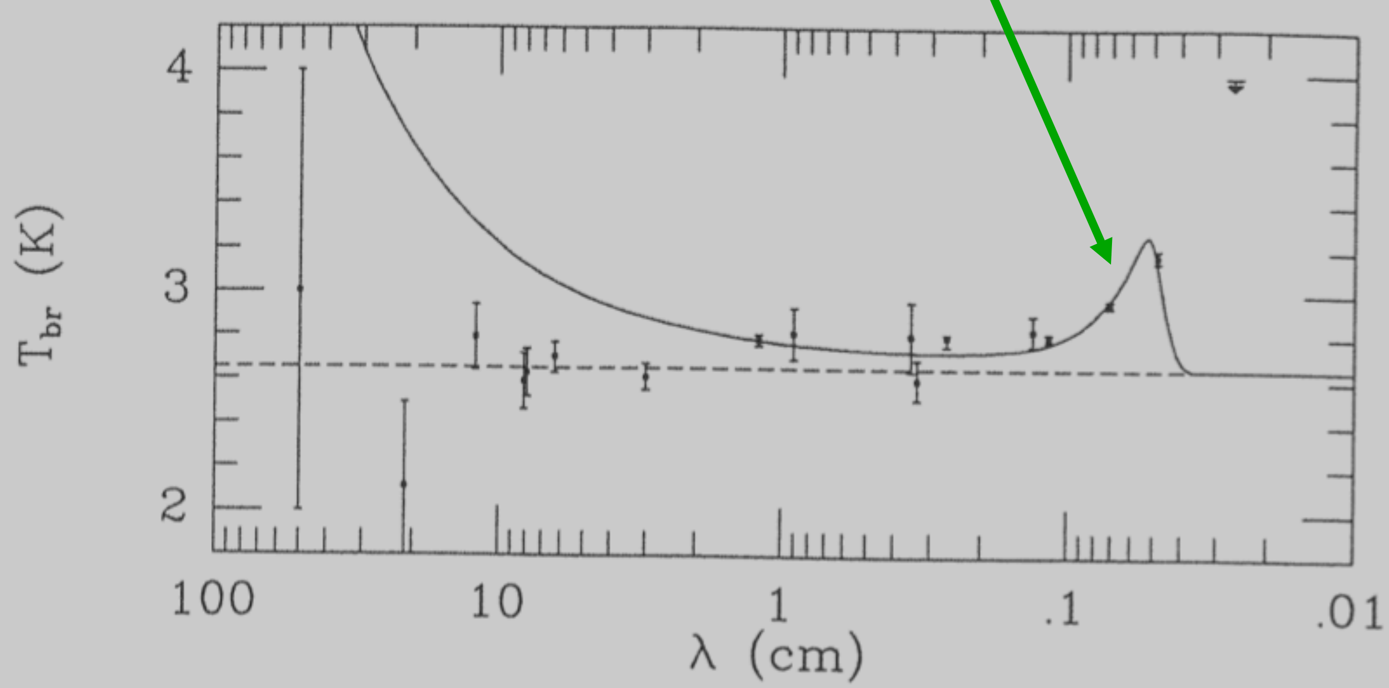

Figure 10. An example of CMB spectral distortions due to a late decay of a very light weakly interacting particle: $m_X = 5 \times 10^{-3}$ eV, $\tau = 0.9 \times 10^{10}$ yr, $n_{X_0} = 100\,\mathrm{cm}^{-3}$, $T_0 = 2.65\,K$, $H_0 = 50$, $\Omega = 1$.

"So far, no fully satisfactory explanation of he sub-mm excess has been found."
L. Danese, CB, L. Toffolatti, G. de Zotti, A. Franceschini, 1990, in The Cosmic Microwave Backgrond: 20 Years Later

Recent long wavelengths experiments (cm–dm)

Crucial for free-free distortions
Where Bose-Einstein like distortions are more prominent
Complementarity of long wavelengths and short (<cm) wavelengths

Sensitive to processes at different & common phases
Breaking "approximate degeneracies" in constraining distortion parameters

TRIS, ground experiment
Gervasi, M., et al. 2008, ApJ, 688, 24

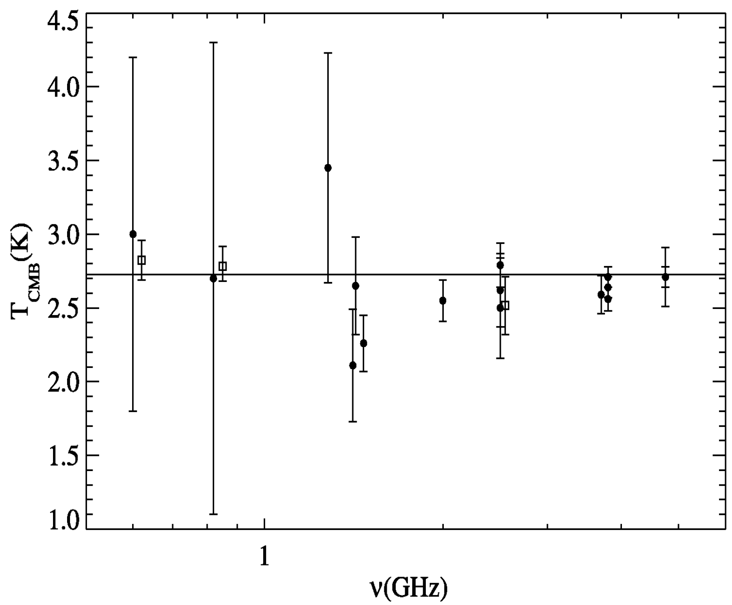

FIG. 5.—CMB thermodynamic temperature measured at low frequencies (see Table 1). For easier comparison with previous measurements (*filled circles*), TRIS data points (*open squares*) have been slightly shifted in frequency. The horizontal solid line is the CMB temperature obtained by FIRAS at higher frequencies.

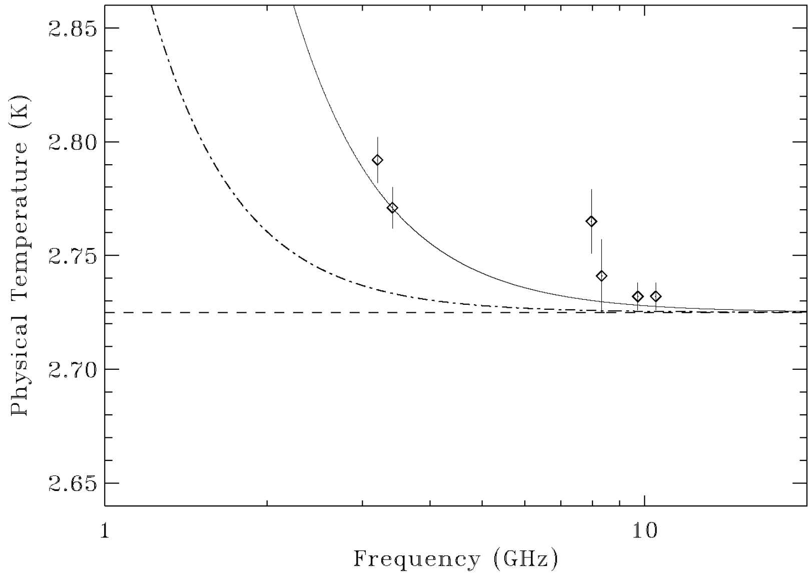

FIG. 1.— Detection of extragalactic radio emission by ARCADE 2 beyond the contribution of discrete radio sources and the expectation of 2.725 K blackbody radiation. Data points are the ARCADE 2 results from Fixsen et al. (2008), and have been corrected for Milky Way Galactic emission described by Kogut et al. (2008). The dashed curve is a constant 2.725 K blackbody, consistent with FIRAS measurements of the CMB. The dot dash curve is an estimate of the discrete radio source contribution from Gervasi et al. (2008a) model "Fit1" added to the 2.725 blackbody. The data points lie significantly above this dot dash curve, indicating our detection of unexplained, excess emission. The solid curve is the best fit of the combined data of Table 1 and FIRAS to a power law plus a constant CMB temperature.

ARCADE 2, balloon
Fixsen, D.J., et al. 2011, ApJ, 734, id. 5

Impact of various sources of errors: note the atmosphere relevance → Needs for balloon/space/Moon observations

Temperature (K)	ν (GHz) 2.5	3.8	4.75	7.5	7.5 1988	1989
$G(S_a - S_{load})$	...	-0.009 ± 0.008	-0.045 ± 0.013	...	-0.146 ± 0.012	-0.126 ± 0.013
Source ($T_{a,load}$)	3.73 ± 0.15	3.762 ± 0.019	3.682 ± 0.010	3.621 ± 0.009	3.671 ± 0.023	
Atmosphere ($T_{a,atm}$)	1.155 ± 0.300	1.109 ± 0.060	0.997 ± 0.060	1.083 ± 0.055	1.083 ± 0.059	1.222 ± 0.064
Galaxy ($T_{a,gal}$)	0.118 ± 0.025	0.055 ± 0.015	0.035 ± 0.025	0.010 ± 0.005	0.010 ± 0.005	0.007 ± 0.004
Ground ($T_{a,gr}$)	0.030 ± 0.050	0.006 ± 0.008	0.020 ± 0.010	0.013 ± 0.010	0.013 ± 0.010	0.022 ± 0.015
System (ΔT_{sys})	...	0.034 ± 0.034	0.0 ± 0.020	0.052 ± 0.034	0.052 ± 0.034	0.023 ± 0.025
RFI ($T_{a,RFI}$)	...	...	...	0.0 ± 0.005	...	0.0 ± 0.005
Sun ($T_{a,sun}$)	0.0 ± 0.005	...	...	...	...	...
$T_{a,ex}$	0.016 ± 0.005	...	...	...	...	...
T^{th}_{CMB}	2.50 ± 0.34	2.64 ± 0.06	2.70 ± 0.07	2.60 ± 0.07	2.64 ± 0.06	
Site	SP	WM/SP	WM	WM	WM	SP
Reference	Sironi, 1991	De Amici, 1991	Mandolesi, 1986	Kogut, 1990	Levin 1992	

Table 8: Values and errors of the recent experiments

Theory of Spectral Distortions

Physical processes involved (+ source terms):

Compton scattering

$$\left(\frac{\partial\eta}{\partial t}\right)_C\bigg|_{x_e=cost} = n_e\sigma_T c\frac{k_B T_e}{mc^2}\frac{1}{x_e^2}\frac{\partial}{\partial x_e}\left\{x_e^4\left[\frac{\partial\eta}{\partial x_e}+\eta(1+\eta)\right]\right\}$$

Bremsstrahlung

$$\left.\frac{\partial\eta}{\partial t}\right)_{ff} = K_0 g_{ff}(\nu, T_e)\frac{e^{-x_e}}{x_e^3}\left[1+\eta(1-e^{x_e})\right]$$

Radiative Compton

$$\left.\frac{\partial\eta}{\partial t}\right)_{DC} = K_{DC}\frac{g_{DC}}{x_e^3}\left[1-\eta\left(e^{x_e}-1\right)\right]$$

The Kompaneets equation in cosmological context provides the best tool to compute the evolution of the photon distribution function, but a numerical code is needed.

$$\frac{\partial\eta}{\partial t} = \left.\frac{\partial\eta}{\partial t}\right)_C + \left.\frac{\partial\eta}{\partial t}\right)_{ff} + \left.\frac{\partial\eta}{\partial t}\right)_{DC}$$

An extremely precise fortran based code, able to simulate the effects of the primordial physical processes that can affect the thermodynamic equilibrium of the CMBR (Kyprix)

CMB distortions @ different cosmic times

Current accurate & general numerical codes, able to ingest many kinds of source terms: KYPRIX: P. Procopio & C. Burigana 2009, A&A, 507, 1243; CosmoTherm: J. Chluba & R.A. Sunyaev, 2012, MNRAS, 419, 1294

BIG

BANG

Blackbody Photoshpere

Intermediate distortions

today

$z_{thermalization}$ z_{BE} z $z_{recombination}$ z

Zeldovich & Sunyaev 1969; Illarionov & Sunyaev 1974; Danese & de Zotti 1977; Burigana et al. 1991; Hu & Silk 1993

Primordial distortions

Bose-Einstein like

$$\eta_\nu = \frac{1}{e^{(h\nu/kT)+\mu} - 1}$$

with μ function of x $\mu(x) \simeq \mu_0\, e^{(-x_C/x)}$

Late distortions

Superposition of black bodies

$$\eta(x, y^*) \simeq (4\pi y^*)^{-1/2} \int_0^\infty \eta_0(x')\exp\left[-\frac{(\ln(x/x') + 3y^*)^2}{4y^*}\right]\frac{dx'}{x'}$$

where $y^* = \int \frac{k_B(T_e - T_r)}{m_e c^2} d\tau$

Burigana et al. '04

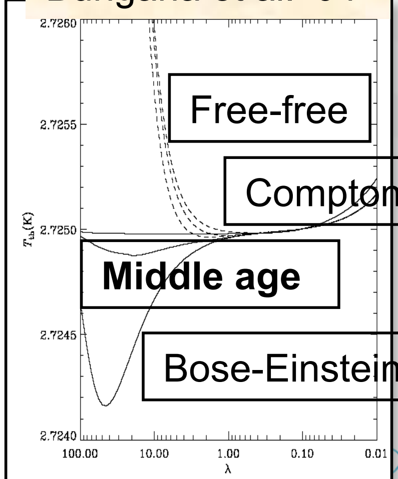

+ Free-free distortions

$$y_B \simeq x^2\left(\frac{T_{br} - T_r\phi_i}{T_r} - 2u\phi_i\right)$$

Late distortions

Related (mainly) to the reionization history of the universe

$\mu \sim 1.4\, \Delta\varepsilon/\varepsilon_i$ $y \sim (1/4)\, \Delta\varepsilon/\varepsilon_i$

Ideas of future CMB spectrum space missions

- The current limits on CMB spectral distortions and energy dissipation processes in the plasma, $|\Delta\varepsilon/\varepsilon_i| \leq 10^{-4}$, are mainly set by the NASA COBE/FIRAS experiment.
- High accuracy CMB spectrum experiments from space, like DIMES at $\lambda \geq 1$ cm (Kogut 1996) and FIRAS II at $\lambda \leq 1$ cm (Fixsen & Mather 2002), have been proposed to constrain (or probably detect) energy exchanges 10–100 times smaller than the FIRAS upper limits possibly generated by heating (but also by cooling) mechanisms at different cosmic epochs.
- These perspectives have been recently renewed in the context of a new CMB space mission like PIXIE (Kogut et al. 2011) proposed to NASA or even in the possible inclusion of spectrum measures in the context of a polarization dedicated CMB space mission, of high sensitivity and up to arcmin resolution, like PRISM proposed to ESA in 2013.

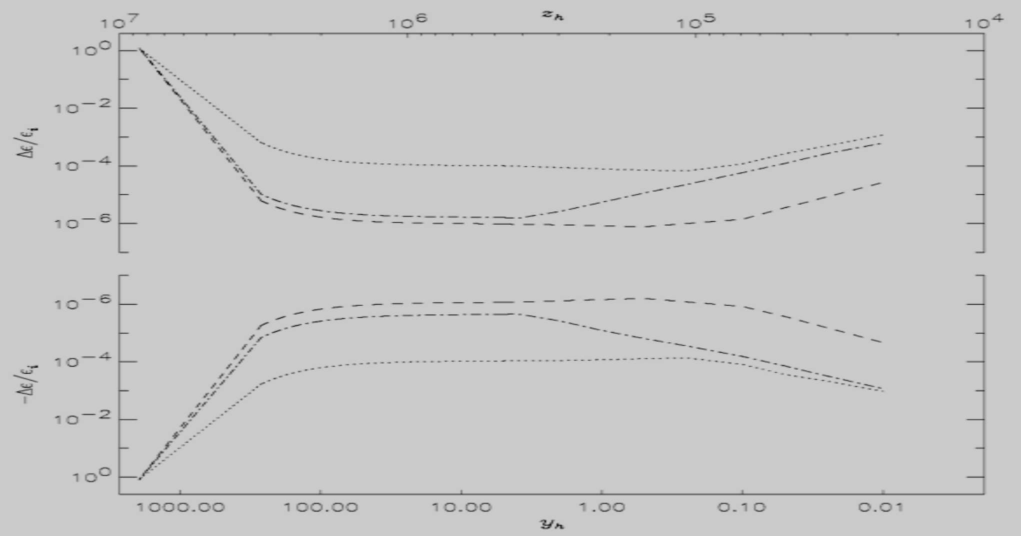

Figure 2. Comparison between the constraints on the energy exchanges derived from current measures – FIRAS and long wavelength data – (dotted lines; in practice FIRAS data alone set the current constraints, see Salvaterra & Burigana 2002), from FIRAS data jointed to a simulated data set from a *DIMES*-like experiment (dash-dotted lines; see Burigana & Salvaterra 2003), and, finally, from simulated data sets from a *DIMES*-like experiment jointed to a FIRAS II-like experiment (dashed lines). An underlying blackbody spectrum is here assumed for the simulated data sets. In the first two cases (dotted lines and dash-dotted lines) we report the constraints on $\Delta\epsilon/\epsilon_i(y_h)$ allowing for a later energy exchange at $y_h \ll 1$ but neglecting free-free distortions (i.e. assuming $y_B = 0$). In the last case (dashed lines) we relax the assumption $y_B = 0$, i.e. we jointly consider three kinds of spectral distortions. See also the text.

DIMES & FIRAS II, about 100 better than FIRAS - Constraints in the absence of detection of distortions

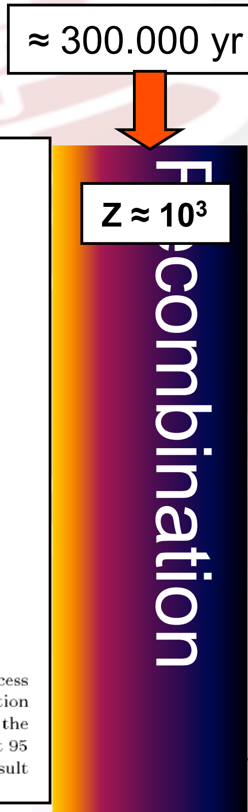

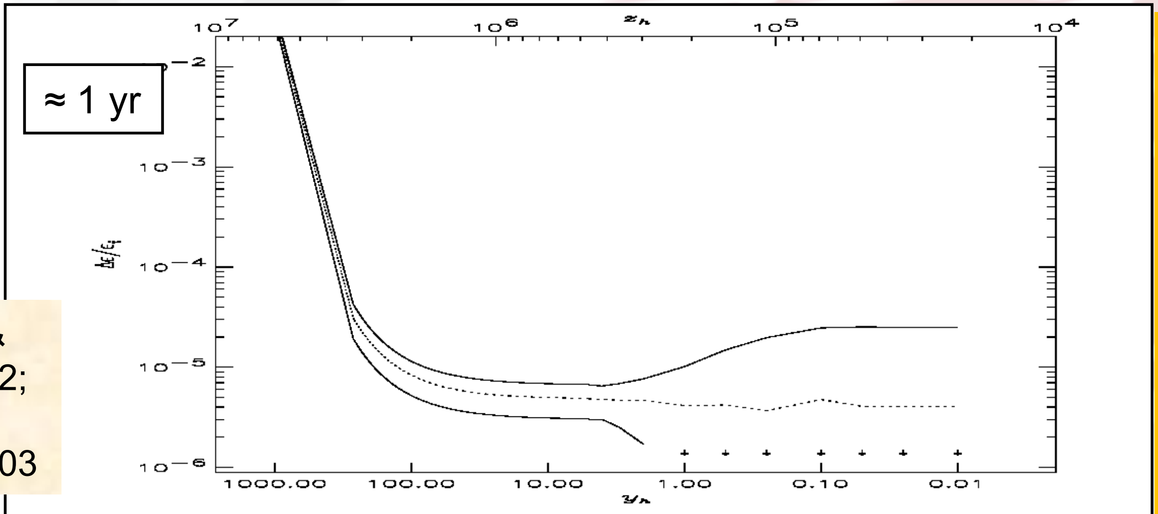

Figure 3. Constraints on the energy exchanges derived at different cosmic times by considering the case of a single dissipation process on the basis of the FIRAS data calibrated according to Mather et al. 1999 and data simulated as in the case of an energy injection with $\Delta\epsilon/\epsilon_i \geq 5 \times 10^{-6}$ and observed with a DIMES-like experiment. The dissipation epoch is assumed to be known (is the same in the generation of simulated data and in the fit). The different lines refer to the best fit result (dots) and to the upper and lower limits at 95 per cent CL (solid lines). The arrows indicate that the sign of the lower limit changes at $y_h \simeq 1$, where lower and upper error bars result to be very similar.

Savaterra & Burigana '02; Burigana & Salvaterra '03

Or in the presence of detection of an early distortion (Bose-Einstein like)

Toward 1000 times better than FIRAS!!!

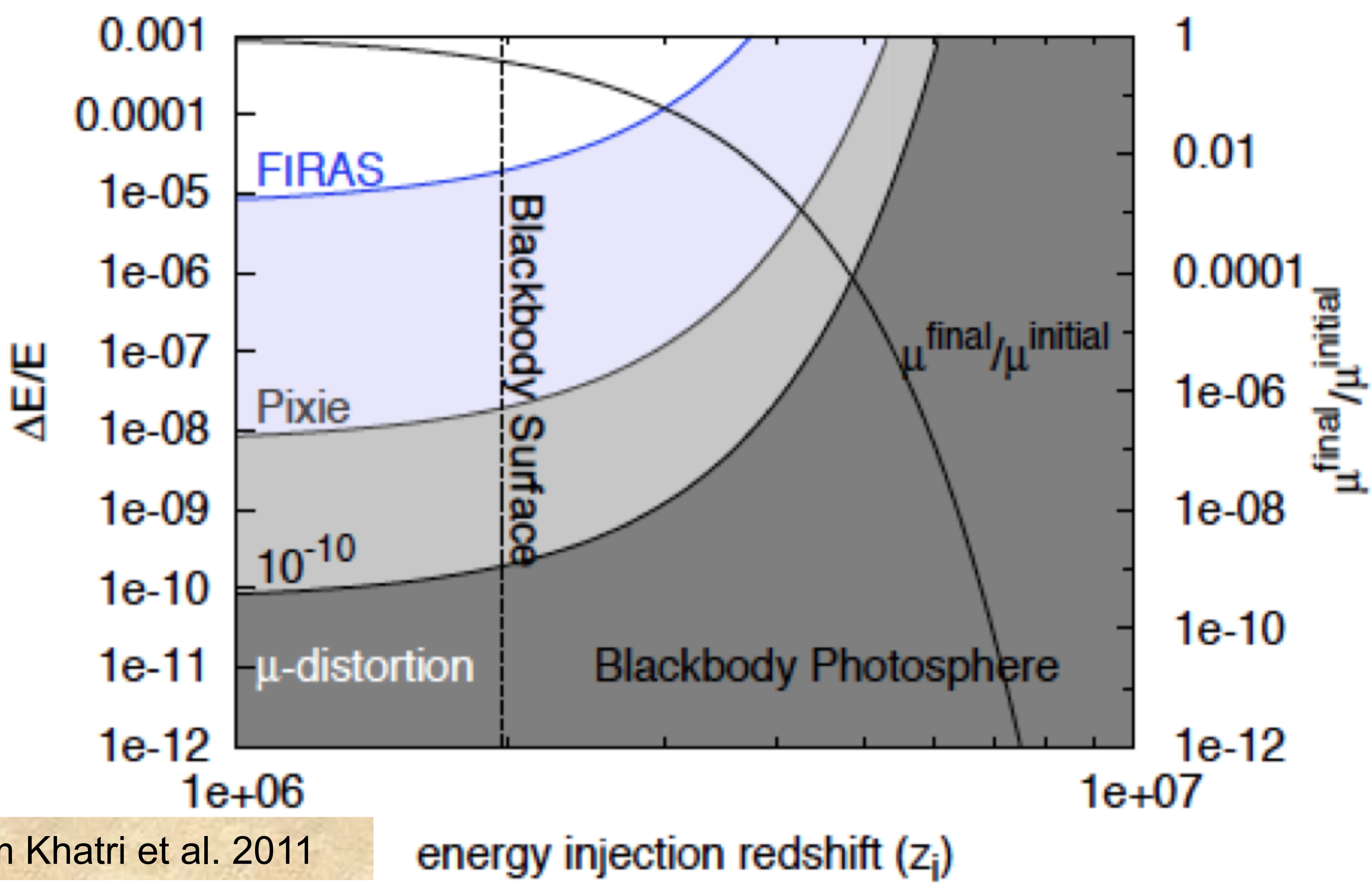

From Khatri et al. 2011

Probing primordial power spectrum on very small scales using spectral distortion

- Current constraints on the power spectrum (and the spectral index n_s) are limited by the size of current horizon (CMB quadrupole) on large scales, and by nonlinearity and Silk damping on small scales.
- Little improvement can be expected from galaxy surveys and SKA because of these fundamental limitation.
- The small scale primordial power dissipated by Silk damping does not disappear completely, but leaves its imprint in **spectral distortions** from the perfect CMB blackbody spectrum. **Important target for the PRISM spectrometer.**

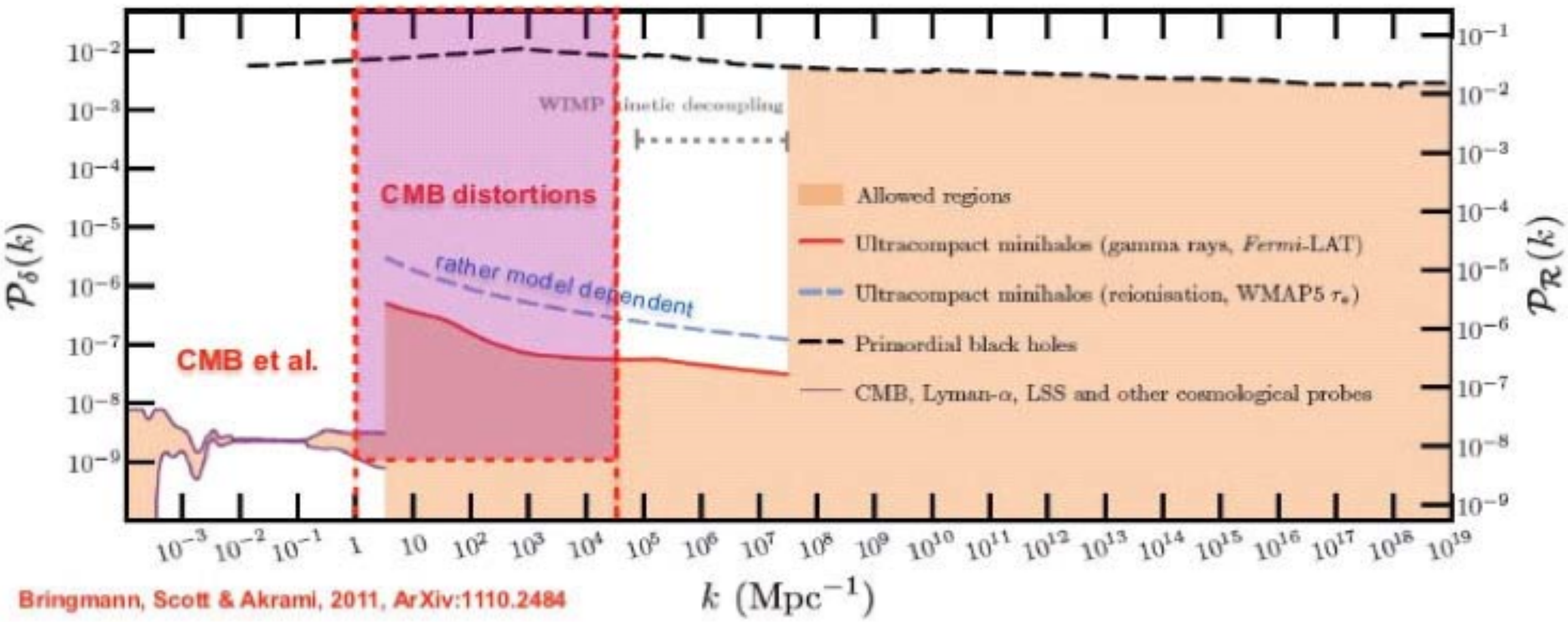

Bringmann, Scott & Akrami, 2011, ArXiv:1110.2484

Adiabatic cooling (BE condensation) vs perturbation dissipation

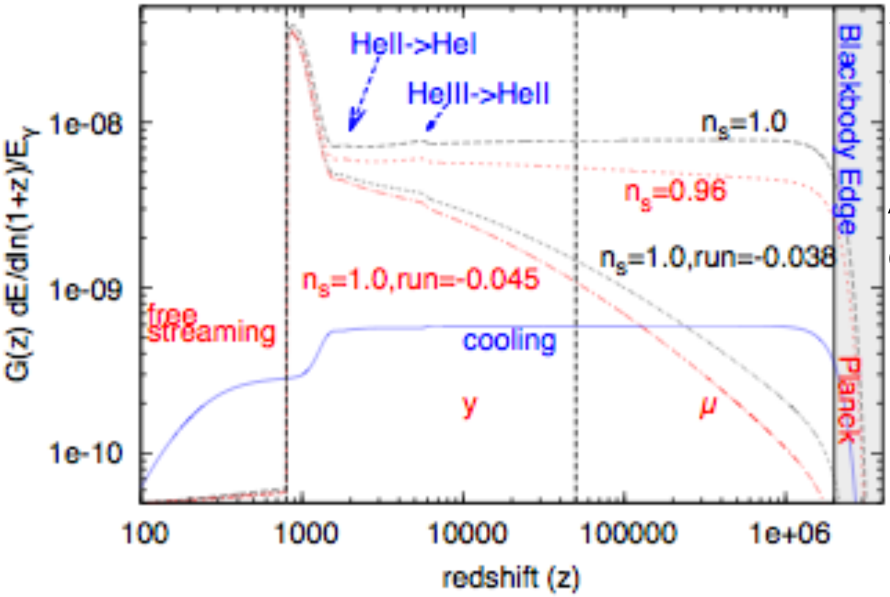

Sketch of fractional rate of energy release due to Silk damping and free streaming for different initial power spectra.
Also shown for comparison is the rate of energy loss due to adiabatic cooling of baryonic matter.

n_s	$\Delta E/E$
1.07	6.8×10^{-8}
1.04	4.7×10^{-8}
1.0	2.9×10^{-8}
0.96	1.8×10^{-8}
0.92	1.1×10^{-8}
BEC	-2.2×10^{-9}

Energy injection in μ distortions during $5 \times 10^4 < z < 2 \times 10^6$ for different initial power spectra without running compared with energy losses due to Bose-Einstein condensation.

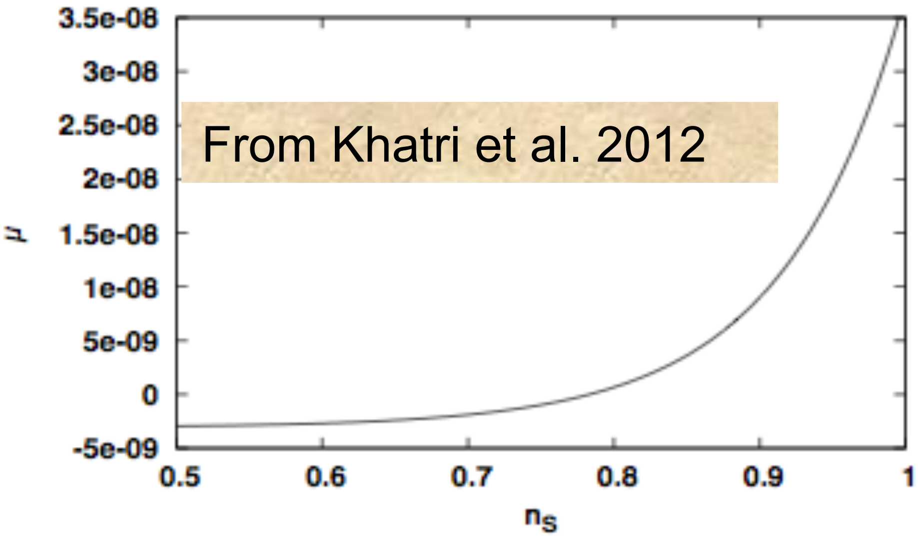

$\mu \sim 1.4\, \Delta\varepsilon/\varepsilon_i$ as a function of spectral index n_s (without running)

Chluba et al. 2012: also amplitude unknown @ small scales → larger range of μ

"Exotic" spectral distortions

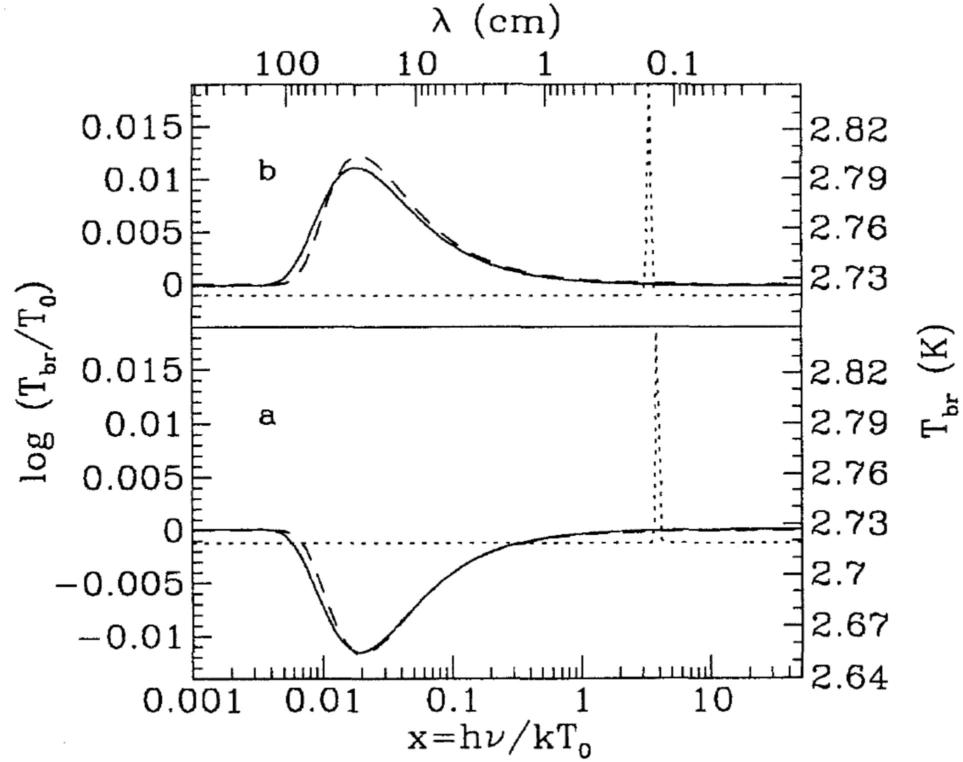

Fig. 4. Relaxation to a Bose–Einstein like spectrum of early distortions in presence of radiative decay with $\Delta n_\gamma/n_i = 7.5\,10^{-3}$ and $\Delta\epsilon/\epsilon_i$ such that $\mu = 10^{-3}$ (a) and $\mu = -10^{-3}$ (b) (see eq. (28), $\Delta\epsilon/\epsilon_i \simeq 0.01$). The initial spectrum is a black–body plus a "line" due to the radiative decay (dotted lines). The numerical results for the present spectrum (solid lines) and the approximation of Burigana et al. (1991a) (dashed lines) are showed. The agreement results to be quite good ($\Omega_b = 0.1$, $H_0 = 50$, $\Omega_T = 1$).

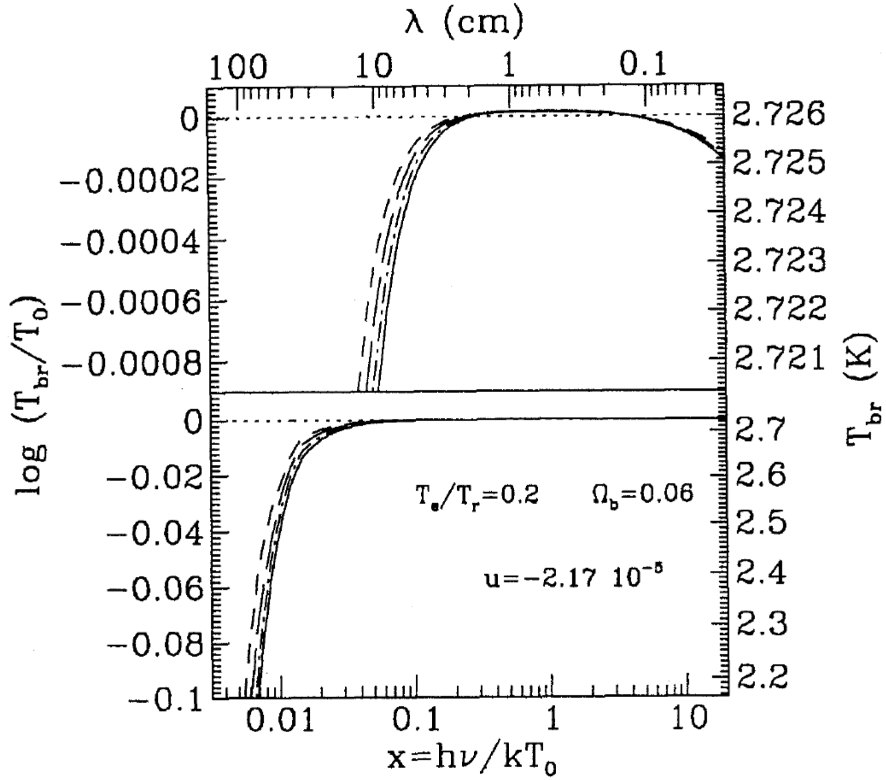

Fig. 13. Evolution of a BB spectrum since $z = 1500$ (dotted line) for the case of ionized matter with a constant ratio $T_e/T_r = 0.2$ between the matter and radiation temperature. The spectrum at several times is showed: $z = 749$ (dashed line), 499 (long dashes), 245 (dots plus dashes) and present time (solid line) ($H_0 = 50$, $\Omega_T = 1$). The distorted spectrum is characterized by negative values of u and y_B as a consequence of the assumption on the ratio T_e/T_r (see eqq. (35) and (46)). Of course at very long wavelengths, where bremsstrahlung is very efficient, the spectrum approaches to that of a black–body with temperature $T = T_e$. The top panel is only a blow–up of a part of the bottom one for sake of comparison between the distortions at submillimetric and RJ spectral regions.

$$\mu \simeq 1.4\left(\frac{1+\Delta\epsilon/\epsilon_i}{(1+\Delta n_\gamma/n_i)^{\frac{4}{3}}}-1\right) = 1.4\left(\frac{1+R_X B_\gamma x_X/\bar{x}_{CMB}}{(1+R_X B_\gamma)^{\frac{4}{3}}}-1\right)$$

$R_x = (3/8)(g_l/X)$

g_l is the number of states per momentum mode and X is the effective number of relativistic interacting species at the decay epoch

Danese & Burigana '94, Lecture Notes Phys., 429, 28

Decay and spectral distortions

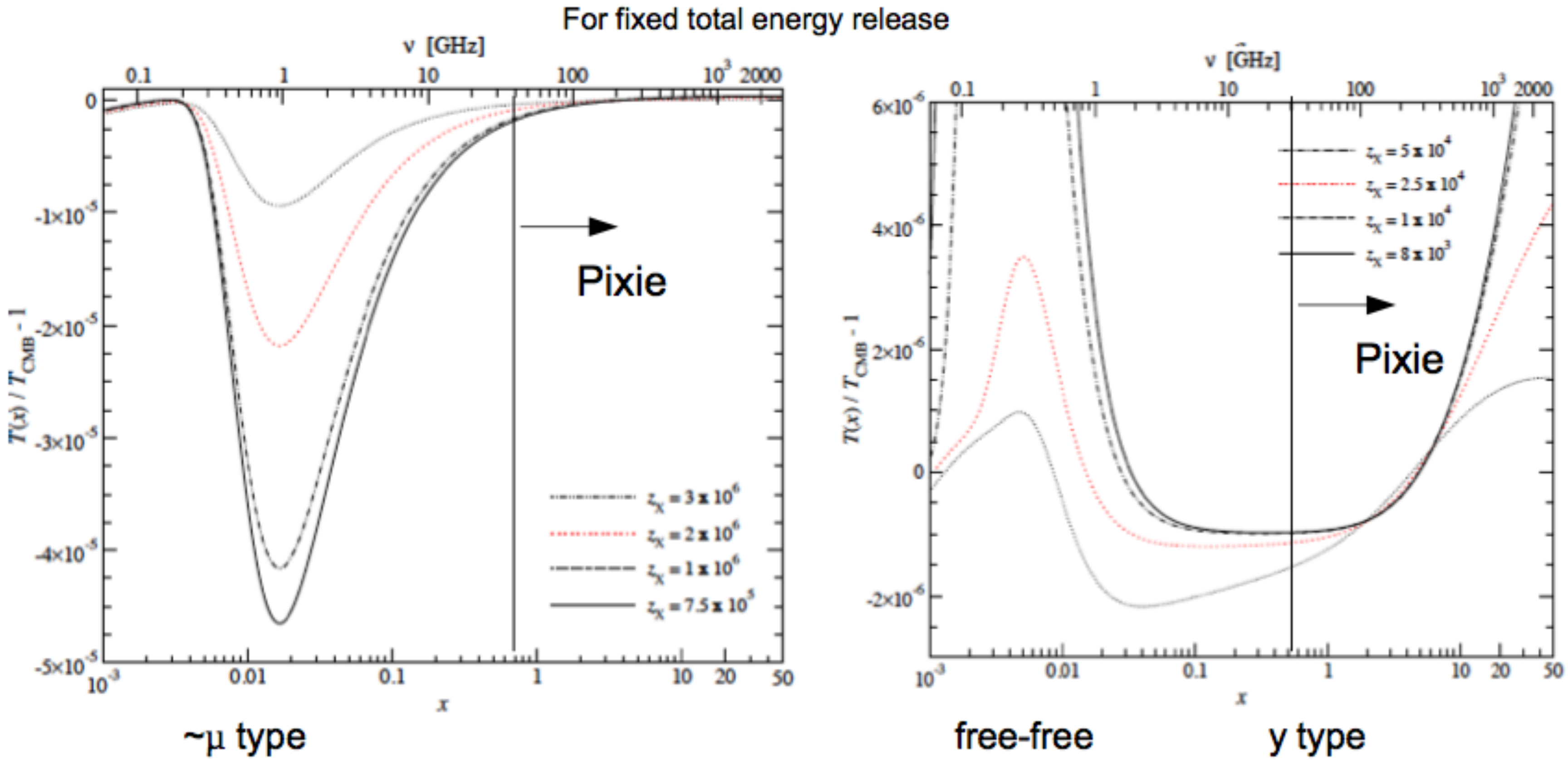

Decay with different lifetimes produce different spectral distortions

Chluba & Sunyaev 2012

Predictions in the view of extreme sensitivity projects

Visibility functions for atomic species

Courtesy Jeans Chluba

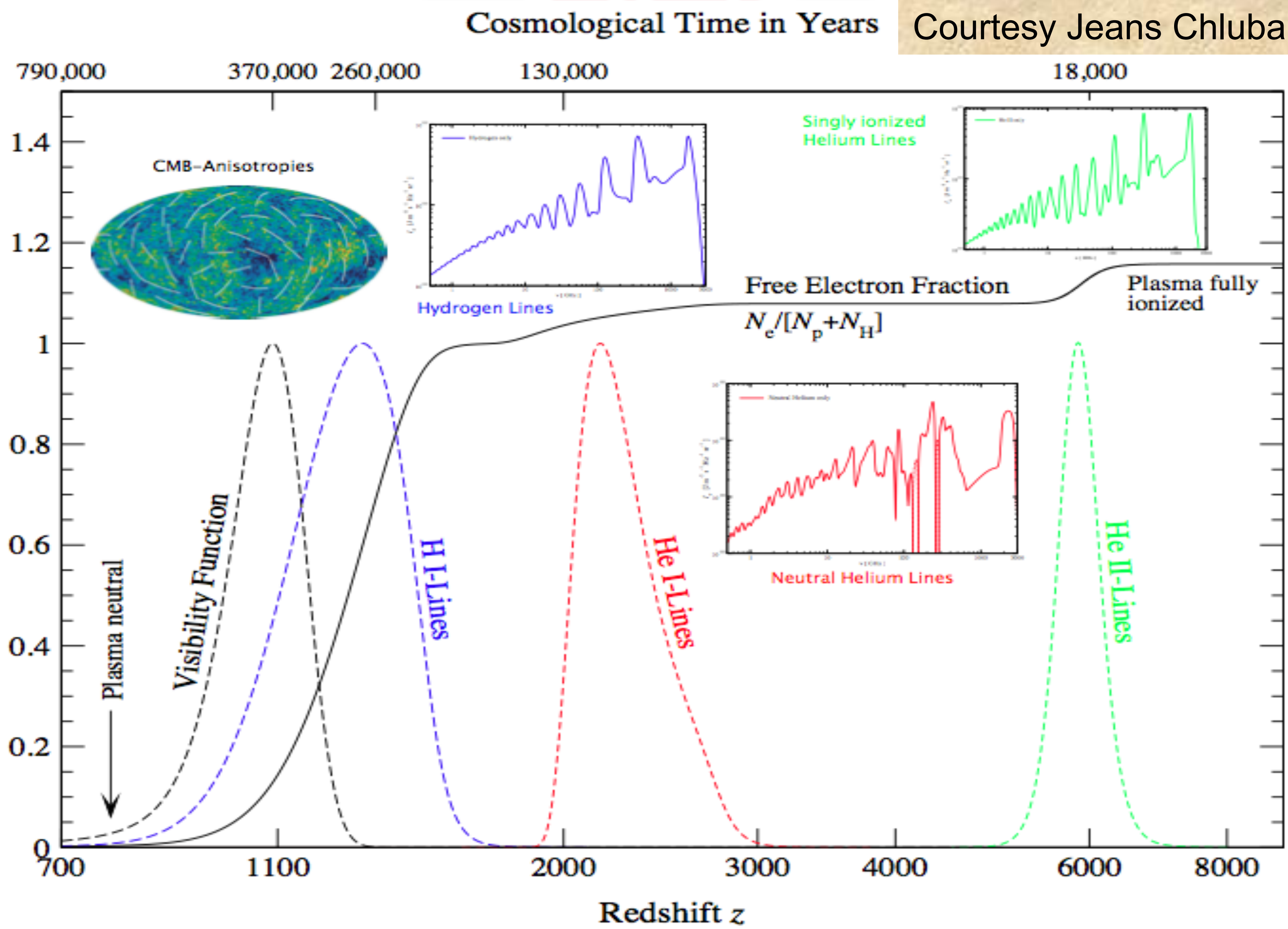

Numerical code for recombination lines

The standard computation

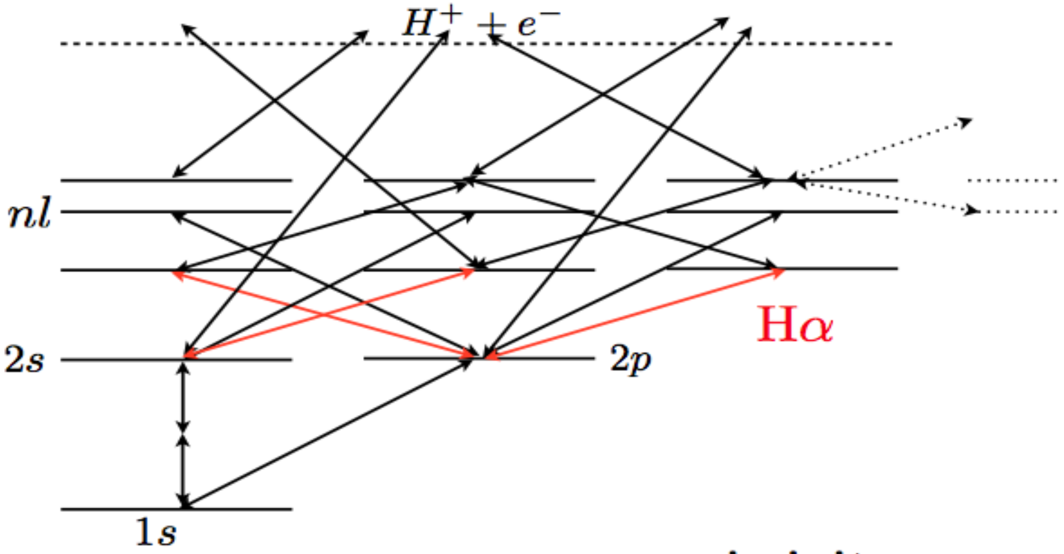

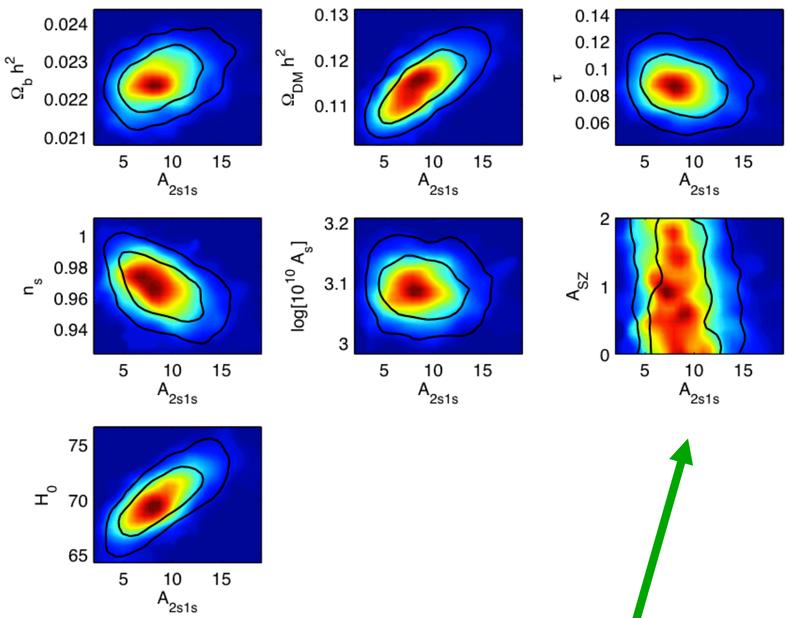

emissivity:

$$j_\nu^{(n'n)} = n_H \sum_l \frac{h\nu}{4\pi} \left[x_{n'l'} R_{n'l,nl} - x_{nl} R_{nl,n'l'} \right] \delta(\nu - \nu_{n'n})$$

Courtesy Yacine Ali-Haïmoud

Hints from TT & Pol anisotropies
Expectation from Planck
→ ±6%

Current limits from cosmology on A_{2S1S} around 8.22458 s^{-1} (±34%)

From Mukhanov et al. JCAP06(2012)040

Recombination lines

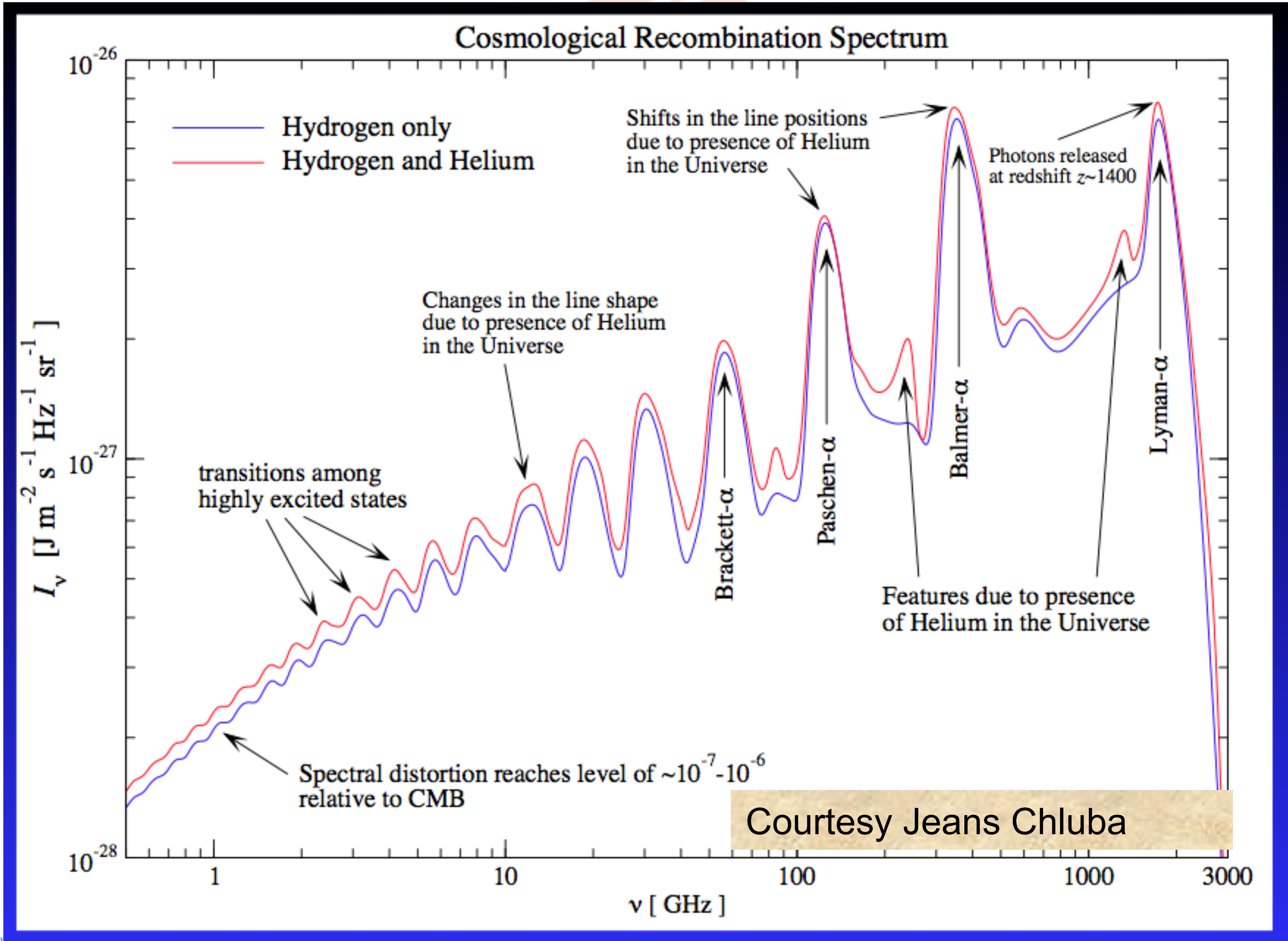

❖ Without any particular assumption about complex haloes physics, **a robust lower limit to the global averaged free-free distortion signal expected from the diffuse ionized IGM** in a given cosmological reionization scenario can be derived from fundamental arguments based only on density contrast evolution on cosmological models and well-known radiative emission mechanisms (T. Trombetti & C. Burigana 2014, MNRAS, 437, 2507):

✓ Boltzmann codes for the matter variance evaluation;

✓ a dedicated code for the free-free distortion including the correct time and frequency dependence of Gaunt factor.

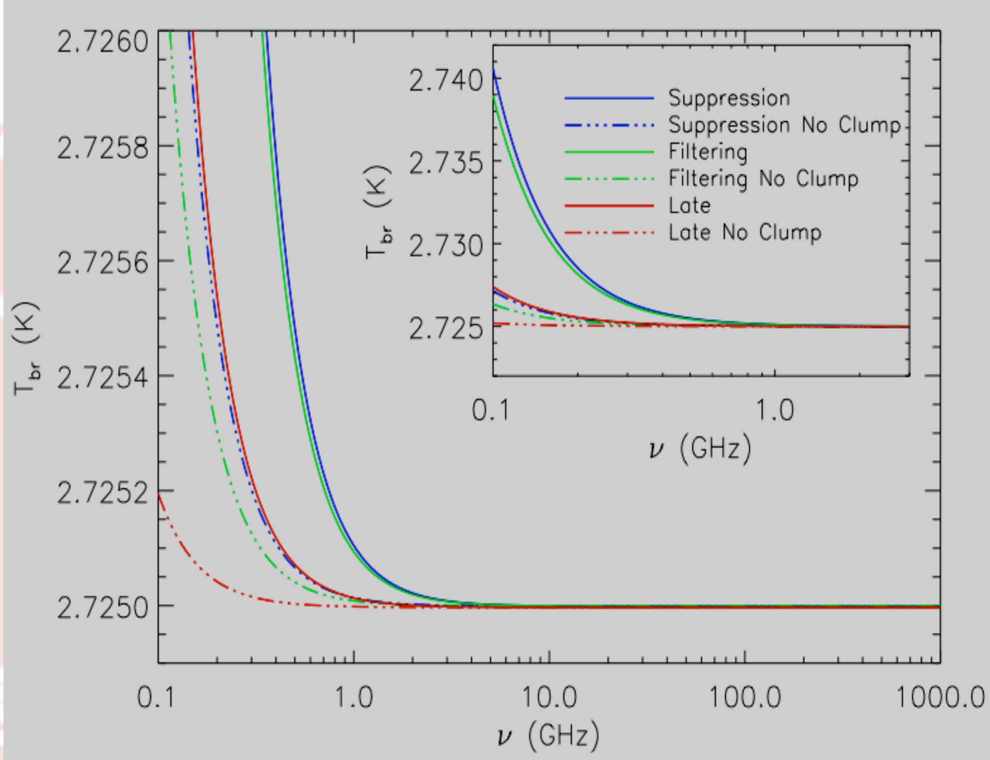

As shown in the figure, where signals from both free-free distortion and Comptonization decrement are included, the expected excess is at ~ mK level at decimeter wavelengths & a few % of Comptonization decrement expected in these models at $\lambda < 1$ cm.

Modest but not negligible impact for CMB space missions, main target for ground-based observations.

Summary of CMB spectral distortions in intensity

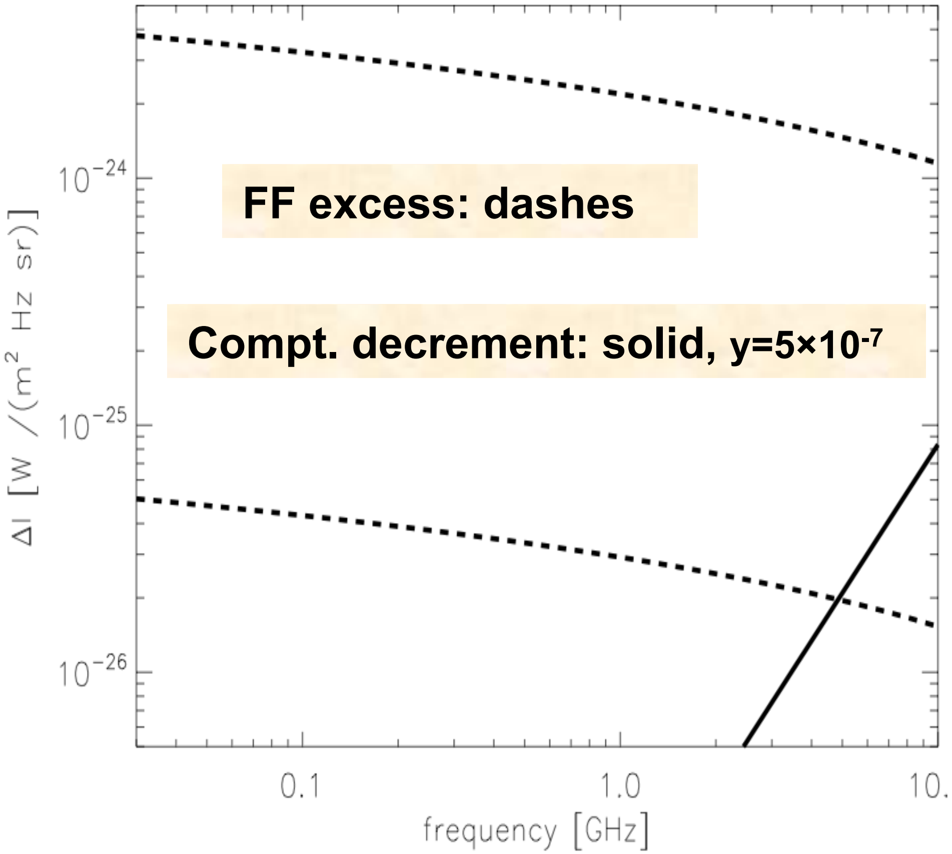

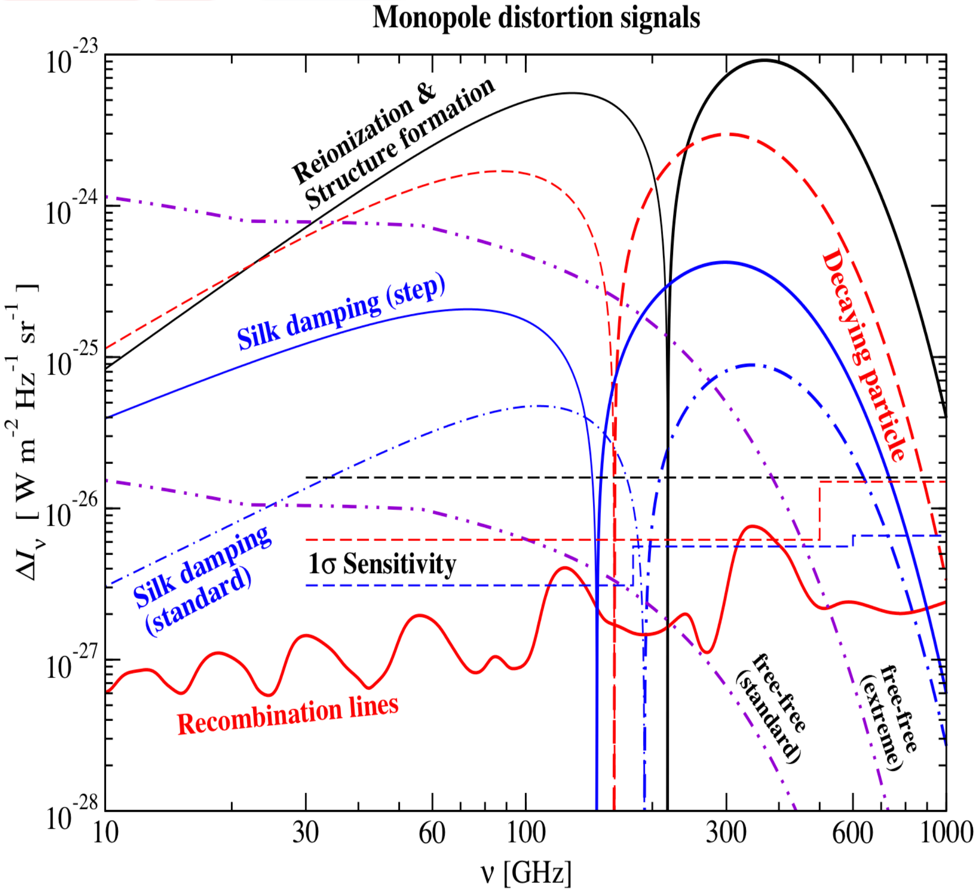

Low freqs.

Ground experiments, DIMES, ARCADE 2, SKA & its precursors

High freqs.

FIRAS II, Pixie, PRISM

From PRISM studies

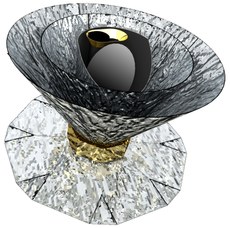

CMB spectral distortions - I

❖ Current observations *consistent with Blackbody & Standard Big-Bang Model* … **but:**

- **Very small distortions** in continuum spectrum are
  - ❖ **strongly predicted** to be generated during ***late epochs*** ($z < 10^4$), as Comptonization, free-free distortions associated to **reionization / structure formation,** hot galaxy clusters: **clearly detectable by PRISM (≳100σ!)**
  - ❖ **or may be produced or have to be produced** at ***earlier epochs***

    (Bose-Einstein distortions, intermediate shapes, "exotic shapes") by "exotic" processes, as decays, annihilation, cooling/Bose condensation, damping of primordial perturbations probing the *power spectrum on very small scales (inflation)*: **detectable by PRISM → New physics!**
- → **"Direct" reconstruction** of thermal history & thermodyn. processes **up to $z \cong 10^7$**
- ➢ N.B.: fully analogy with CMB anisotropy before COBE/DMR:

  Standard model would be untenable if no distortion were detected

➢ **H & He recombination lines from $z \simeq 10^3$**

➢ *HI Balmer & Paschen-α lines detectable with* ***PRISM***

➢ ***additional anisotropic signal detectable with PRISM***

➢ **Resonant scattering signals of metals during the *dark ages***

CMB spectral distortions - II

- **Feasibility/robustness of theoretical studies**
- **Accurate codes** for the Kompaneets eq. & lines predictions exist, **versatile & fast enough**
  - to ingest many physical / astrophysical processes at both high & low z
  - for implementations with different source terms
  - for comparison with future ultra-precision data (also with MCMC methods)

- **"By-products" of absolute temperature high-precision data**
  - better calibration, inter-frequency calibration of all astrophysical microwave/mm/sub-mm data, also of future ground-based facilities (@ higher resolution)
  - accurate **assessment of 0-levels** of microwave/mm/sub-mm maps
  - crucial link with radio & IR surveys, also for improving **component separation** results by **combining *imaging with spectroscopy!***

Thanks for the attention!